

ATTACHMENT B

ANALYSIS OF PLANT RESPONSE DURING JANUARY 25, 1982
STEAM GENERATOR TUBE FAILURE AT THE R.E. GINNA NUCLEAR POWER PLANT

NOVEMBER, 1982

Prepared by: E. C. Volpenhein

Westinghouse Electric Corporation
Nuclear Energy Systems
P. O. Box 355
Pittsburgh, Pennsylvania 15230

Prepared for

Rochester Gas and Electric
89 East Avenue
Rochester, N. Y. 14649

8211290439 821122
PDR ADCK 05000244
P PDR

TABLE OF CONTENTS

<u>SECTION</u>	<u>PAGE</u>
ABSTRACT	i
LIST OF TABLES	ii
LIST OF FIGURES	iii
 I. INTRODUCTION	 1
 II. ANALYSIS OF PLANT RESPONSE	 2
II.1 Systems Analysis Code	2
II.2 Plant Data	4
II.3 Initial Leak Rate	5
II.4 Pre-trip System Response	7
II.5 Post-trip System Response	16
5.1 Primary System Pressure	21
5.2 Reactor Coolant Flow	28
5.3 Reactor Coolant Temperature	33
5.4 Pressurizer Level	52
5.5 Break Flow	55
5.6 Reactor Coolant Voiding	58
5.7 Steam Generator Overfill	60
II.6 Long Term Recovery	62
 III. SUMMARY AND CONCLUSIONS	 65
 REFERENCES	 67
 Appendix A: Initial Leak Rate Calculation	 68
 Appendix B: Best Estimate Break Flow Model	 70
 Appendix C: Calculation of Upper Head Void Size	 74

ABSTRACT

Plant response to the January 25, 1982 steam generator tube failure at the R. E. Ginna nuclear power plant has been analyzed using the computer code LOFTRAN to provide additional insight into reactor coolant voiding, natural circulation loop flows, and primary-to-secondary leakage during the event. Results are compared to available plant data.



LIST OF TABLES

TABLE II.1-1	SEQUENCE OF MAJOR EVENTS
TABLE II.3-1	PRE-TRIP PRESSURIZER LEVEL
TABLE II.5.1-1.	SEQUENCE OF PORV OPERATION
TABLE C-1	UPPER HEAD VOID SIZE

LIST OF FIGURES

FIGURE II.1-1	GINNA SAFETY INJECTION CAPACITY
FIGURE II.4-1	PRE-TRIP NORMALIZED CORE POWER
FIGURE II.4-2	PRE-TRIP SECONDARY SYSTEM PRESSURE
FIGURE II.4-3	PRE-TRIP PRESSURIZER PRESSURE
FIGURE II.4-4	PRE-TRIP PRESSURIZER LEVEL
FIGURE II.4-5	PRE-TRIP AVERAGE RCS COOLANT TEMPERATURE
FIGURE II.4-6	PRE-TRIP PRESSURIZER PRESSURE: CONSTANT COOLANT TEMPERATURE
FIGURE II.4-7	PRE-TRIP PRESSURIZER LEVEL: CONSTANT COOLANT TEMPERATURE
FIGURE II.5-1	NORMALIZED PRE-TRIP STEAM FLOW
FIGURE II.5.2	NORMALIZED PRE-TRIP FEEDWATER FLOW
FIGURE II.5.3	INTACT STEAM GENERATOR PRESSURE
FIGURE II.5-4	INTACT LOOP COLD LEG TEMPERATURE
FIGURE II.5.1-1	REACTOR COOLANT SYSTEM PRESSURE
FIGURE II.5.1-2	PRIMARY-TO-SECONDARY LEAKAGE AND TOTAL SAFETY INJECTION FLOW
FIGURE II.5.1-3	PRESSURIZER WATER VOLUME
FIGURE II.5.1-4	UPPER HEAD FLUID MASS
FIGURE II.5.2-1	VOLUMETRIC LOOP FLOW RATES
FIGURE II.5.2.1-1	COMPARISON OF "MIXED TEMPERATURE" REVERSE FLOW THROUGH FAULTED LOOP AND BREAK FLOW FROM THE SG OUTLET PLENUM
FIGURE II.5.2.1-2	FAULTED LOOP COLD LEG INLET AND OUTLET FLOWS
FIGURE II.5.3-1	POST-TRIP REACTOR COOLANT TEMPERATURES
FIGURE II.5.3.1-1	STEAM DUMP VALVE OPERATION AND AFW FLOW DURING COOLDOWN OF THE RCS
FIGURE II.5.3.1-2	GINNA CORE EXIT AND INTACT LOOP COLD LEG TEMPERATURES
FIGURE II.5.3.2-1	COMPARISON OF INTACT AND FAULTED LOOP COLD LEG TEMPERATURES FOLLOWING REACTOR TRIP
FIGURE II.5.3.2-2	FAULTED LOOP COLD LEG TEMPERATURES
FIGURE II.5.3.2-3	MIXING VOLUME FOR VESSEL DOWNCOMER TEMPERATURE CALCULATION
FIGURE II.5.3.2-4	MIXING VOLUME LOOP FLOW AND SAFETY INJECTION FLOW
FIGURE II.5.3.2-5	MIXING VOLUME FLOW TEMPERATURES
FIGURE II.5.3.2-6	BEST ESTIMATE REACTOR VESSEL DOWNCOMER TEMPERATURE
FIGURE II.5.3.3-1	CORE EXIT FLUID TEMPERATURE



LIST OF FIGURES (Cont.)

FIGURE II.5.3.4-1	BREAK FLOW FROM SG INLET AND OUTLET PLENUMS
FIGURE II.5.3.4-2	LOFTRAN FAULTED LOOP HOT LEG TEMPERATURE
FIGURE II.5.3.5-1	FAULTED SG TUBE BUNDLE FLUID TEMPERATURE
FIGURE II.5.3.6-1	POST-TRIP UPPER HEAD FLUID TEMPERATURE
FIGURE II.5.3.6-2	LOFTRAN UPPER HEAD FLUID TEMPERATURE
FIGURE II.5.4-1	PRESSURIZER LEVEL INDICATION
FIGURE II.5.5-1	LOFTRAN AND BEST ESTIMATE BREAK FLOWS
FIGURE II.5.5-2	FAULTED STEAM GENERATOR PRESSURE
FIGURE II.5.7-1	FAULTED STEAM GENERATOR WATER VOLUME
FIGURE II.6-1	RCS AND FAULTED STEAM GENERATOR PRESSURES
FIGURE II.6-2	LONG TERM PRESSURIZER LEVEL RESPONSE
FIGURE B-1	SG TUBE RUPTURE FLOW MODEL DIAGRAM
FIGURE C-1	UPPER HEAD VOIDING ILLUSTRATION

I. INTRODUCTION

At the request of Rochester Gas and Electric (RGE), Westinghouse has analyzed the January 25, 1982 steam generator tube rupture event at the R. E. Ginna nuclear power plant. The principle objective of this effort is to supplement the existing data base^(1,2) to provide a more thorough understanding of the plant response and actual sequence of events. Of particular interest are voiding of the reactor coolant, natural circulation loop flow behavior, and primary-to-secondary leakage. The LOFTRAN⁽³⁾ computer code was used for these analyses. A number of auxiliary calculations are also described which complement LOFTRAN by providing more detailed modelling of localized effects.

The plant response to the steam generator tube failure and subsequent recovery actions is presented for three different phases of the event. The pre-trip data record provides information for estimating the initial leak rate and extent of tube failure. LOFTRAN analysis of this period extrapolates this data to determine the approximate time of tube failure and history of tube leakage. Following reactor trip, several automatic protection systems were actuated in rapid succession and a sequence of emergency recovery actions was initiated to mitigate the consequences of the accident. This emergency recovery period culminated in termination of safety injection. The plant response to the automatic protection systems and recovery actions during this phase was also investigated using LOFTRAN. Finally, the long term plant response and additional leakage into the faulted steam generator after termination of safety injection is discussed.

A brief discussion of LOFTRAN modelling is presented. Several limitations are identified which are significant when applied to the Ginna event and must be considered when evaluating the analysis results. These results are compared to the available plant data in the following sections.



II. ANALYSIS OF PLANT RESPONSE

II.1 Systems Analysis Code

LOFTRAN is a fast running, digital computer code developed to simulate transient behavior in Westinghouse pressurized water reactors. The program models neutron kinetics as well as control and protection systems on the primary and secondary systems. The most significant of the protection systems, the Emergency Core Cooling System (ECCS) and the Auxiliary Feedwater (AFW) system, are described below.

The ECCS was represented by the combined capacity of three high head safety injection pumps shown in Figure II.1-1. Safety injection initiated automatically on low pressurizer pressure of 1740 psia and was assumed equally distributed between loops. The suction of these pumps was initially aligned to two boric acid tanks (BAT) containing approximately 4320 gallons of borated water at 140 F. On low level, suction was automatically re-aligned to the Refueling Water Storage Tank (RWST) which contained cooler water. In the analyses presented, 60 F water from the RWST was assumed to be injected through the BAT containing a 140 F boric acid solution. Reactor coolant makeup from the normal charging pumps was also simulated with suction from these pumps aligned to the RWST. Charging flow is discussed on a case by case basis in the following sections.

Two motor driven AFW pumps automatically started on a safety injection signal. Each motor driven pump provided approximately 200 GPM of water from the Condensate Storage Tank (CST) and delivered to one of the two steam generators. One steam driven AFW pump started automatically on low-low steam generator level. The steam driven pump supplied a total of 400 GPM which was available to both steam generators. AFW pump operation was simulated as described in the sequence of events in Table II.1-1. A purge volume of 200 ft³ containing normal feedwater was also simulated. This represented a delay of approximately 4 minutes before cold CST water entered the tube region of the intact steam generator.

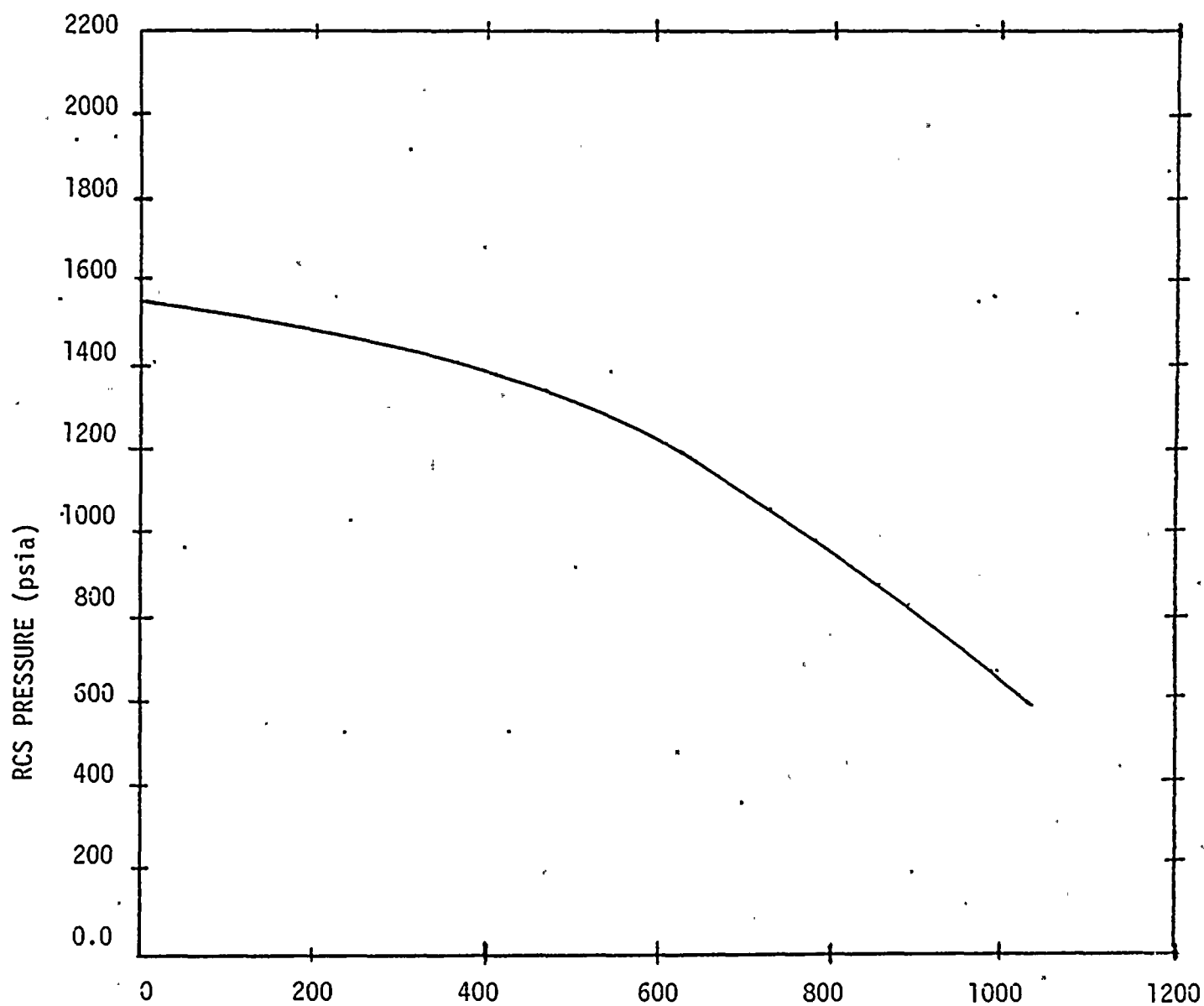


FIGURE II.1-1. GINNA SAFETY INJECTION CAPACITY.

Previous LOFTRAN analyses have simulated the Prairie Island tube failure event well⁽⁴⁾. However, LOFTRAN is somewhat limited by the modelling of the upper head region, steam generator secondary side, and primary-to-secondary leakage. The upper head modelling assumes homogeneous, thermodynamic equilibrium conditions during flashing of the upper head fluid. Refilling of the upper head region is artificially constrained to simulate non-equilibrium behavior. Effectively, the upper head region can not refill during natural circulation flow. Furthermore, flow into the upper head region via guide tubes is not represented. Consequently, the calculated upper head fluid temperature may be unrealistic for plants with smaller upper head "spray" nozzles, such as Ginna. LOFTRAN is also limited by the homogeneous, saturated conditions within the secondary which promotes an unrealistically lethargic tube bundle region temperature response to AFW flow and secondary-to-primary heat transfer. In addition, these conditions result in artificially reduced steam generator pressures when no steam flow occurs since the steam is effectively assumed to be in contact with the steam generator tubes. The break flow calculations within LOFTRAN are based on conservative, i.e. maximum flow, critical flow correlations. The accuracy of these correlations in predicting critical flow trends over a wide range of system conditions is uncertain. Furthermore, the break flow modelling does not consider flow resistance through the failed tube, or fluid temperature variations between the steam generator inlet and outlet plenums. Finally, LOFTRAN does not permit reverse flow to occur in the coolant loop to which the pressurizer is connected. For the results presented, the pressurizer was modelled on the intact loop although during the Ginna event the pressurizer was on the faulted loop. This may result in unrealistic loop flows during refilling of the pressurizer.

II.2 Plant Data

The plant data which forms the basis of the analyses that follow was obtained from various computer records, strip charts of system parameters, and the sequence of events as reconstructed by RGE. The Ginna plant computer is a real time central processing unit which stores selected plant parameters for use during normal operations. Several peripheral devices serviced by this central unit provide the principal data for post-accident analyses which includes primary and secondary pressures, reactor coolant temperatures, and



pressurizer level. These devices include a pre-trip event recorder, a TI-7000 teletype terminal, an alarm typewriter, and a log typewriter. Communications with RGE personnel supplemented this data and provided additional insight into the event. The sequence of operator actions was extracted from the sequence of events provided by RGE and the chronology of plant alarms, when possible. The major events are presented in Table II.1-1. Comprehensive plant data and the complete sequence of events is available in reference 1.

II.3 Initial Leak Rate

The pre-trip pressurizer level response to the loss of reactor coolant was analyzed to estimate the initial primary-to-secondary leak rate. Rapid variations in reactor coolant temperature due to turbine runback and automatic steam dump to the condenser tended to mask the inventory loss. However, an average leak rate prior to trip was estimated by considering the indicated pressurizer level response between times of constant average coolant temperature. Since the coolant temperatures at these times were approximately the same, the effect of the turbine runback on this calculation was minimized. The pre-trip pressurizer level, adjusted for instrumentation calibration, is presented in Table II.3-1:

Based on discussions with RGE personnel, two charging pumps were operating prior to the tube failure, one in manual and the other in automatic. Each pump was delivering approximately 25 GPM of flow. Total letdown, including reactor coolant pump seal leakoff, was 50 GPM. Following tube failure, one charging pump automatically increased to the maximum capacity of 60 GPM as pressurizer level decreased. Although a third charging pump was manually started approximately 40 seconds before reactor trip, 9:27:30, it would have provided little flow before trip. Consequently, the normal charging system was supplying an excess of approximately 35 GPM during this period.

The average pre-trip leak rate was estimated to be 573 GPM (Appendix A). An initial leak rate of 634 GPM was calculated by extrapolating the average leak rate to the initial system conditions based on subcooled critical⁽⁵⁾ flow through the failed tube. An effective break area of 0.0033 ft² was determined by proportioning the critical flow rate as calculated by LOFTRAN for the initial system conditions to match the initial leak rate.



TABLE II.3-1 PRE-TRIP PRESSURIZER LEVEL

Time (A.M.)	Indicated Level (% span)	Adjusted* Level (% span)	Tavg (°F)
9:26:18	32.5	32.7	571.2
9:26:26	30.6	31.0	571.2
9:26:34	30.5	30.8	571.9
9:26:42	30.5	30.9	573.2
9:26:58	30.2	30.7	575.2
9:27:06	30.2	30.5	576.4
9:27:14	30.2	30.6	576.8
9:27:22	28.9	29.4	576.1
9:27:30	26.2	26.9	575.3
9:27:38	20.8	22.0	574.5
9:27:46	17.9	19.5	573.4
9:27:54	14.8	16.8	572.4
9:28:02	11.7	14.1	571.4
9:28:10	9.0	11.9	570.1

*See Appendix A



II.4 Pre-Trip System Response

The first indications of abnormal conditions were recorded at approximately 9:25 when a number of alarms sounded nearly simultaneously. These included low pressurizer pressure, low pressurizer level, condenser air ejector radiation, and B steam generator level deviation alarms. The alarm recorder indicates that the low pressurizer pressure alarm sounded first. System conditions were normal at 9:22 with no apparent symptoms of primary-to-secondary leakage.

The reactor coolant system pressure and temperature prior to reactor trip were analyzed using normalized core power, Figure II.4-1, and secondary pressure, Figure II.4-2, data as forcing functions for the calculations. Alternative secondary side boundary conditions were also considered as forcing functions for the pre-trip calculations, including normalized steam and feedwater flows. Although these produced reasonable results, the instrument uncertainties and response times were not as conducive as secondary pressure to pre-trip analysis. The pressurizer pressure and level responses calculated using LOFTRAN agreed very well with plant data as illustrated in Figures II.4-3 and II.4-4, respectively. Extrapolation of this data with an initial leak rate of 634 GPM suggests that tube failure occurred at 9:25:10 (ϕ min). The calculated pressure at the actual time of reactor trip was approximately 30 PSI greater than indicated. The average reactor coolant temperature is compared with pre-trip data in Figure II.4-5. The increase in temperature due to turbine runback momentarily masked the decrease in primary coolant inventory. Similarly, when the steam dump valves opened, the associated cooldown enhanced reactor coolant system depressurization. Figures II.4-6 and II.4-7 illustrate the predicted pressurizer pressure and level responses when reactor coolant temperature was maintained constant. As demonstrated, the pressure and level responses are significantly affected by coolant temperature trends.



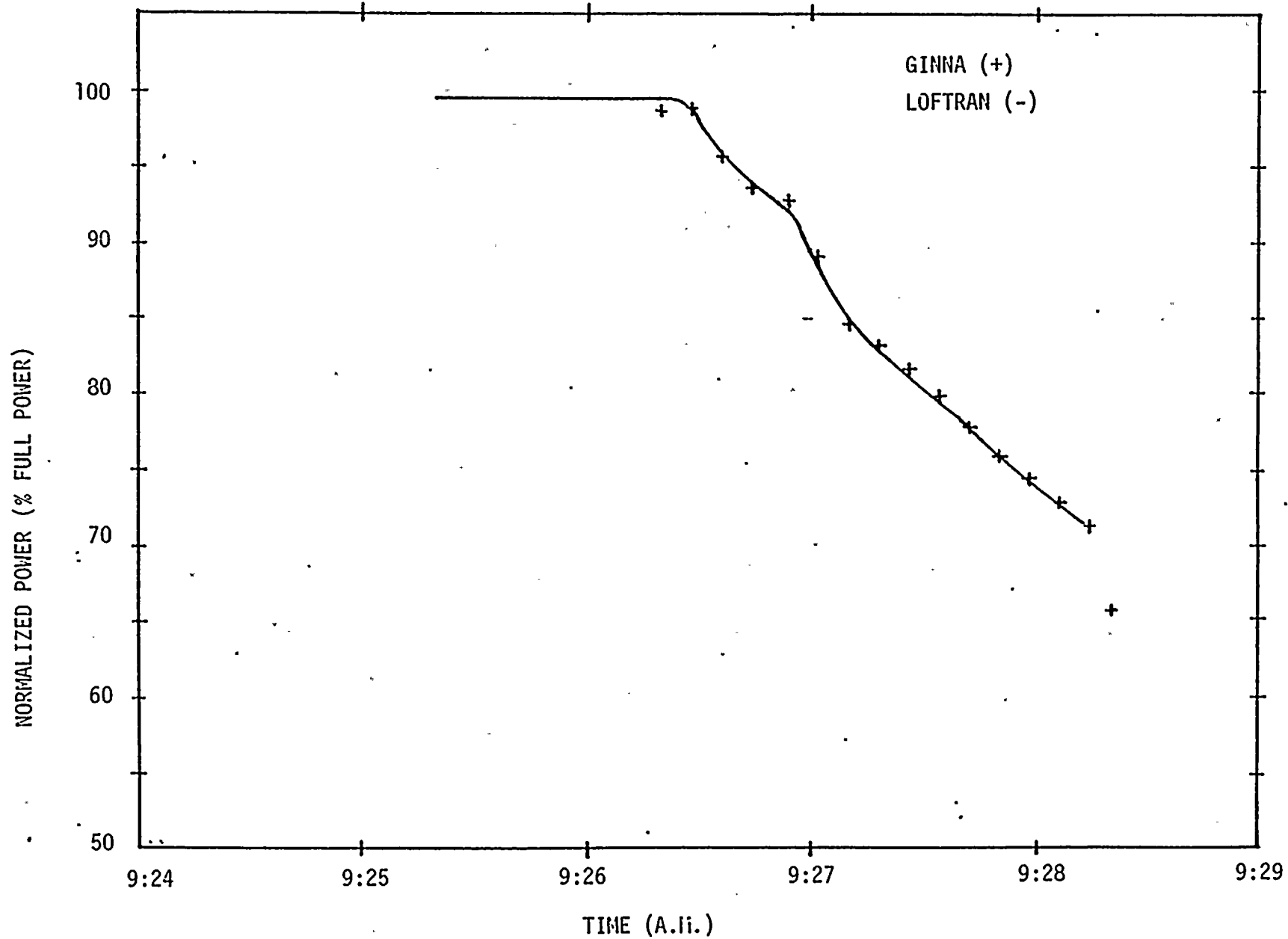


FIGURE II.4-1. PRE-TRIP NORMALIZED CORE POWER.



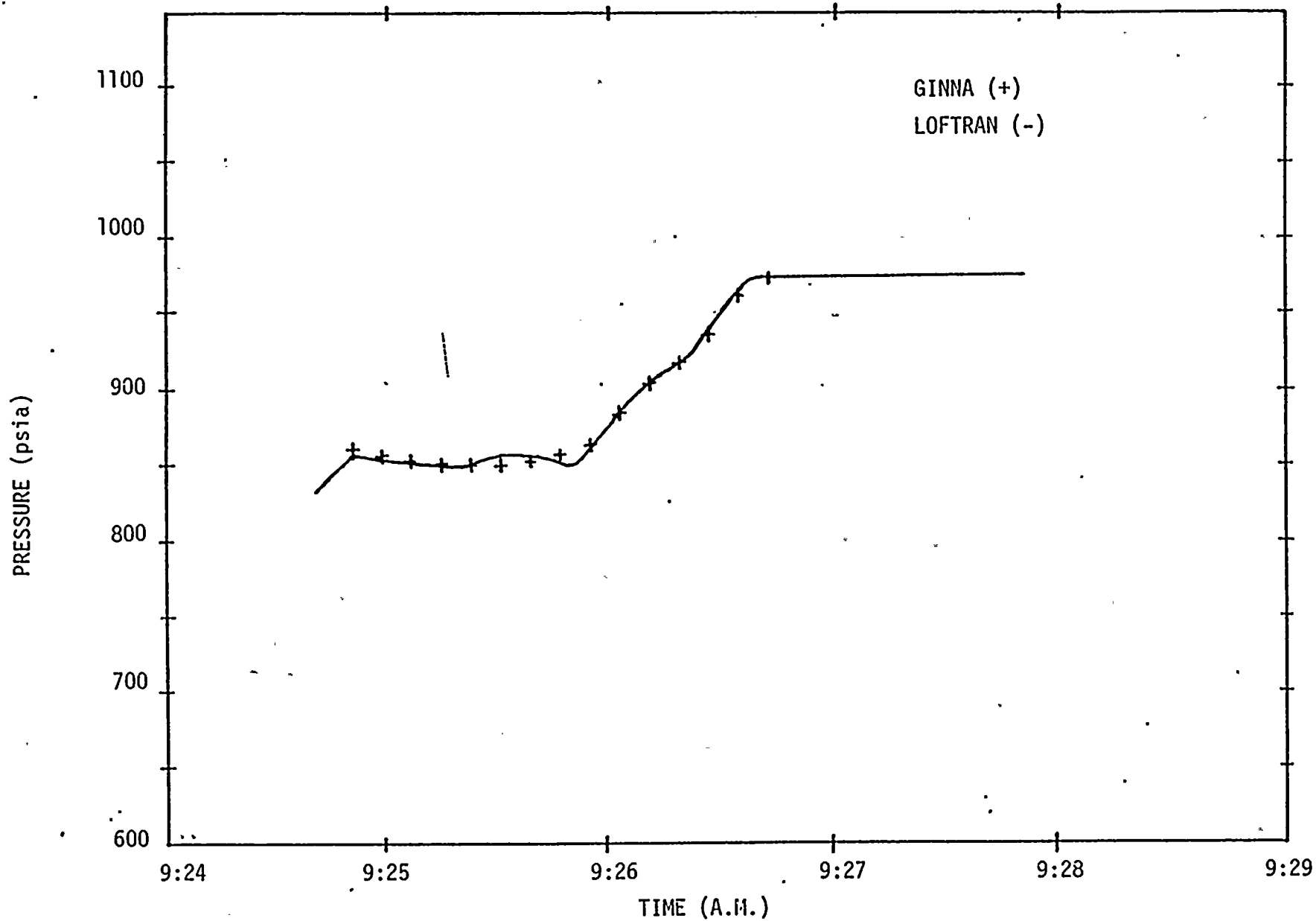


FIGURE II.4-2. PRE-TRIP SECONDARY SYSTEM PRESSURE

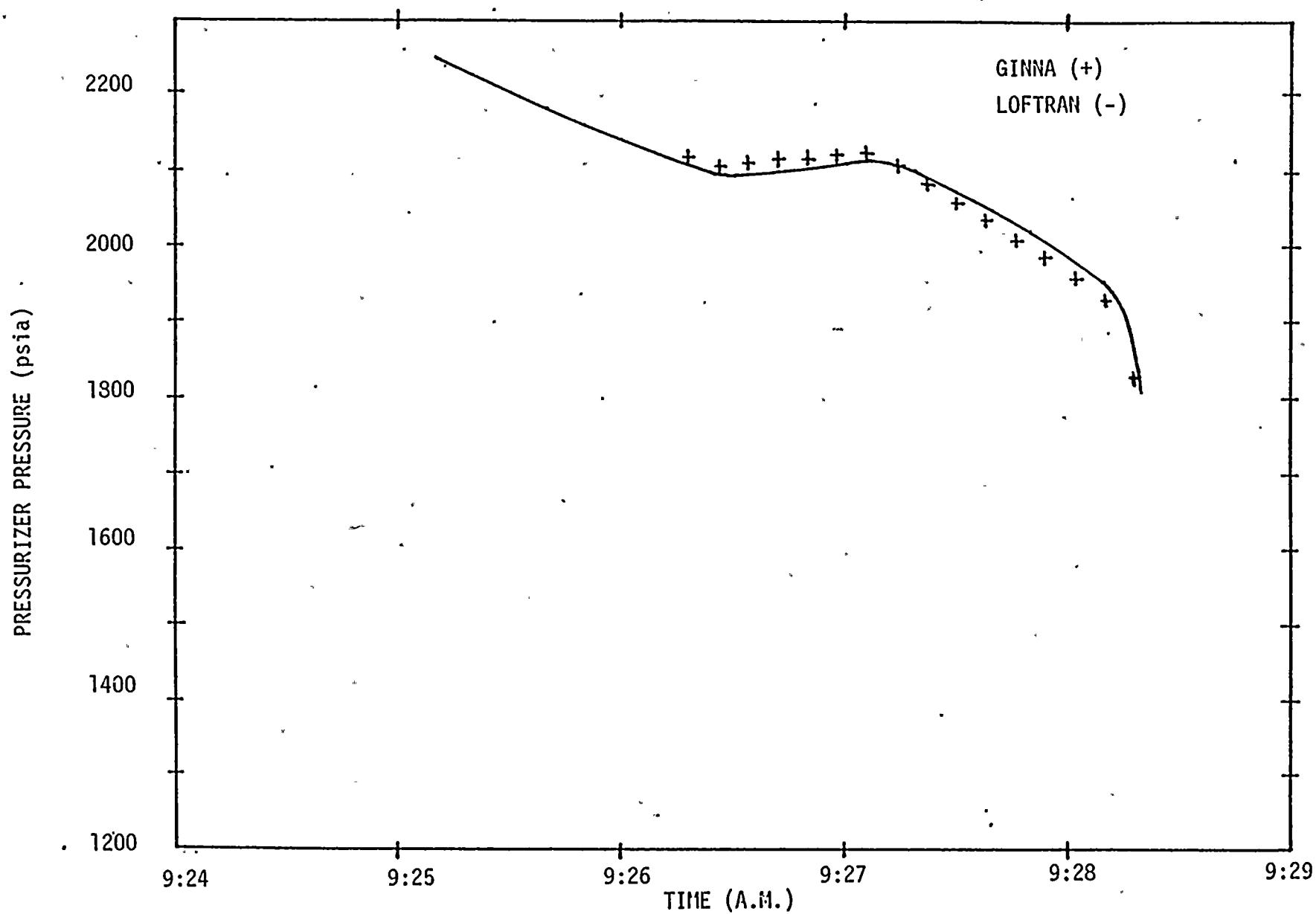


FIGURE II.4-3. PRE-TRIP PRESSURIZER PRESSURE.

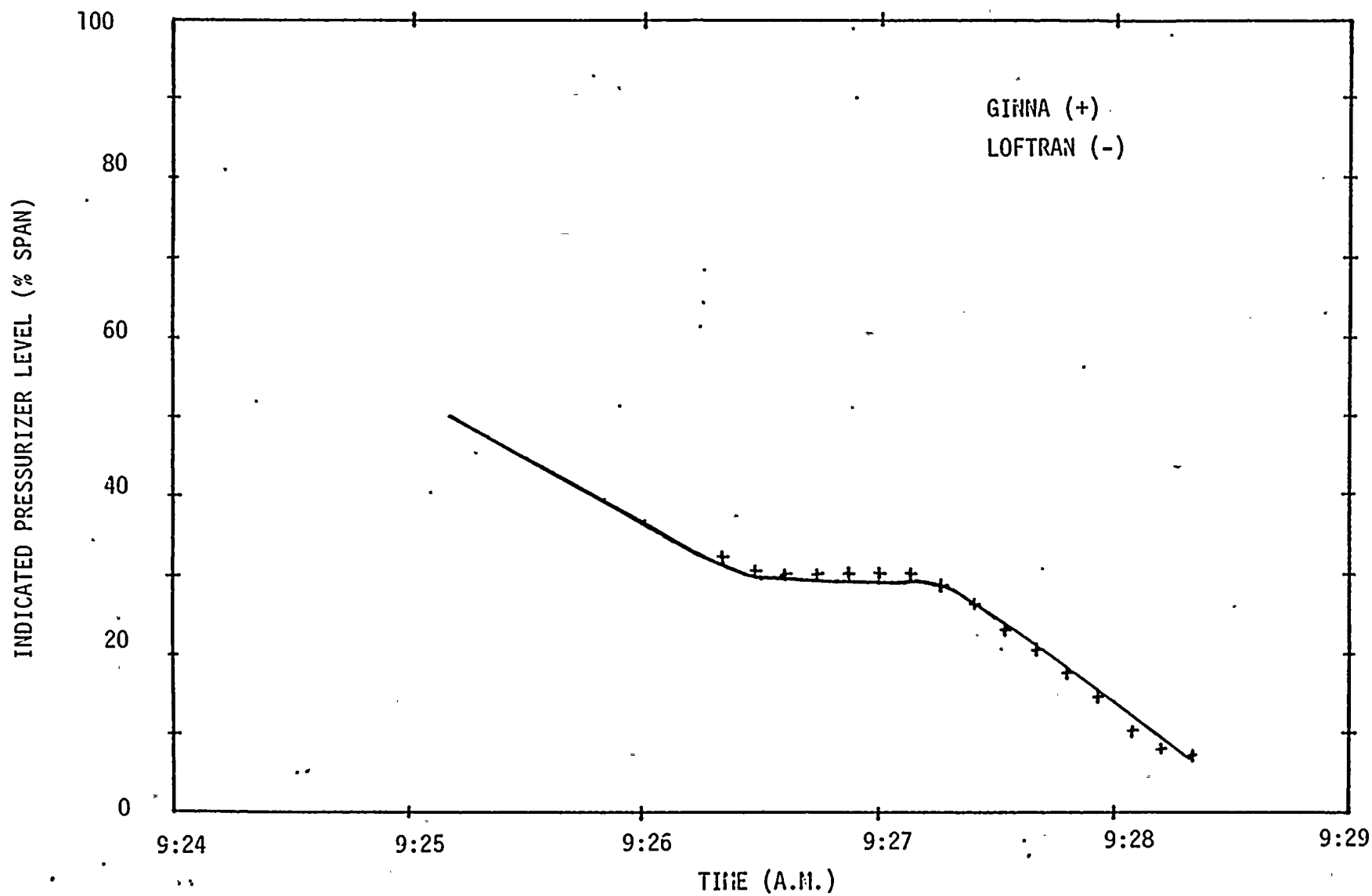


FIGURE II.4-4. PRE-TRIP PRESSURIZER LEVEL.

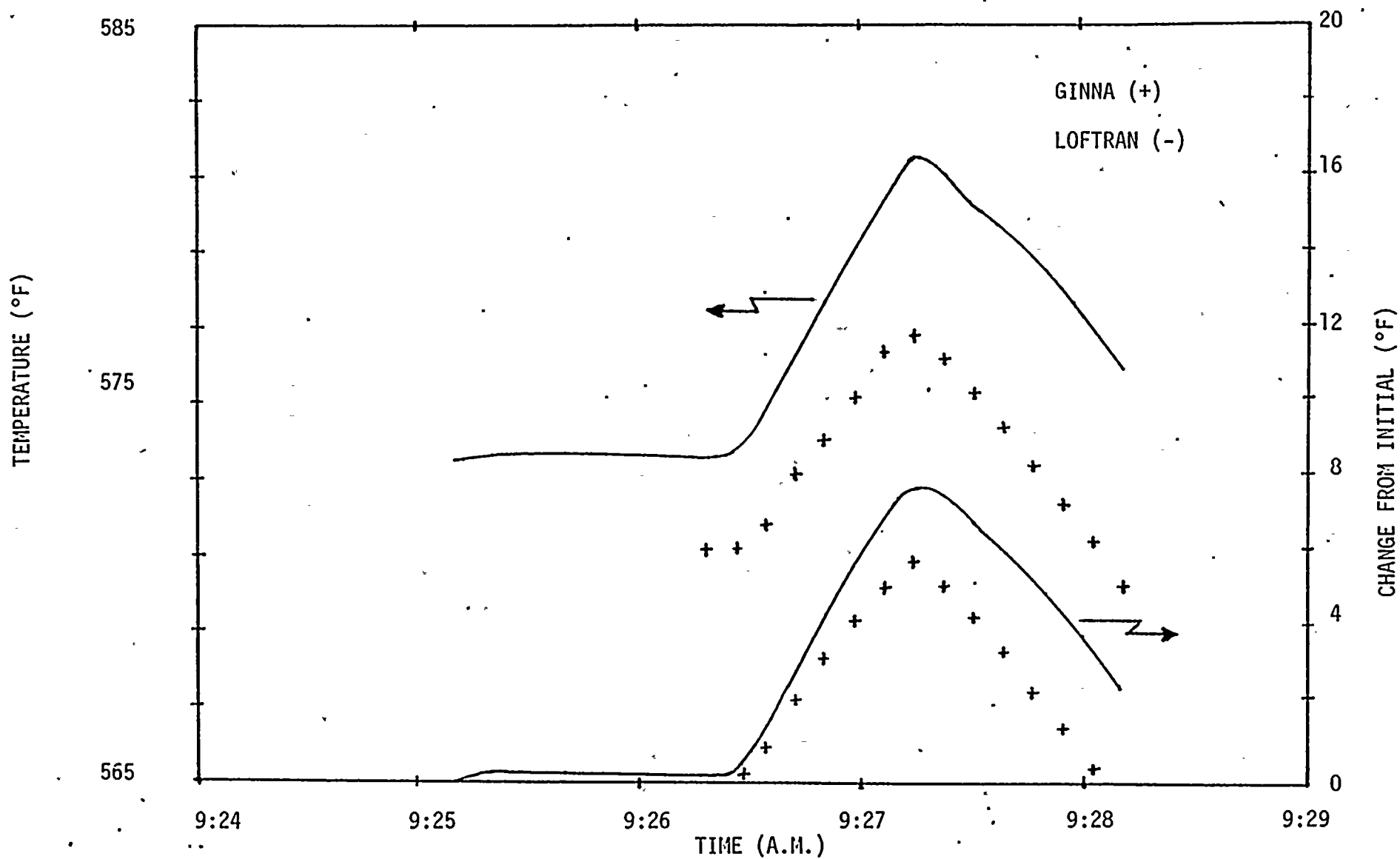


FIGURE II.4-5. PRE-TRIP AVERAGE RCS COOLANT TEMPERATURE



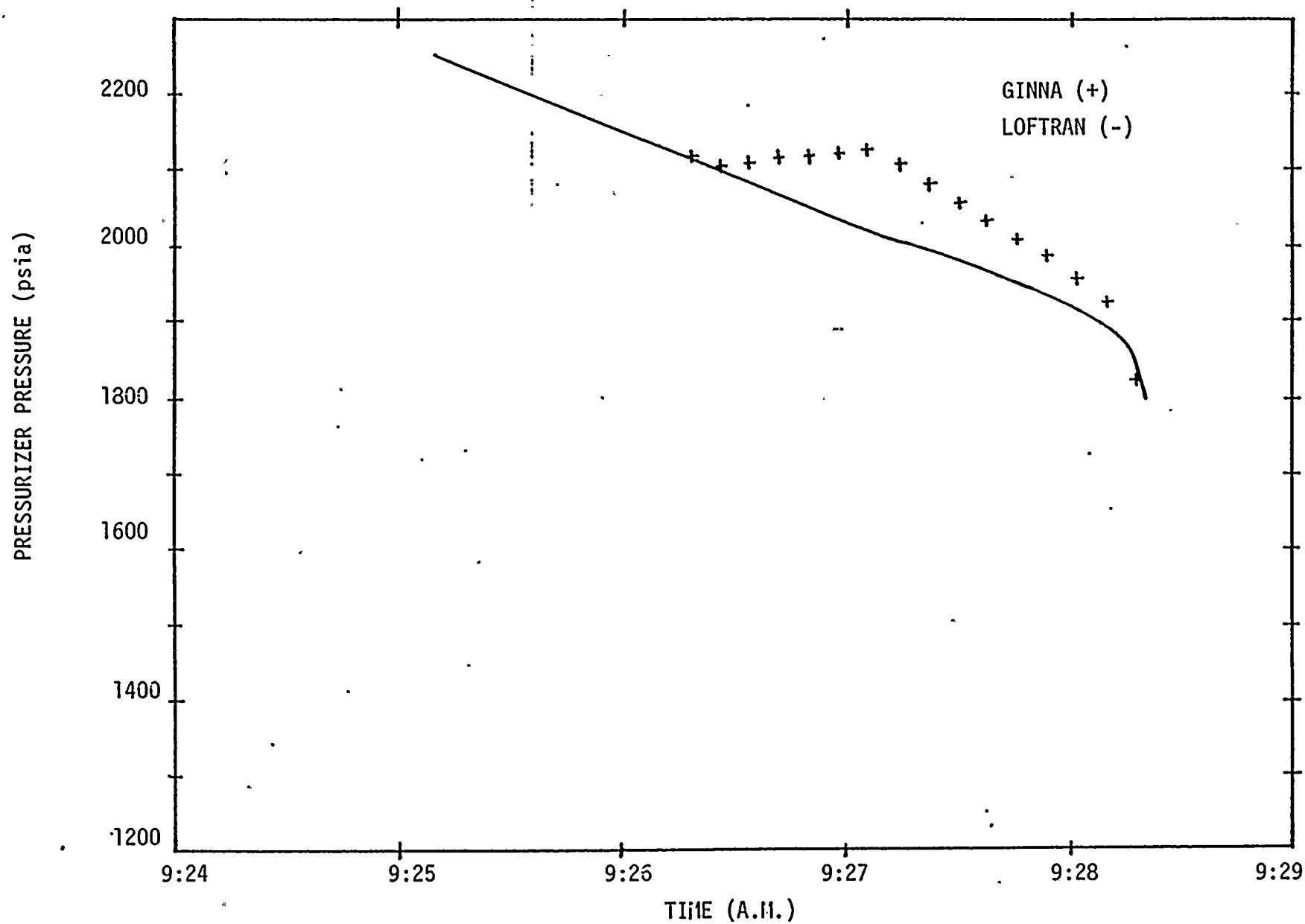


FIGURE II.4-6. PRE-TRIP PRESSURIZER PRESSURE: CONSTANT COOLANT TEMPERATURE

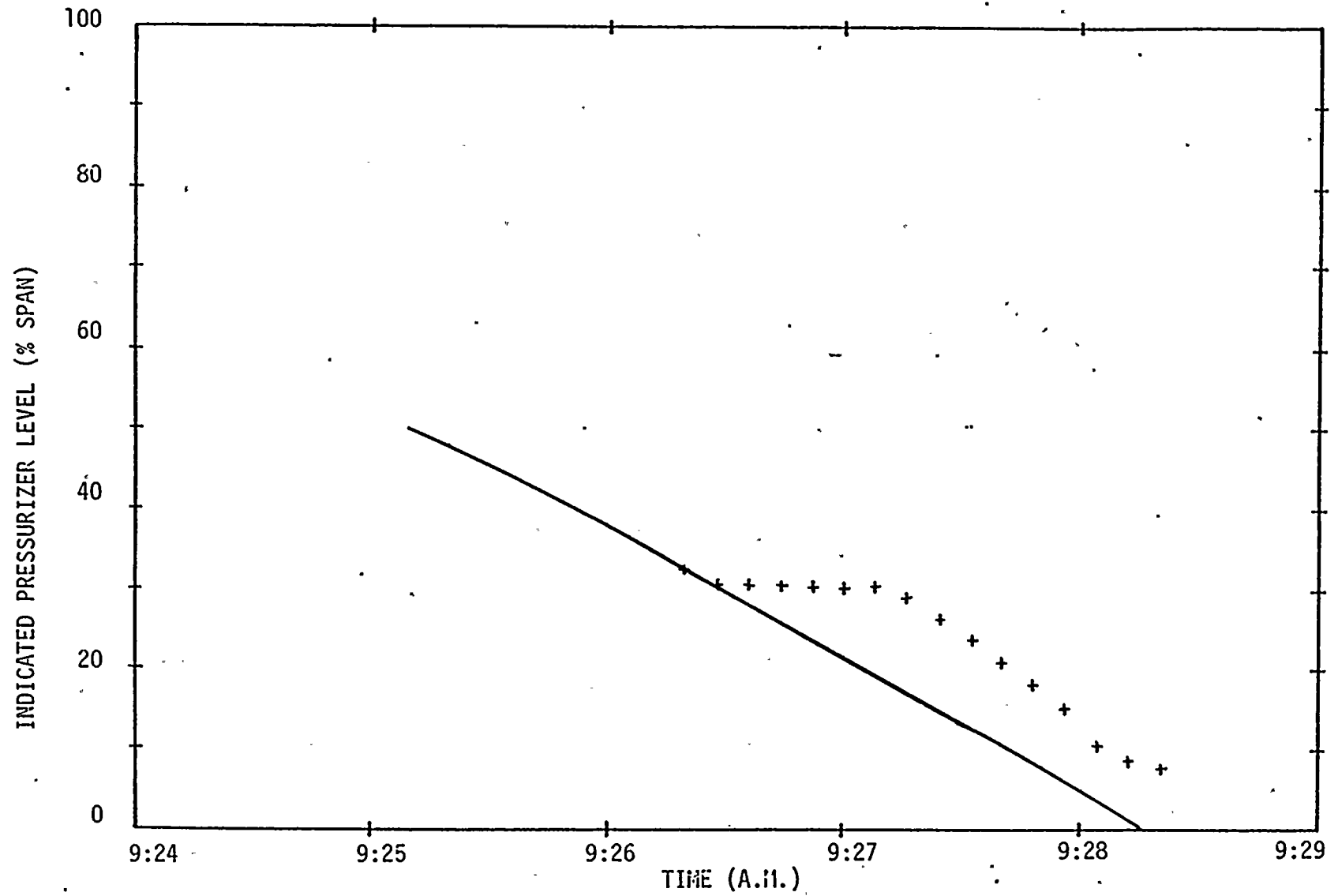


FIGURE II.4-7. PRE-TRIP PRESSURIZER LEVEL: CONSTANT COOLANT TEMPERATURE



TABLE II.1-1: SEQUENCE OF MAJOR EVENTS

Event	Manual (O)	TIME (Sec)	
	Automatic (A)	Actual	Simulated
Tube Failure	-	0	0
Turbine Runback	0	78	70
Automatic Steam Dump	A	110	118
Reactor Trip	A	182	182
Safety Injection Signal	A	190	198
Feedwater Isolation	A	192	198
Auxiliary Feedwater Start	A	220	239
Reactor Coolant Pump Trip	0	230	246
B Motor Driven AFW Pump Off	0	410 ⁽¹⁾	410
Manual Steam Dump	0	770 ⁽¹⁾	530 ⁽²⁾
B Loop MSIV Closed	0	890 ⁽¹⁾	530 ⁽²⁾
AFW Throttled A SG	0	950 ⁽¹⁾	950
AFW Stopped to B SG	0	1250 ⁽¹⁾	1250
Charging Pumps Started	0	2330 ⁽¹⁾	2330
PORV Cycled	0	2540	2540
SI Terminated	0	4310 ⁽¹⁾	4310

(1) These times are approximate and typically may vary by up to 60 seconds.

(2) See section II.5 for a discussion on the simulation of these events.



II.5 Post-Trip System Response

Continued leakage of primary coolant in combination with rapid cooldown of the reactor coolant system following actuation of the steam dump system, caused an automatic reactor trip on low pressurizer pressure. Primary system pressure decreased rapidly as power generation was abated, and several supporting systems, including the ECCS and AFW system, started in relatively rapid succession. A series of operator actions commenced in accordance with emergency response procedures to recover the plant to a safe shutdown condition. The plant response to these systems and operator actions was analyzed using LOFTRAN and the results are presented in the following sections. These analyses were limited to the time from initial failure until 10:40 (75 min), shortly after termination of safety injection. Beyond this time, LOFTRAN analysis was not appropriate because of the homogeneous, equilibrium secondary side modelling. Additional leakage into the faulted steam generator was estimated from plant data to determine the mass discharged from the steam generator after overfill.

The steam generator tube failure occurred in the B loop during the Ginna event. Consequently, faulted loop and B loop are synonymous in the following sections. Similarly, intact loop and A loop are used interchangeably. However, A loop and B loop designations generally refer to plant data, and intact and faulted to LOFTRAN calculations.

For these analyses, normalized steam flow, Figure II.5-1, and feedwater flow, Figure II.5-2, from plant data were used prior to trip as forcing functions for the calculations. This provided additional flexibility in modelling subsequent operator actions with LOFTRAN. The LOFTRAN analysis results, which include an adjustment to the input steam flow to account for increased secondary pressure, are also shown for comparison. After reactor trip, the intact steam generator pressure was controlled to reproduce the indicated loop A cold leg temperatures. The intact steam generator pressure input to LOFTRAN is compared to plant data in Figure II.5-3. Figure II.5-4 shows the calculated and measured intact loop fluid temperatures at the cold leg inlet. Note that loop A cold leg fluid was subcooled at the A loop steam generator pressure between approximately 9:32 (7 min) and 9:41 (16 min). Because of the homogeneous equilibrium secondary side modelling with LOFTRAN, such subcooling

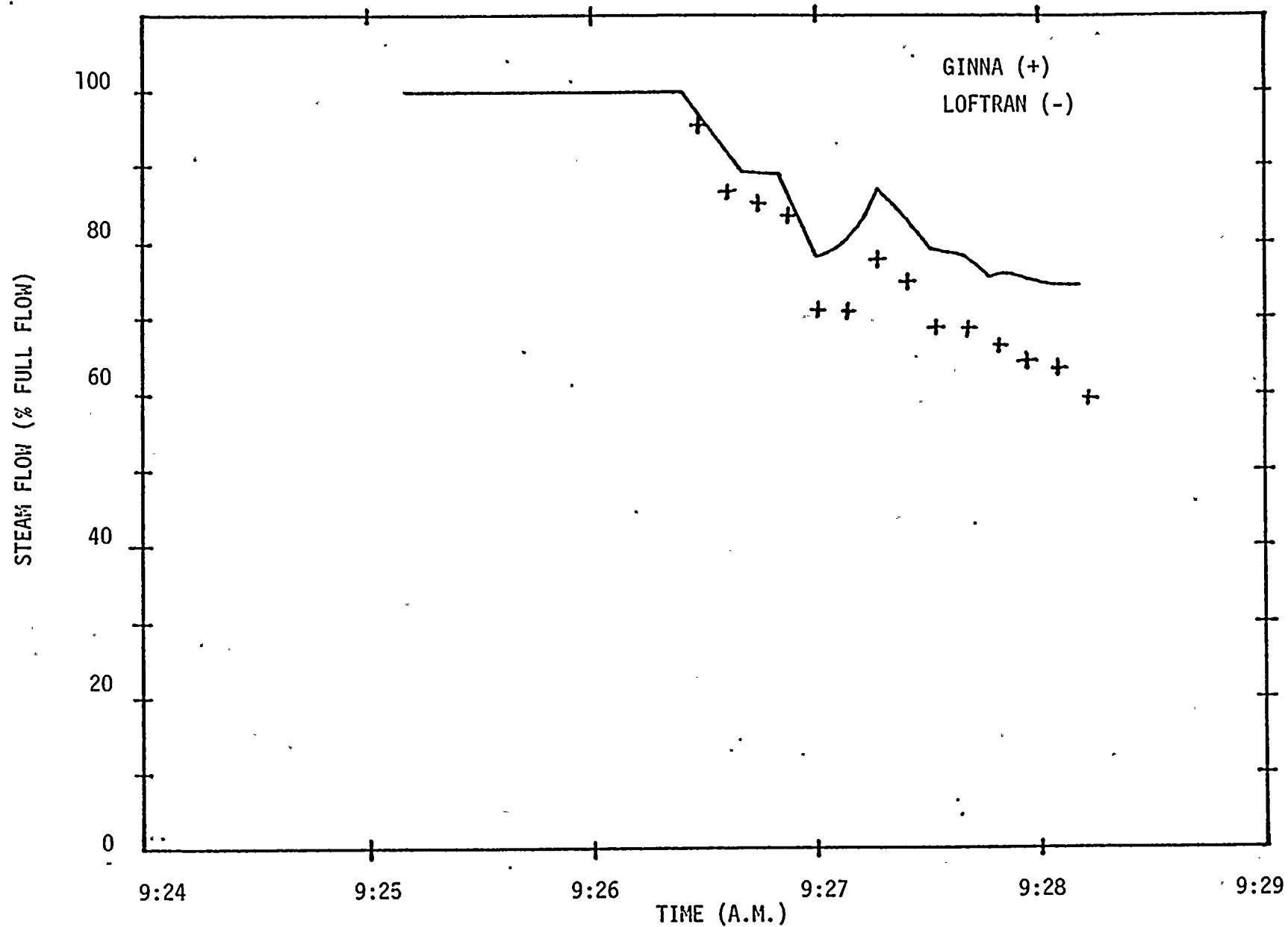


FIGURE II.5-1. NORMALIZED PRE-TRIP STEAM FLOW.



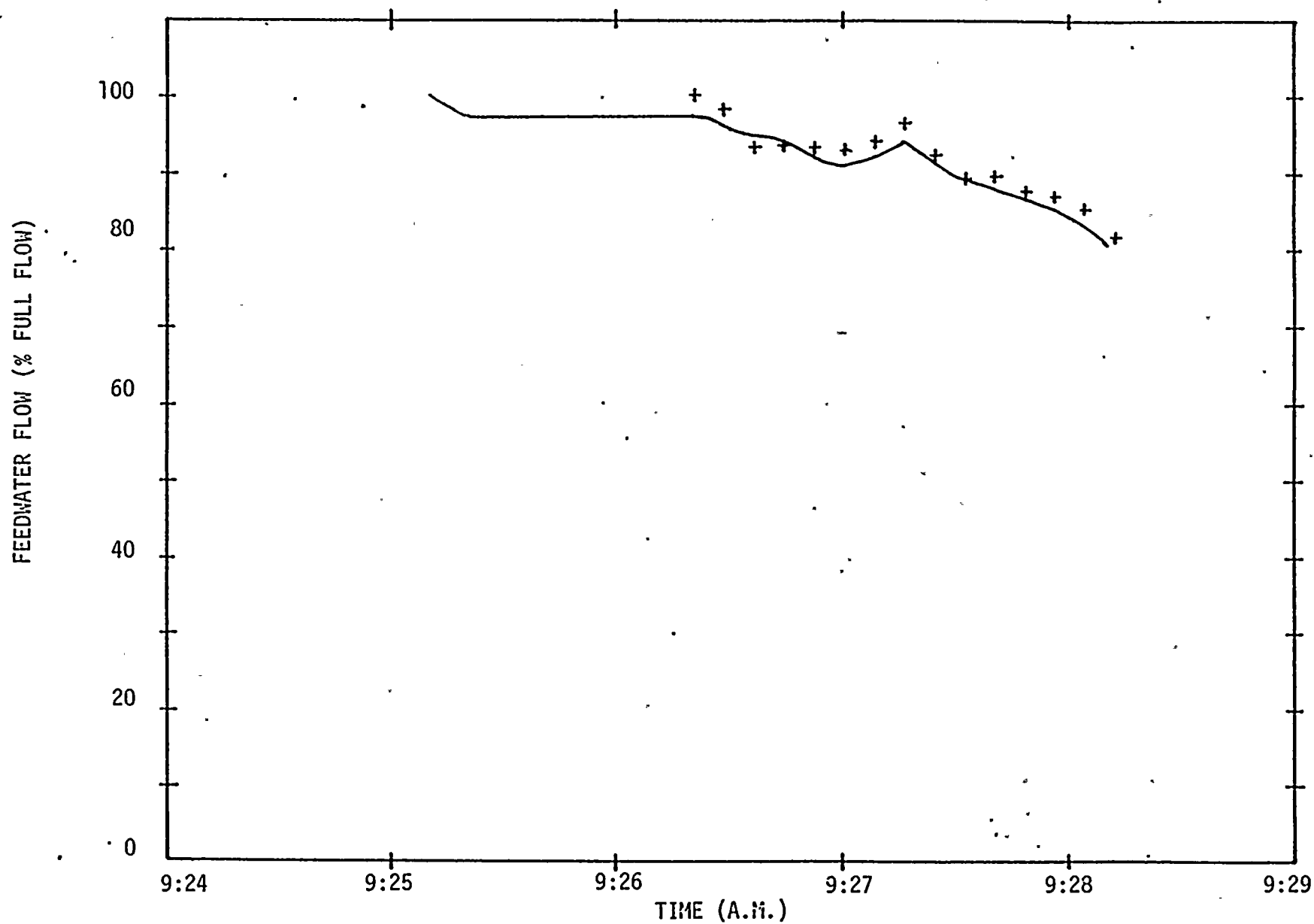


FIGURE II.5-2. NORMALIZED PRE-TRIP FEEDWATER FLOW.



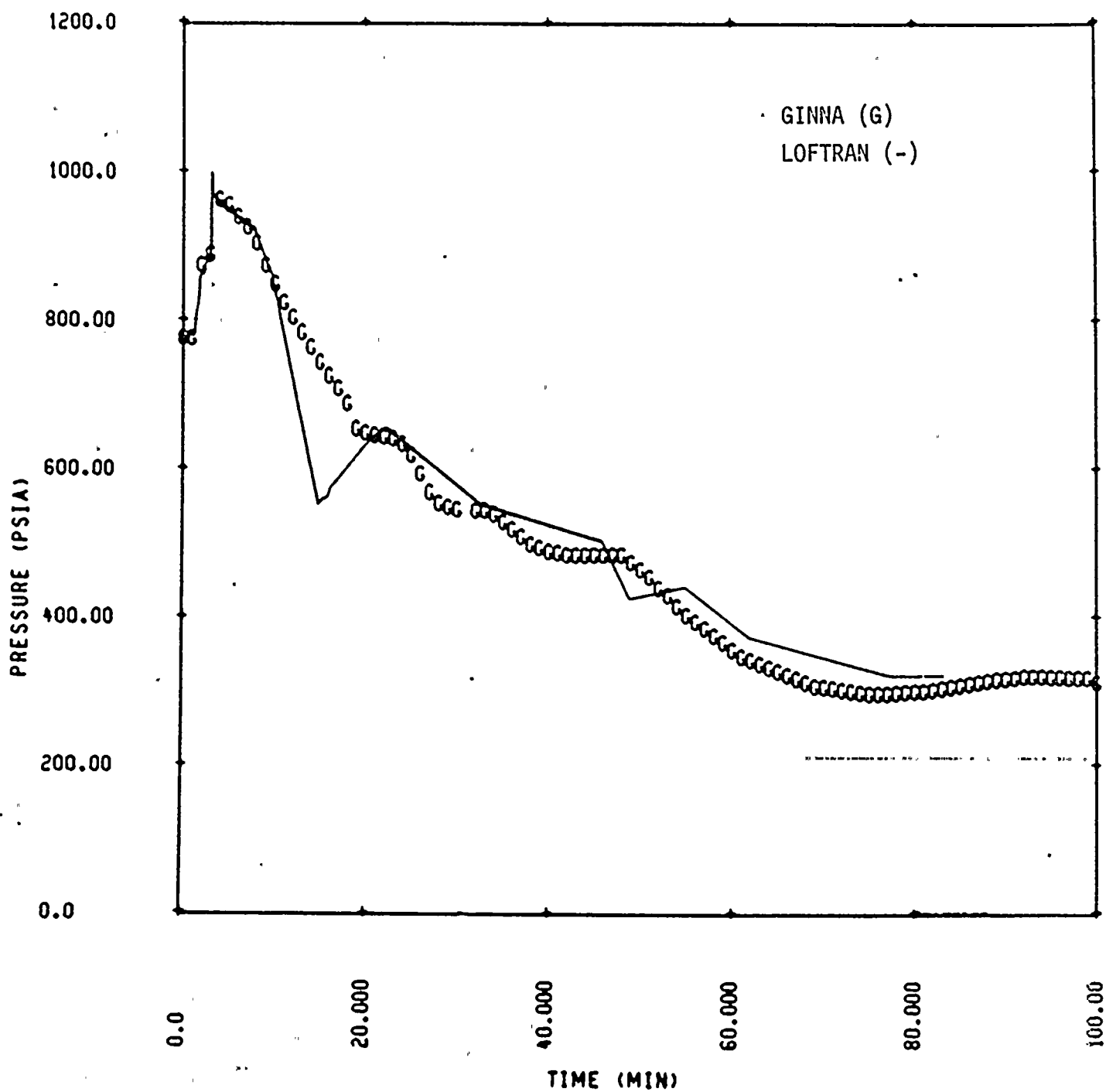


FIGURE II.5-3. INTACT STEAM GENERATOR PRESSURE.



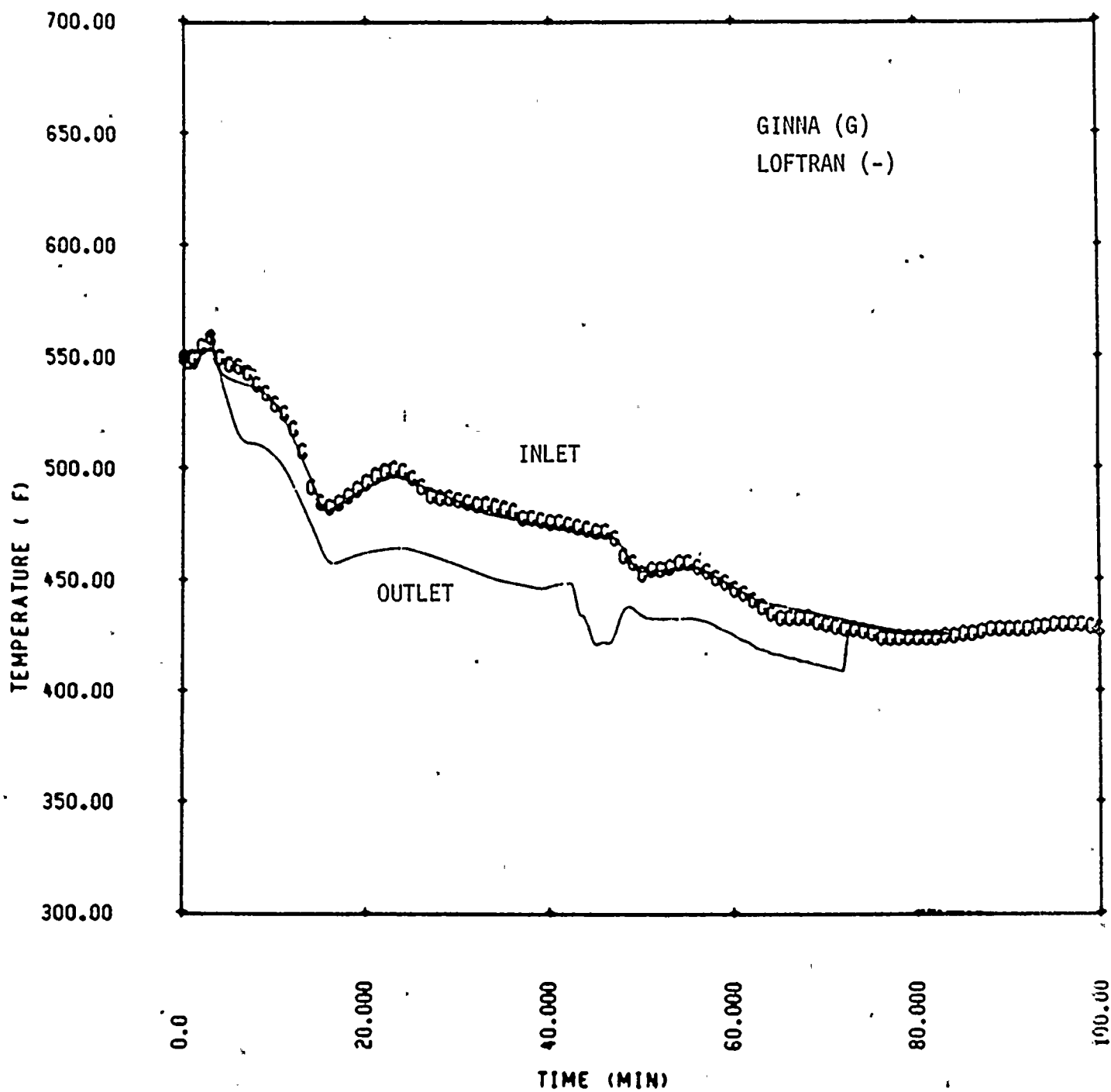


FIGURE II.5-4. INTACT LOOP COLD LEG TEMPERATURE.



could not be reproduced. However, the cooldown of the A loop was simulated by artificially steaming the intact steam generator. Hence, the calculated steam generator pressure was less than measured during this period.

II.5.1 Primary System Pressure

Primary pressure continued to decrease following reactor trip as break flow depleted coolant inventory and automatic steam dump cooled the reactor coolant system. Safety injection was activated within approximately 16 seconds, at 9:28:28 (3.2 min), when pressurizer pressure reached 1740 psia. Three high head safety injection pumps began to inject shortly thereafter to restore coolant inventory. Pressure continued to decrease to a minimum of 1200 psia between 9:29 (4 min) and 9:30 (5 min) as automatic steam dump established no-load RCS temperature. A small void may have developed in the upper head region during this initial depressurization although LOFTRAN did not predict flashing (see section II.5.6.2). The calculated RCS pressure history is compared to plant data in Figure II.5.1-1.

When the post-trip cooldown subsided after no-load temperature had been established, safety injection flow in excess of break flow, Figure II.5.1-2, repressurized the reactor coolant system until approximately 9:32 (7 min). Heat-up of the reactor coolant during the transition from forced to natural circulation due to RCP trip contributed to this repressurization. LOFTRAN analysis demonstrated a more rapid repressurization during this period than actually observed possibly because of collapse of an upper head void during the actual event. Reactor coolant shrinkage, as cold AFW entered the A loop steam generator, in combination with break flow decreased pressure to a minimum of 1140 psia between 9:32 (7 min) and 9:41 (16 min). Manual steam release beginning at approximately 9:38 (13 min) contributed little to this RCS cooldown since the steam generator tube bundle region was subcooled. Although a decrease in primary system pressure is evident in the analysis results shown in Figure II.5.1-1, the actual pressure decreased significantly lower. This is caused in part by the initially higher calculated primary pressure at 9:32 (7 min). In addition, although LOFTRAN indicates a small amount of water remained in the pressurizer during this period, Figure II.5.1-3, the pressurizer may have actually drained. This would have enhanced depressurization of the primary system.



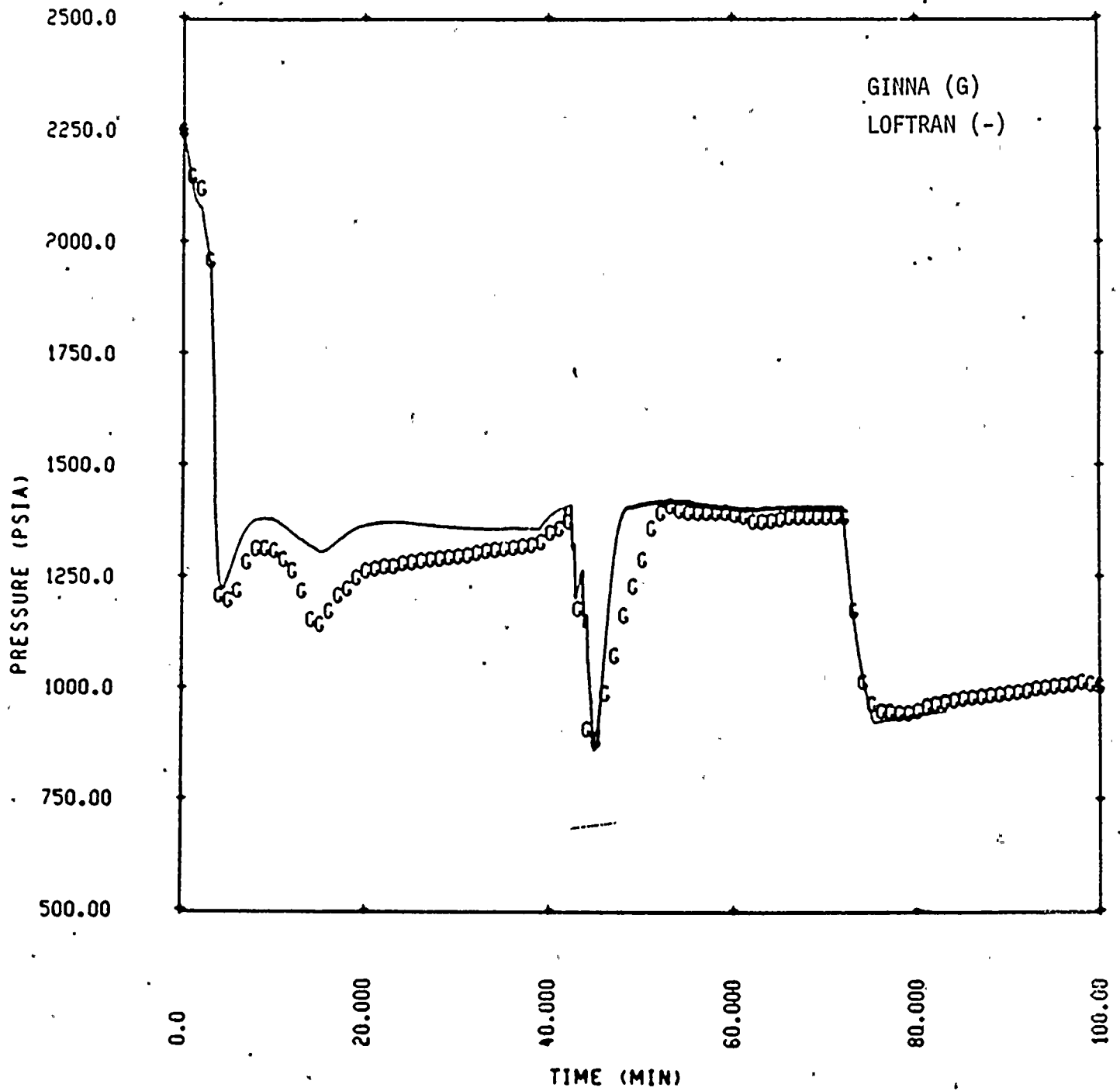


FIGURE II.5.1-1. REACTOR COOLANT SYSTEM PRESSURE.



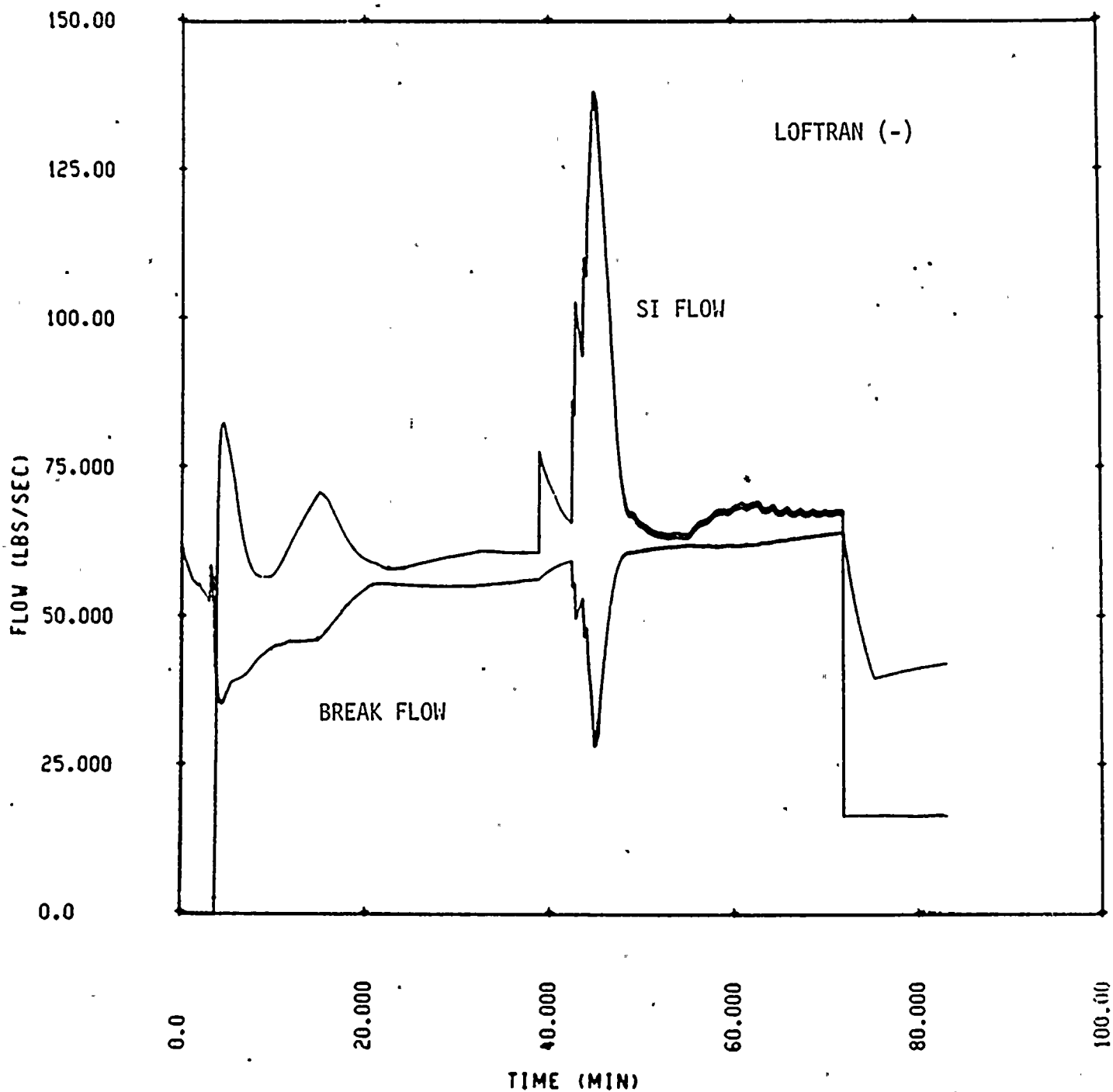


FIGURE II.5.1-2. PRIMARY-TO-SECONDARY LEAKAGE AND TOTAL SAFETY INJECTION FLOW.



3

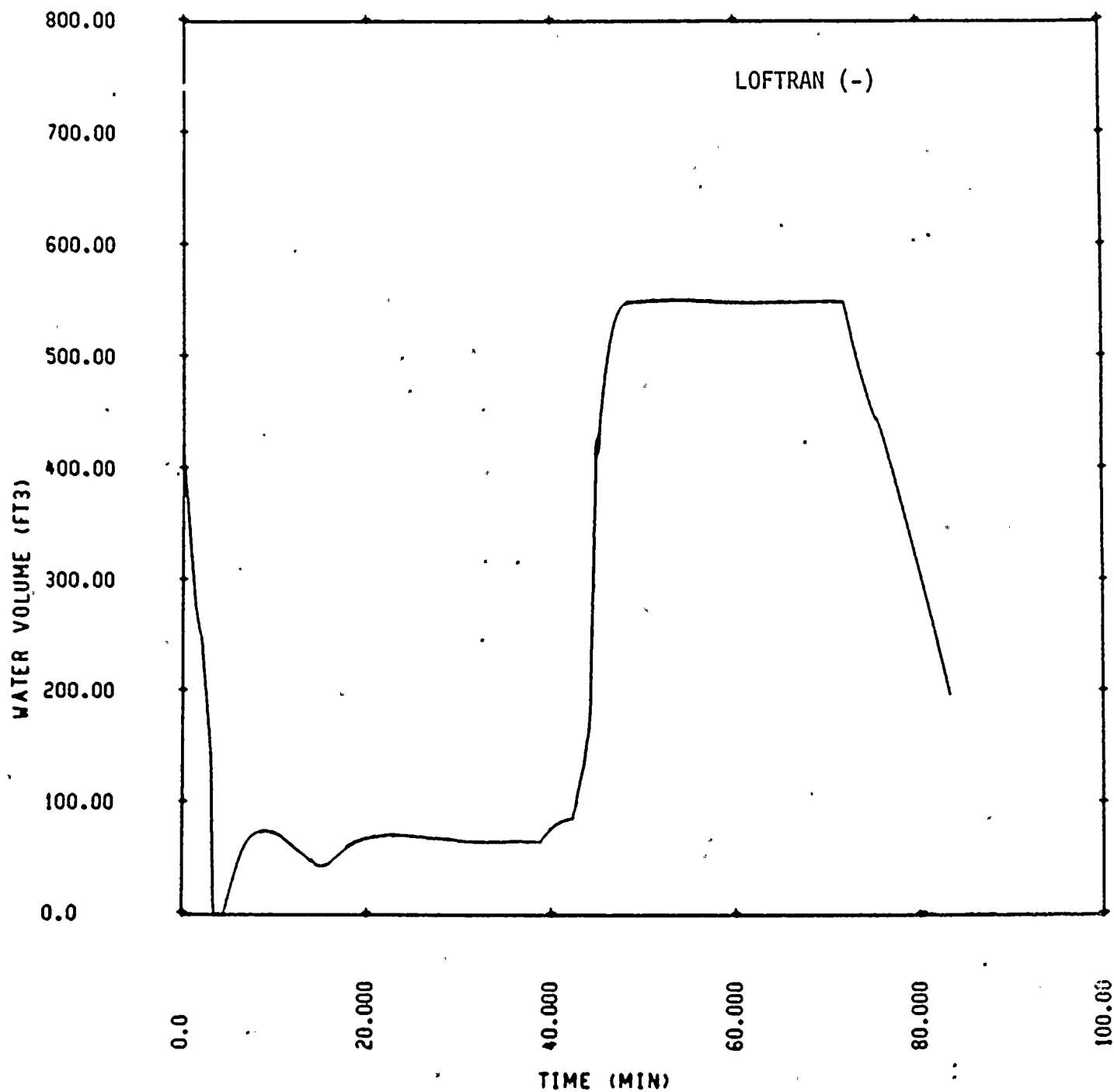


FIGURE II.5.1-3. PRESSURIZER WATER VOLUME.

When AFW flow was terminated to the A loop steam generator at 9:41 (16 min), the cooldown of the reactor coolant system subsided. Safety injection flow repressurized the primary system toward an equilibrium pressure of approximately 1320 psia where break flow and safety injection were nearly equal, as illustrated in Figure II.5.1-2. Operation of the steam dump valves occasionally perturbed this general trend and maintained pressure slightly below equilibrium. LOFTRAN calculations slightly overestimated the reactor coolant system pressure during this period. Two charging pumps with a combined capacity of 120 gpm were assumed to inject into the faulted loop cold leg beginning at 10:04 (39 min), as noted in the sequence of events. As a result, the predicted primary pressure increased toward an equilibrium value of 1410 psia by 10:07 (42 min). This is consistent with plant data which indicates an equilibrium pressure of approximately 1390 psia.

Cycling of a pressurizer Power Operated Relief Valve (PORV) was simulated beginning at 10:07 (42 min) and proceeded as indicated in Table II.5.1-1. The PORV was modelled to fully open or close instantaneously. During the actual event, the PORV failed to close on the fourth cycle and was manually isolated. Although this isolation was assumed completed by 10:10 (45 min), the actual time may have been slightly later. The calculated reactor coolant system pressure response during this period agreed well with available plant data. The minimum pressure during this period was calculated to be 847 psia. Following isolation of the failed PORV, the reactor coolant system pressure increased rapidly to approximately 1400 psia as safety injection flow and reverse flow from the ruptured steam generator increased coolant inventory. The actual repressurization was slower than calculated by LOFTRAN. As noted previously, LOFTRAN inhibits refilling of the upper head region during natural circulation flow, as evidenced by the constant upper head fluid mass beyond 10:10 (45 min) in Figure II.5.1-4. This enhanced refilling of the pressurizer and, consequently, repressurization of the primary system. Hence, the slower increase in pressure observed in the actual event is attributed to at least partial refilling of the upper head region.

By 10:17 (52 min), safety injection and charging flows had reestablished an equilibrium with break flow at approximately 1400 psia. When safety injection

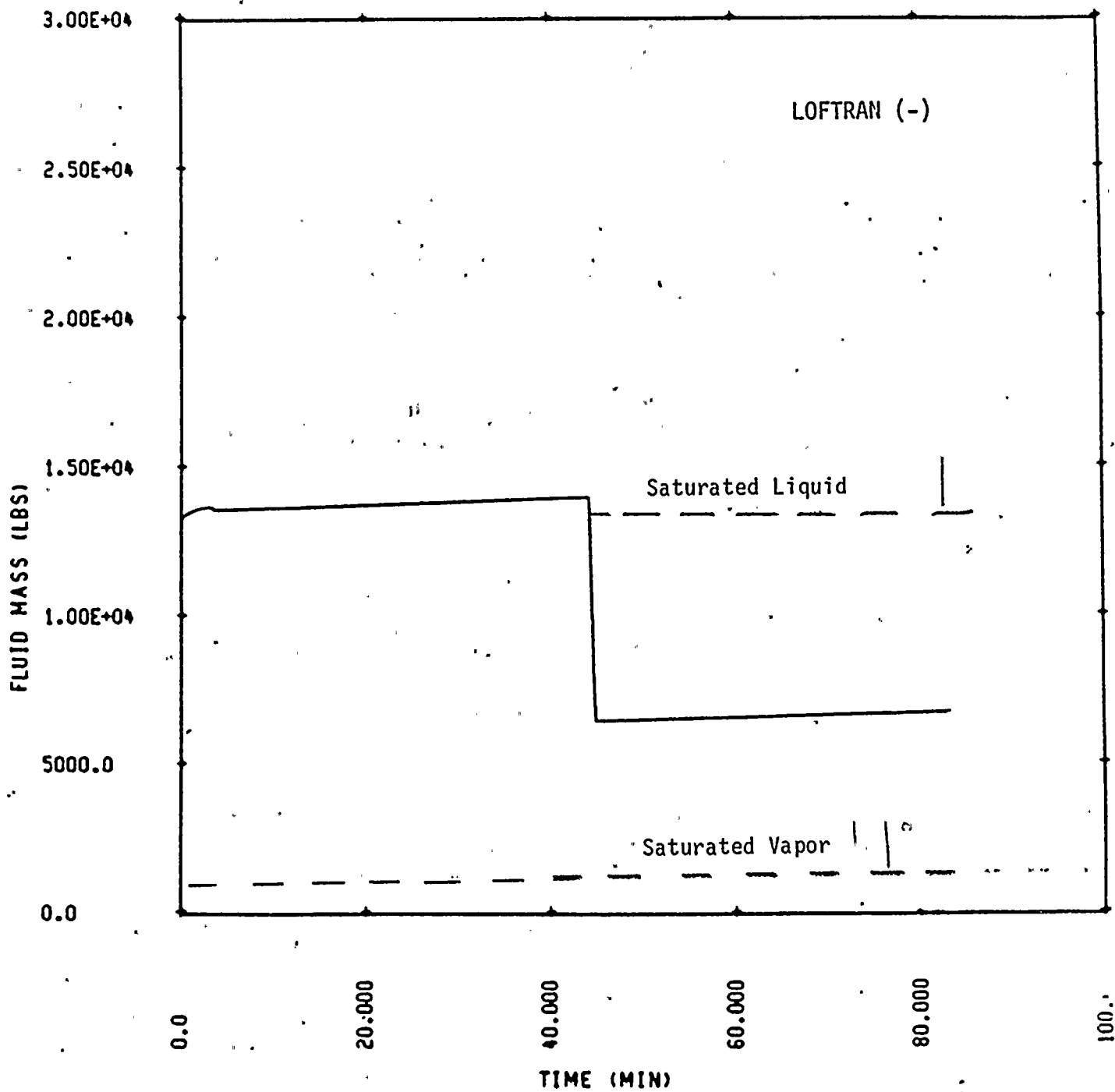


FIGURE II.5.1-4. UPPER HEAD FLUID MASS.

TABLE II.5.1-1 SEQUENCE OF PORV OPERATION

Cycle	Time (A.M.)	
	Opened	Closed
1	10:07:30.5	10:07:35.5
2	10:07:49.3	10:07:57.3
3	10:08:44.0	10:08:52.7
4	10:09:10.1	10:10:0.0 ⁽¹⁾

⁽¹⁾ Actual time of isolation may have been slightly later



was terminated at 10:37 (72 min), primary system pressure decreased rapidly from 1370 psia to 945 psia. LOFTRAN analyses demonstrated a similar depressurization as the pressurizer steam bubble expanded to accommodate residual break flow in excess of reactor coolant makeup. Continued charging flow and pressurizer heater operation maintained primary pressure greater than the faulted steam generator pressure until primary-to-secondary leakage was terminated at 12:30 (185 min).

II.5.2 Reactor Coolant Flow

A transition from forced to natural circulation flow occurred following manual reactor coolant pump trip at 9:29:09 (4 min). This is evidenced by the increasing loop delta-T between 9:29 (4 min) and 9:31 (6 min). AFW flow preferentially cooled the A steam generator which enhanced natural circulation flow in the A loop and retarded flow in the B loop. This response was demonstrated in the LOFTRAN results shown in Figure II.5.2-1 from 9:32 (7 min) to 9:41 (16 min). When AFW flow was throttled at 9:41 (16 min), flow through the A intact loop was calculated to decrease to approximately 4% of initial conditions. Flow through the faulted loop momentarily increased, as AFW flow from the turbine driven AFW pump continued to cool the faulted steam generator, until 9:46 (21 min) when AFW flow was terminated. As the cooldown of the intact steam generator continued, flow through the faulted loop was calculated to stagnate at 10:10 (45 min). Natural circulation flow through the intact loop was maintained between 3% and 4% full flow until the reactor coolant pump was restarted at 11:19 (114 min).

II.5.2.1 Loop B Cold Leg Flow

Although LOFTRAN did not support significant reverse flow through the faulted loop, the effect of break flow modelling on the calculated loop flow was uncertain. Hence, the potential for primary-to-secondary leakage generating sufficient reverse loop flow to produce the observed B loop temperature response was investigated. Figure II.5.2.1-1 compares the total reverse flow, i.e. safety injection flow and loop flow from the vessel downcomer, which would have a mixed temperature identical to the indicated B loop temperature,



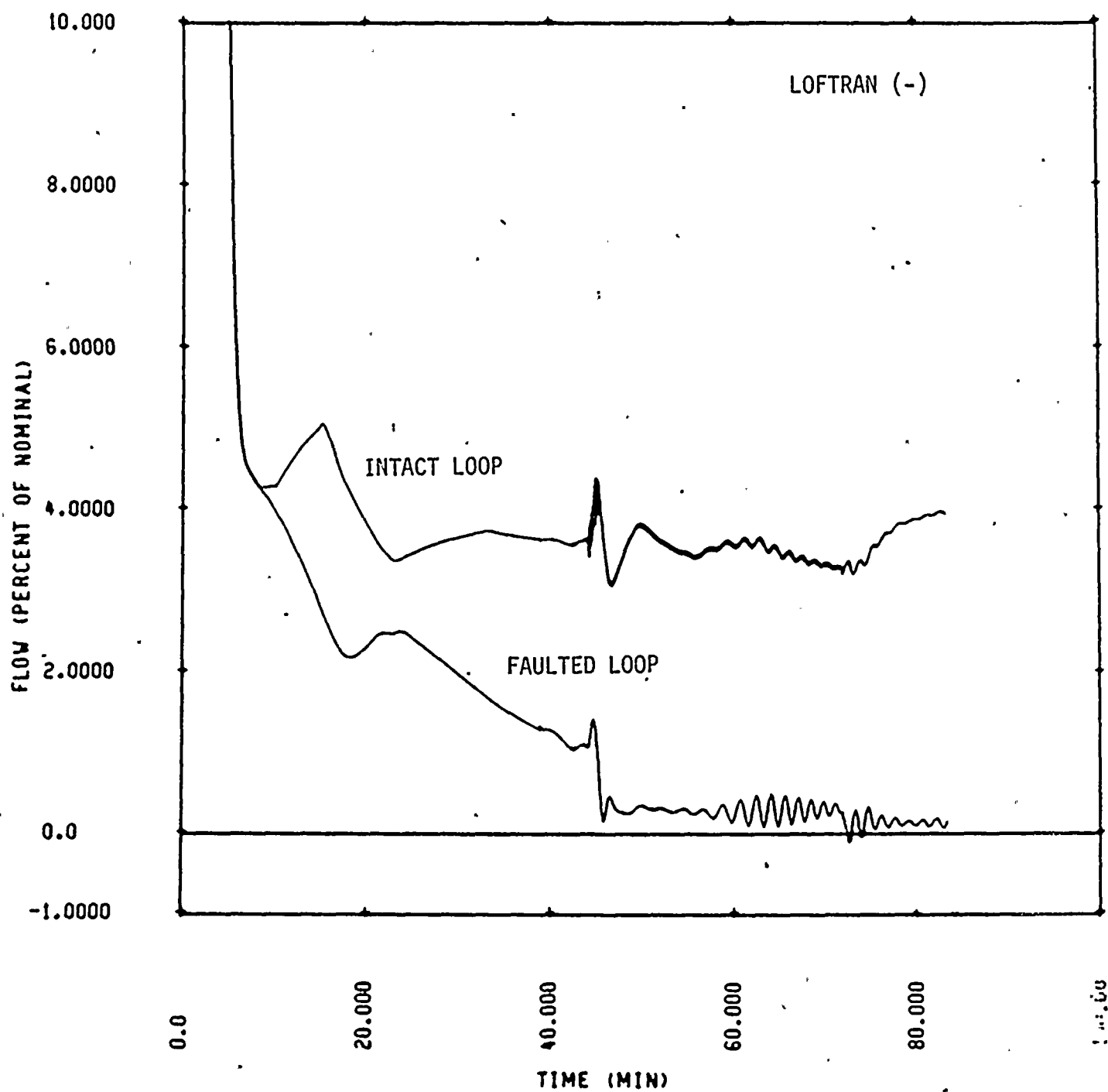


FIGURE II.5.2-1. VOLUMETRIC LOOP FLOW RATES.



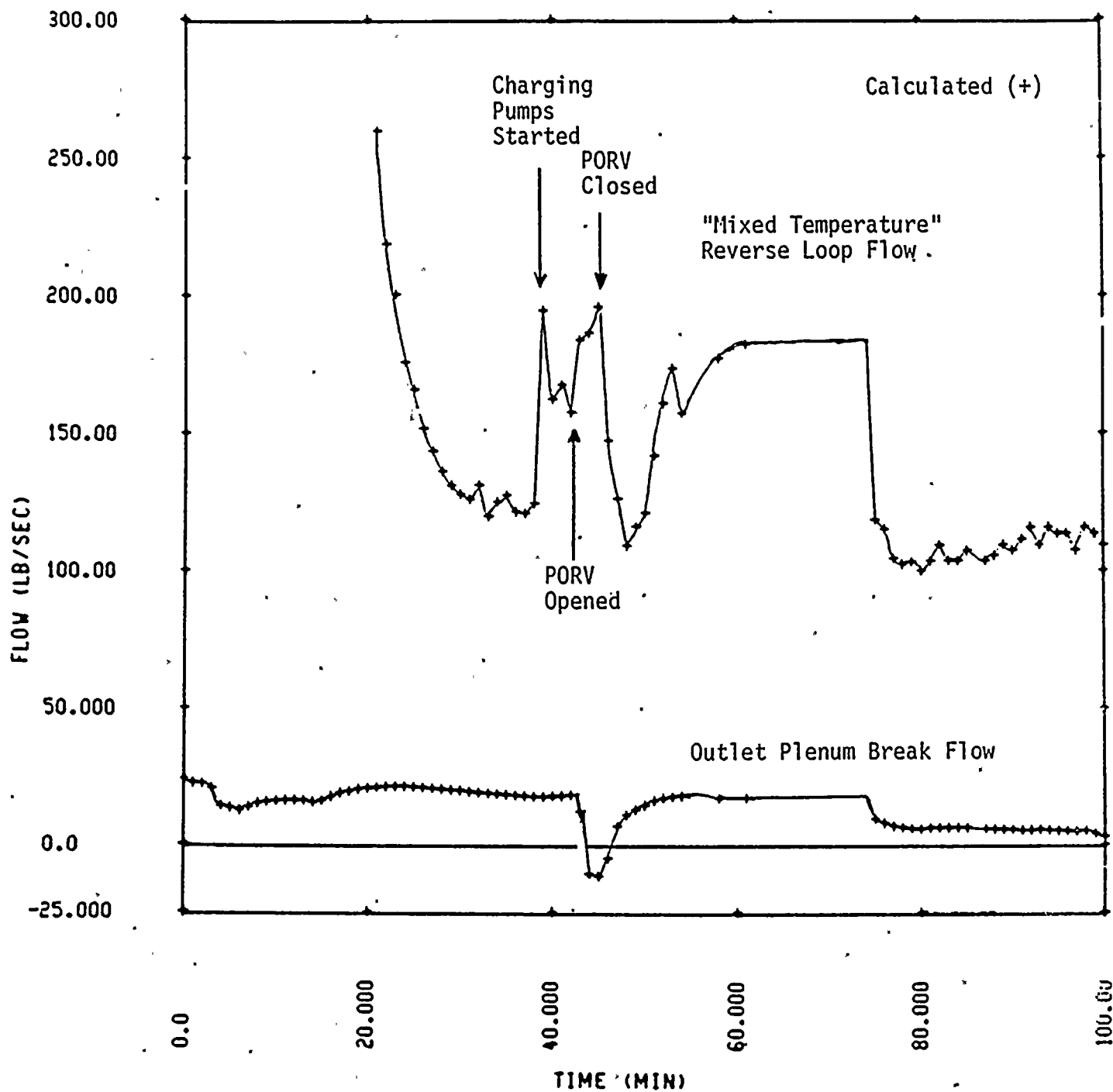


FIGURE II.5.2.1-1. COMPARISON OF "MIXED TEMPERATURE" REVERSE FLOW THROUGH FAULTED LOOP AND BREAK FLOW FROM SG OUTLET PLENUM.

and the calculated break flow from the steam generator outlet plenum. As demonstrated, primary-to-secondary leakage was much less than the required mixed loop flow. As an additional assessment of potential reverse loop flow, the response of the tube bundle fluid temperature in the faulted steam generator was calculated (see section II.5.3.5). These results suggest that if sufficient reverse loop flow did occur and produced a mixed temperature response similar to temperatures actually observed, the faulted steam generator would have been colder than the intact steam generator. Since this would promote forward flow in the faulted loop, it is unlikely that such sustained reverse flow occurred.

Ginna data demonstrated propagation of a portion of the safety injection flow upstream of the injection location beginning at 9:39 (14 min). In addition, the observed B loop cold leg temperature response suggests a continuous supply of warm fluid upstream of the injection nozzle (see section II.5.3.3). The calculated fluid flows into and from the faulted loop cold leg are shown in Figure II.5.2.1-2. Safety injection flow was calculated to split when the faulted loop flow stagnated at 10:10 (45 min); a small portion flowed toward the steam generator while the majority flowed toward the vessel. A continuous flow of warm water was not observed in the LOFTRAN analysis results. No significant temperature increase in the calculated faulted loop cold leg temperature occurred.

These results support the existence of a counter-current type of flow regime upstream of the injection nozzle. The B loop temperature response represents mixing of a portion of the safety injection flow upstream of the injection nozzle with a stream of warmer water from the steam generator. Such mixing is not simulated in the one dimensional modelling of LOFTRAN. The magnitude of flow from the faulted steam generator required to produce the quasi-steady temperature response was estimated from the cold leg inlet temperature and safety injection flow in the faulted loop calculated with LOFTRAN. Experimental evidence^(6,7) suggests that a significant portion of safety injection into a stagnant loop would propagate upstream of the injection nozzle. Based on this evidence, one third of the safety injection flow was assumed to mix upstream of the injection location. The result of this calculation indicates that a minimum loop flow of 21 lbm/sec (170 gpm) existed after 10:07 (42 min).



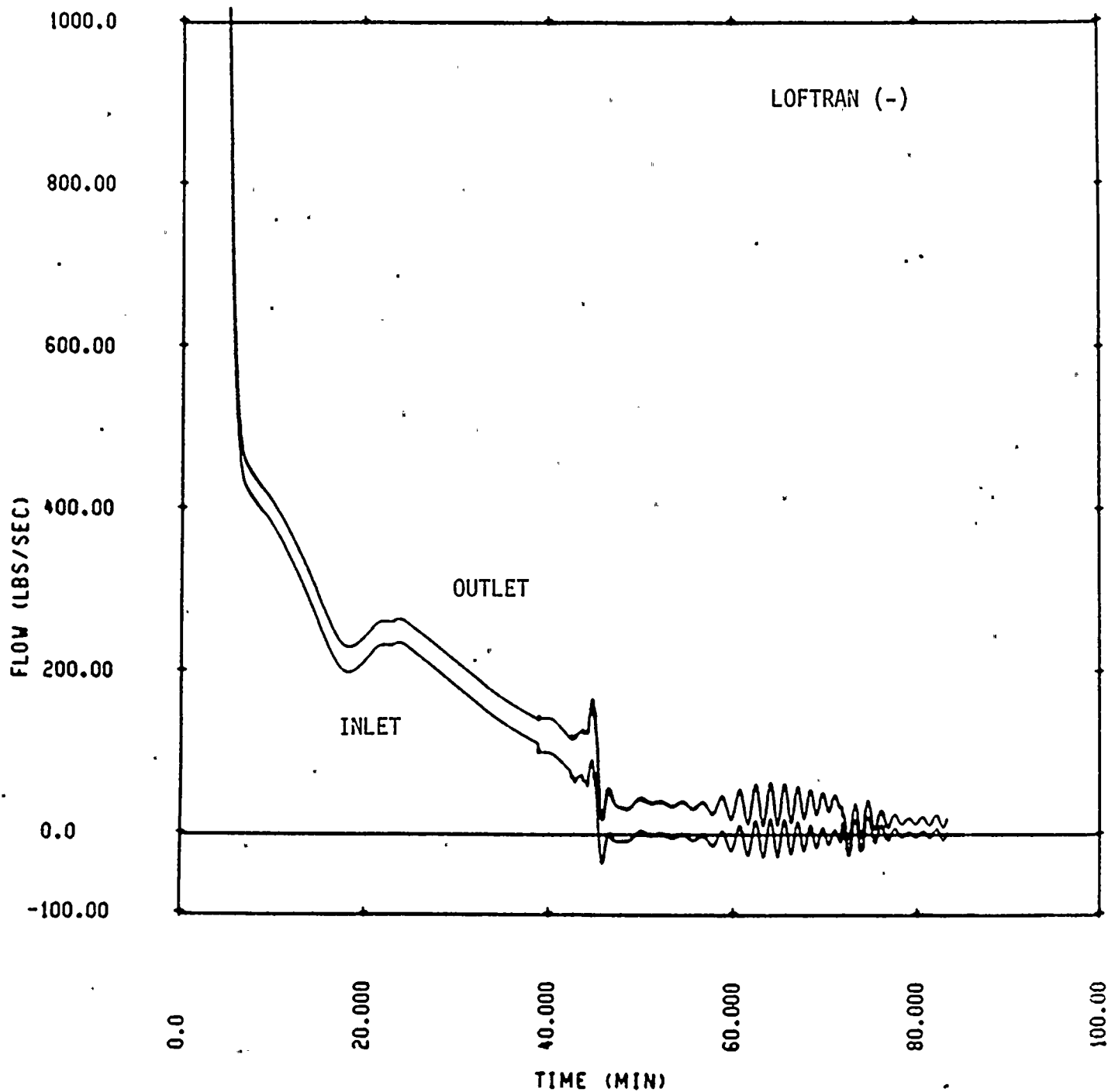


FIGURE II.5.2.1-2. FAULTED LOOP COLD LEG INLET AND OUTLET FLOWS.



II.5.3 Reactor Coolant Temperatures

The early reactor coolant temperature responses were typical of reactor trip. Hot and cold leg temperatures decreased rapidly as the automatic steam dump system and secondary coolant absorbed energy more rapidly than decaying core power. The large flow/power mismatch reduced the core coolant temperature rise to only a few degrees and the steam dump system operated to momentarily stabilize temperatures near no-load. The measured core temperature rise decreased to a minimum of 2°F before reactor coolant pumps were tripped and steadily increased thereafter to approximately 10°F by 9:31 (6 min). From 9:31 (6 min) to 9:38 (13 min) all steam dump valves were closed. During this time, safety injection and auxiliary feedwater flows absorbed decay heat and stabilized temperatures as demonstrated in the LOFTRAN analysis results shown in Figure II.5.3-1.

II.5.3.1 A Loop Cold Leg Temperature

Cold AFW flow rapidly cooled the A loop cold leg beginning at 9:32 (7 min). Although the AFW pumps were automatically started shortly after reactor trip, the steam generator feedlines and downcomer volume delayed injection of cold water from the Condensate Storage Tank (CST) into the tube bundle region. Two steam dump valves were manually opened from about 9:38 (13 min) until 9:39 (14 min) to decrease primary coolant temperature as directed by the emergency operating procedures. This appears to have had little effect on the cold leg temperature since the secondary coolant in the tube bundle region was sub-cooled. The A loop cold leg temperature decreased to a minimum of 485°F at 9:41 (16 min) when AFW flow was terminated to the A steam generator.

The homogeneous equilibrium secondary side modelling within LOFTRAN tended to underestimate the primary system cooling due to auxiliary feedwater. Consequently, the intact steam generator pressure was used as a forcing function to reproduce the A loop cold leg temperature response, as previously noted. Figures II.5-3 and II.5-4 compare the intact steam generator pressure and calculated cold leg temperature, respectively, with plant data. With the exception of the cooldown due to AFW flow, both pressure and temperature match the data reasonably well. Decreases in measured cold leg temperature

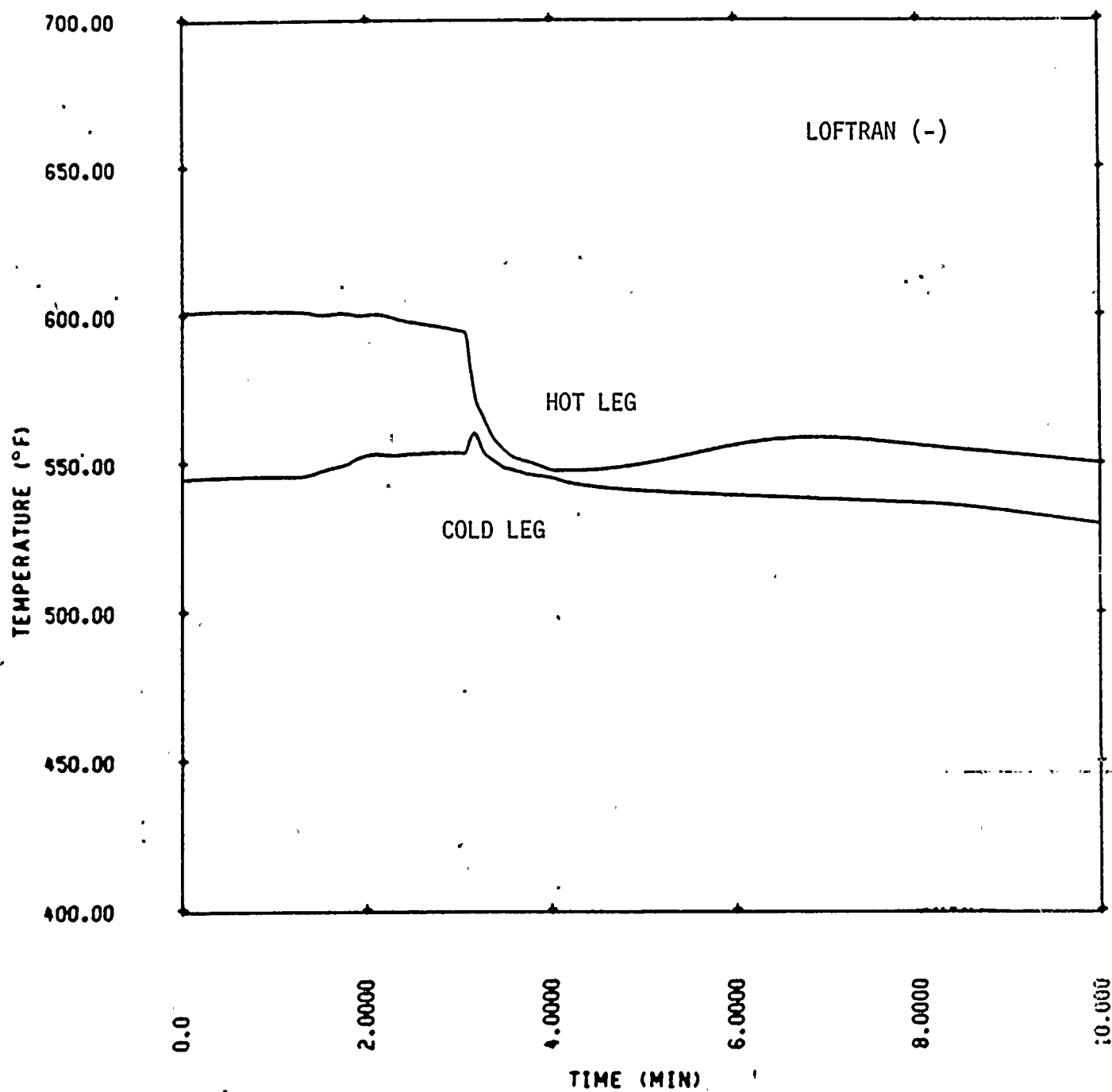


FIGURE II.5.3-1. POST-TRIP REACTOR COOLANT TEMPERATURES.



correlate with the operation of steam dump valves and AFW flow as shown in Figure II.5.3.1-1. The surge of safety injection when the pressurizer PORV was opened, reduced the core exit temperature below the A loop cold leg temperature, as shown in Figure II.5.3.1-2. This suggests that secondary-to-primary heat transfer may have momentarily occurred in the A loop. The LOFTRAN analysis results demonstrated a similar response. However, the decrease in cold leg temperature between 10:12 (47 min) and 10:15 (50 min) was underestimated. This appears to be a consequence of the homogeneous secondary side.

II.5.3.2 B Loop Cold Leg Temperature

The B loop cold leg temperature response was essentially the same as the A loop until AFW flow was reduced to the B steam generator at approximately 9:32 (7 min). From 9:32 (7 min) until 9:39 (14 min) the B loop temperature decreased more slowly as illustrated in Figure II.5.3.2-1. At approximately 9:39 (14 min), the B loop cold leg temperature decreased rapidly, indicative of safety injection flow upstream of the injection nozzle. Beyond this time, two distinct trends are evident in the measured temperature response. The rapid decrease in temperature beginning at 9:39 (14 min) is typical of a "mixing-cup" configuration where a portion of the cold safety injection flow mixes with the warmer fluid within a fixed volume. Since the inventory of warmer water available for mixing is limited, such a system is characterized by a continuous, exponential decrease in fluid temperature to the temperature of the incoming safety injection flow. Equally evident in the B loop cold leg temperature response is a quasi-steady period beginning at approximately 9:57 (32 min). It is clear that "mixing-cup" conditions do not describe this behavior since sufficient mixing volume is not available to support an exponential fit to the temperature time response. Furthermore, the increase in cold leg temperature from 10:11 (46 min) until 10:18 (53 min) cannot be explained by "mixing-cup" behavior. This suggests that a flow of warmer water continued into the B loop cold leg.

The calculated faulted loop cold leg fluid temperatures are compared with B loop data in Figure II.5.3.2-2. The calculated cold leg outlet, i.e. vessel inlet, temperature steadily decreased, as flow through the faulted steam generator decayed, and approached the temperature of the safety injection

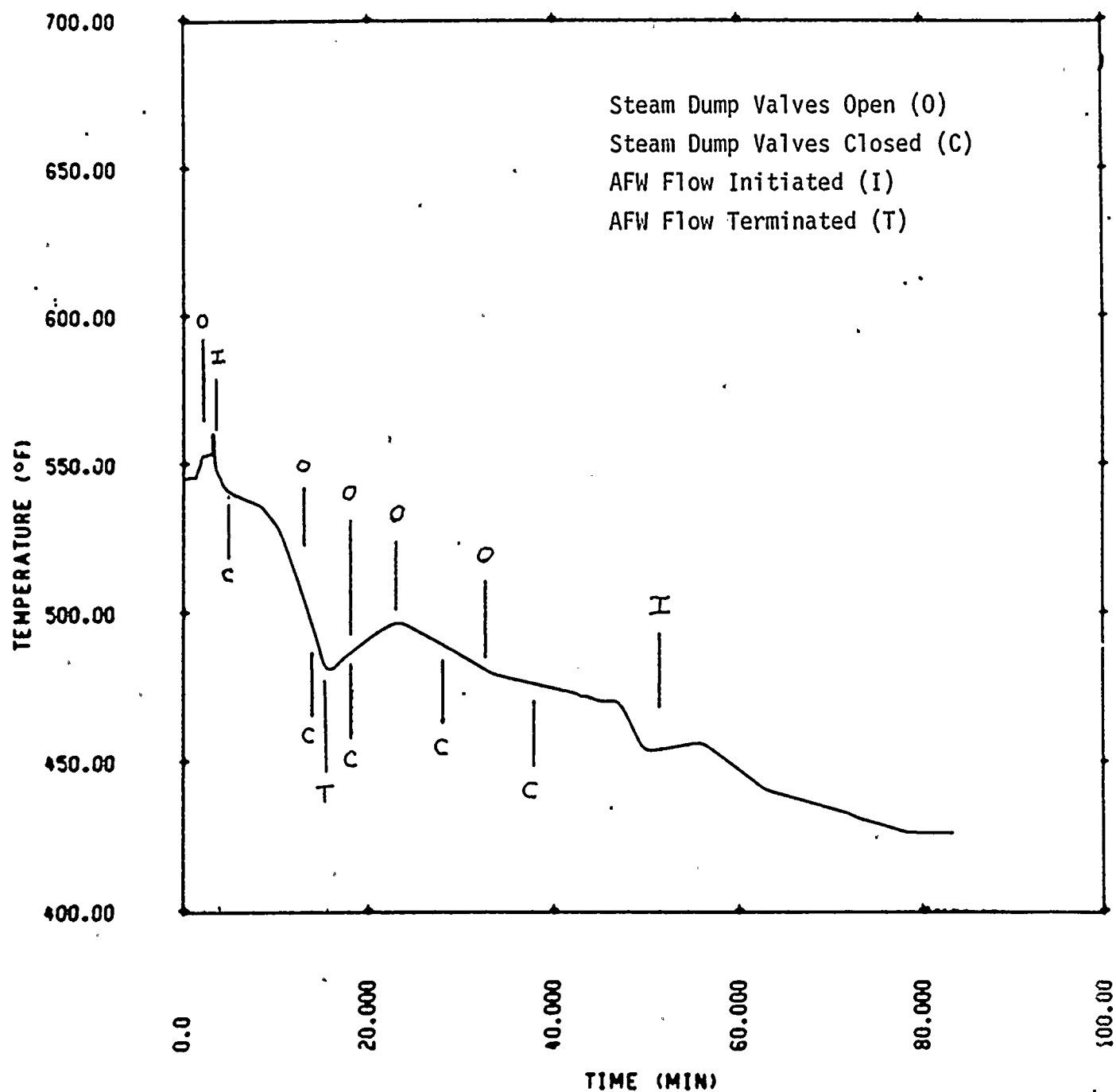


FIGURE II.5.3.1-1. STEAM DUMP VALVE OPERATION AND AFW FLOW DURING COOLDOWN OF THE RCS.

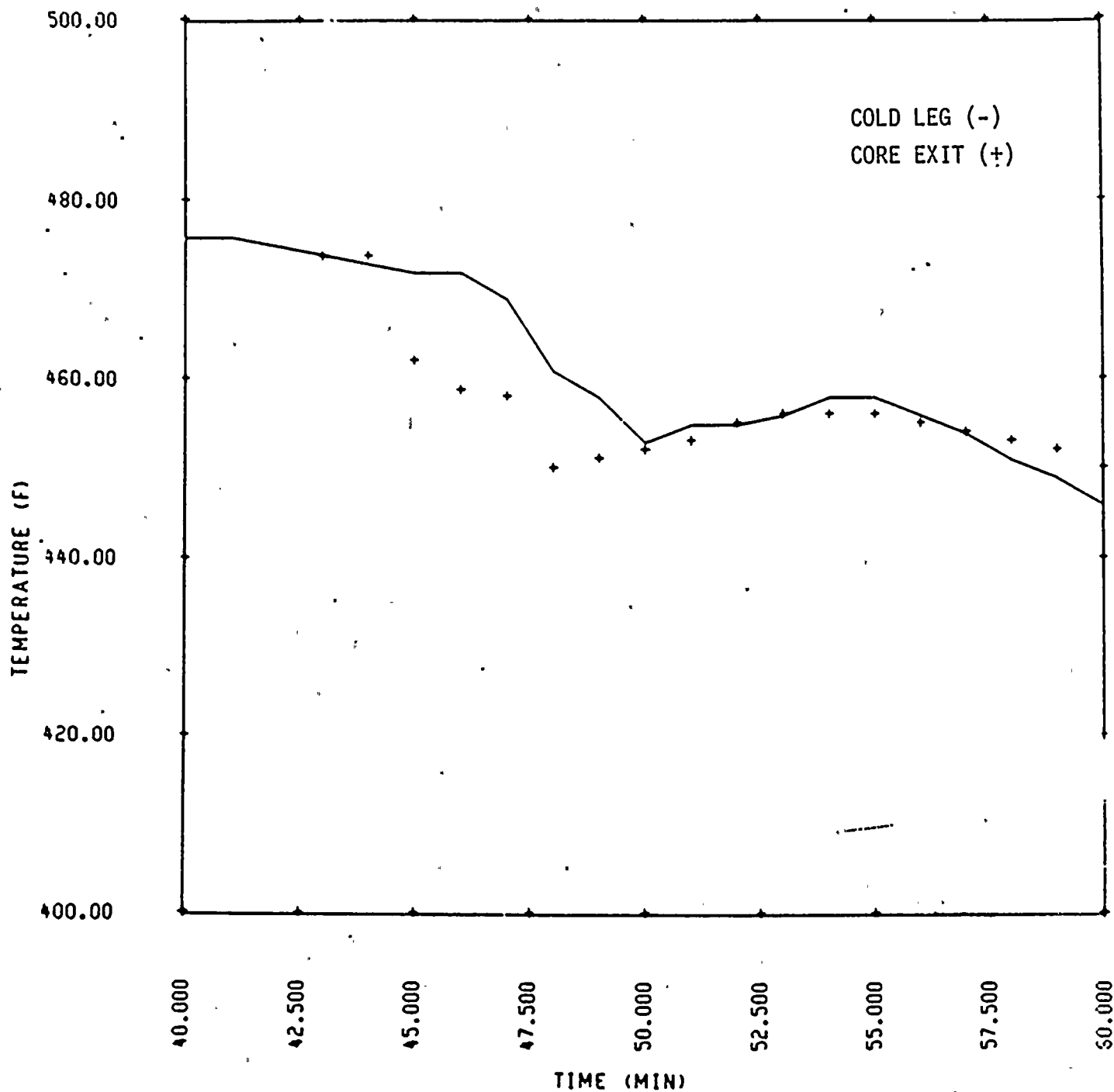


FIGURE II.5.3.1-2. GINNA CORE EXIT AND INTACT LOOP COLD LEG TEMPERATURES.

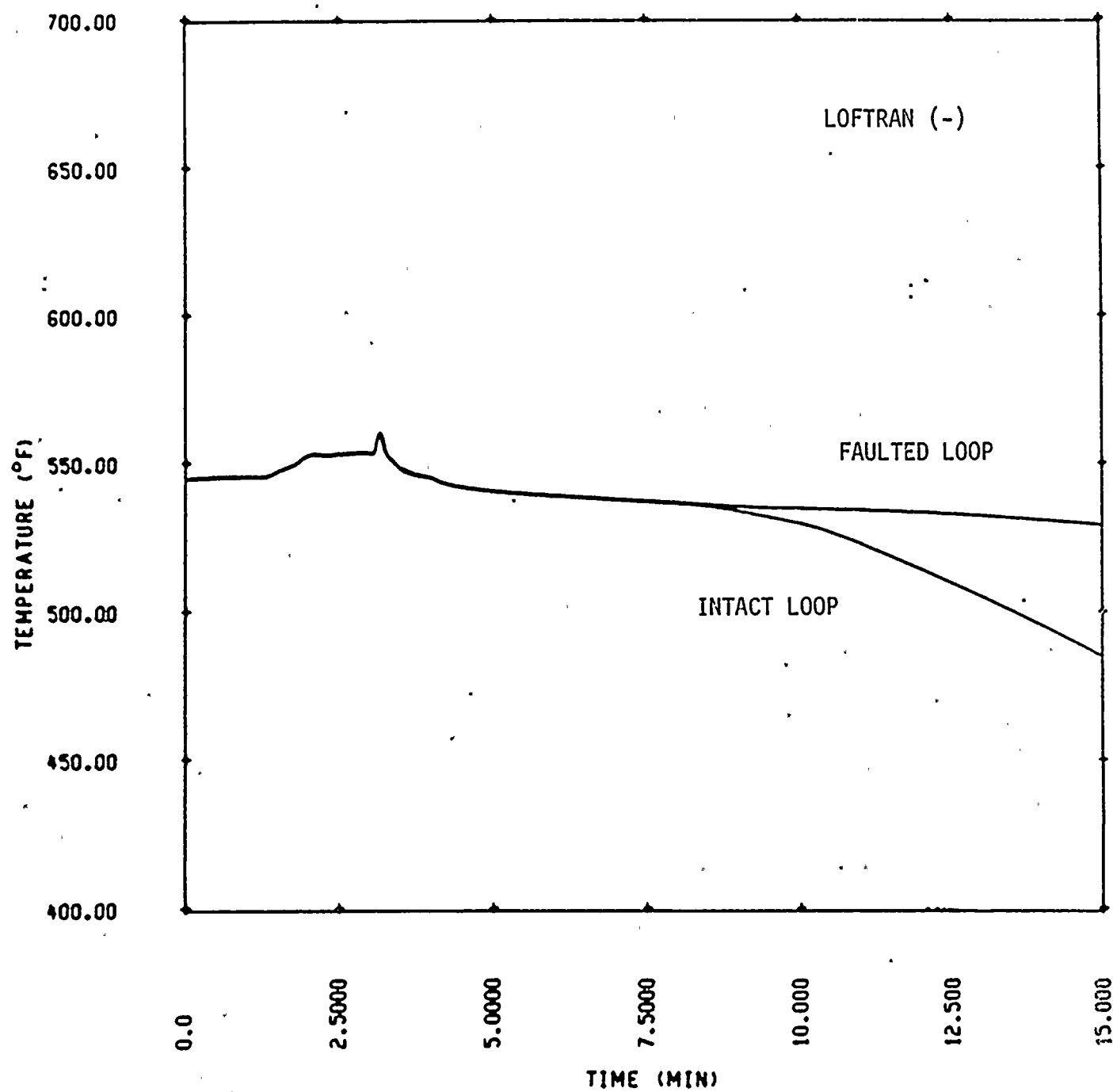


FIGURE II.5.3.2-1. COMPARISON OF INTACT AND FAULTED LOOP COLD LEG TEMPERATURES FOLLOWING REACTOR TRIP.

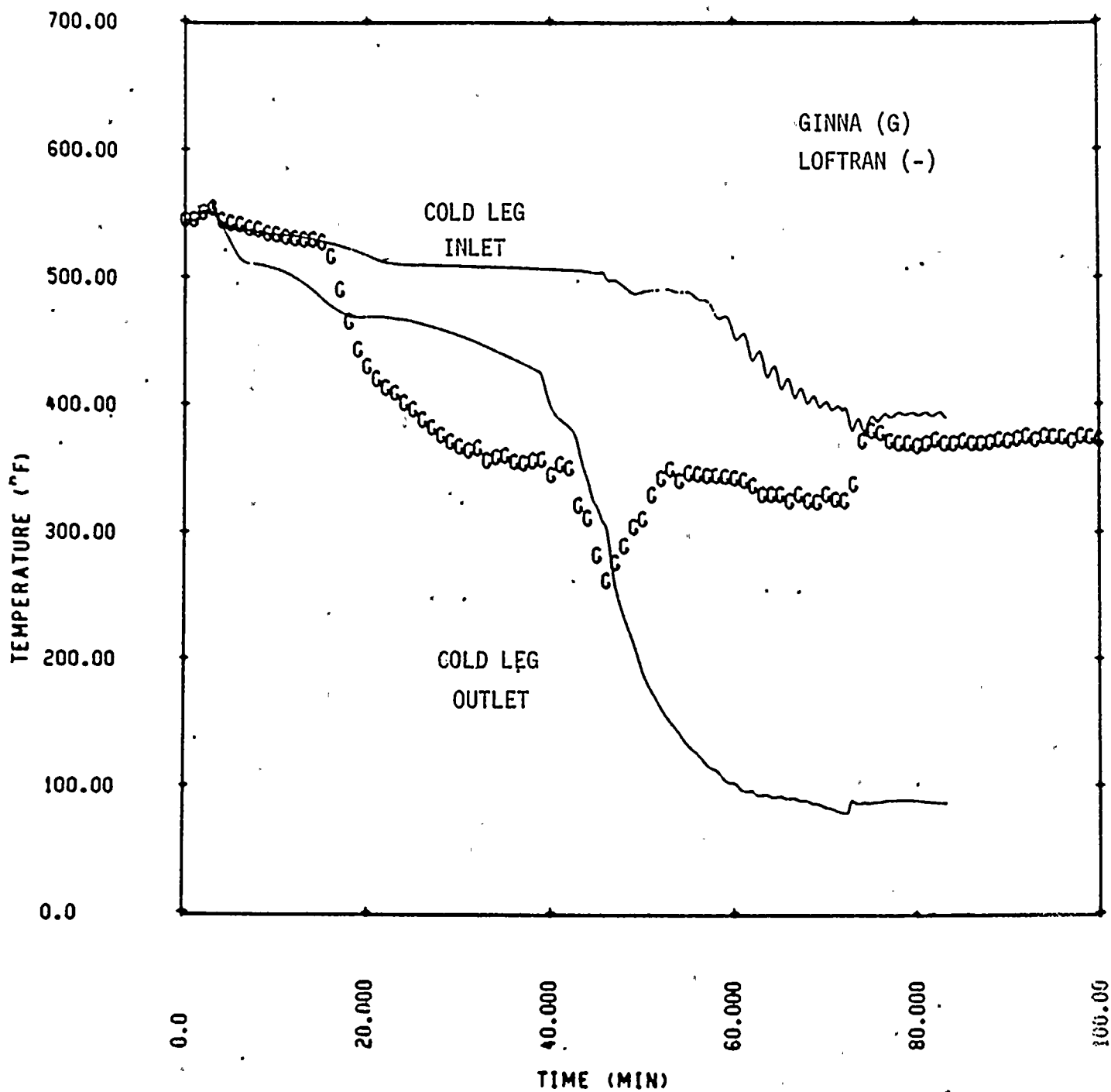


FIGURE II.5.3.2-2. FAULTED LOOP COLD LEG TEMPERATURES.



flow. Although this is similar to the B loop transition period, the calculated cold leg outlet temperature continued to decrease. The calculated temperature upstream of safety injection remained relatively hot until approximately 10:10 (45 min), at which time safety injection flow was first predicted by LOFTRAN to propagate upstream of the injection nozzle.

When the pressurizer PORV was cycled beginning at 10:07 (42 min), a surge of safety injection flow decreased the B loop fluid temperature. The calculated vessel inlet temperature demonstrated a similar response. Although the calculated faulted loop cold leg inlet temperature was not significantly affected, the location of the pressurizer may have artificially promoted flow toward the vessel. No increase in fluid temperature is observed in the LOFTRAN analysis results after isolation of the failed PORV.

Evaluation of the potential flow distributions within the faulted loop cold leg (see section II.5.2.1) suggests that multi-dimensional behavior may have significantly affected the actual temperature response. Such effects are beyond the capabilities of LOFTRAN. However, the B loop temperature response indicates an additional flow of warm fluid into the cold leg which is not observed in the LOFTRAN analysis results. Consequently, the calculated cold leg outlet temperature shown in Figure II.5.3.2-2 underestimates the expected minimum bulk fluid temperature at the vessel inlet.

In order to more realistically estimate the minimum fluid temperature in the reactor vessel, the vessel downcomer, cold leg and crossover leg piping, and reactor coolant pump were modelled as a single, mixing volume as shown in Figure II.5.3.2-3. The temperature response of this configuration to flow from the faulted steam generator and safety injection flow, Figure II.5.3.2-4, was calculated assuming perfect fluid mixing. These flows and associated temperatures, Figure II.5.3.2-5, were obtained from the LOFTRAN analysis results; however, a minimum loop flow of 21 lbm/sec (170 gpm) was assumed, as discussed in section II.5.2.1. Metal heat addition from the reactor vessel, piping, and coolant pump was determined from a one dimensional conduction/convection heat transfer model based on the measured fluid temperature in the B loop cold leg. The calculated mixing volume fluid temperature is compared to the LOFTRAN analysis vessel inlet temperature and B loop temperature data in Figure II.5.3.2-6. The metal heat and additional loop flow increased the



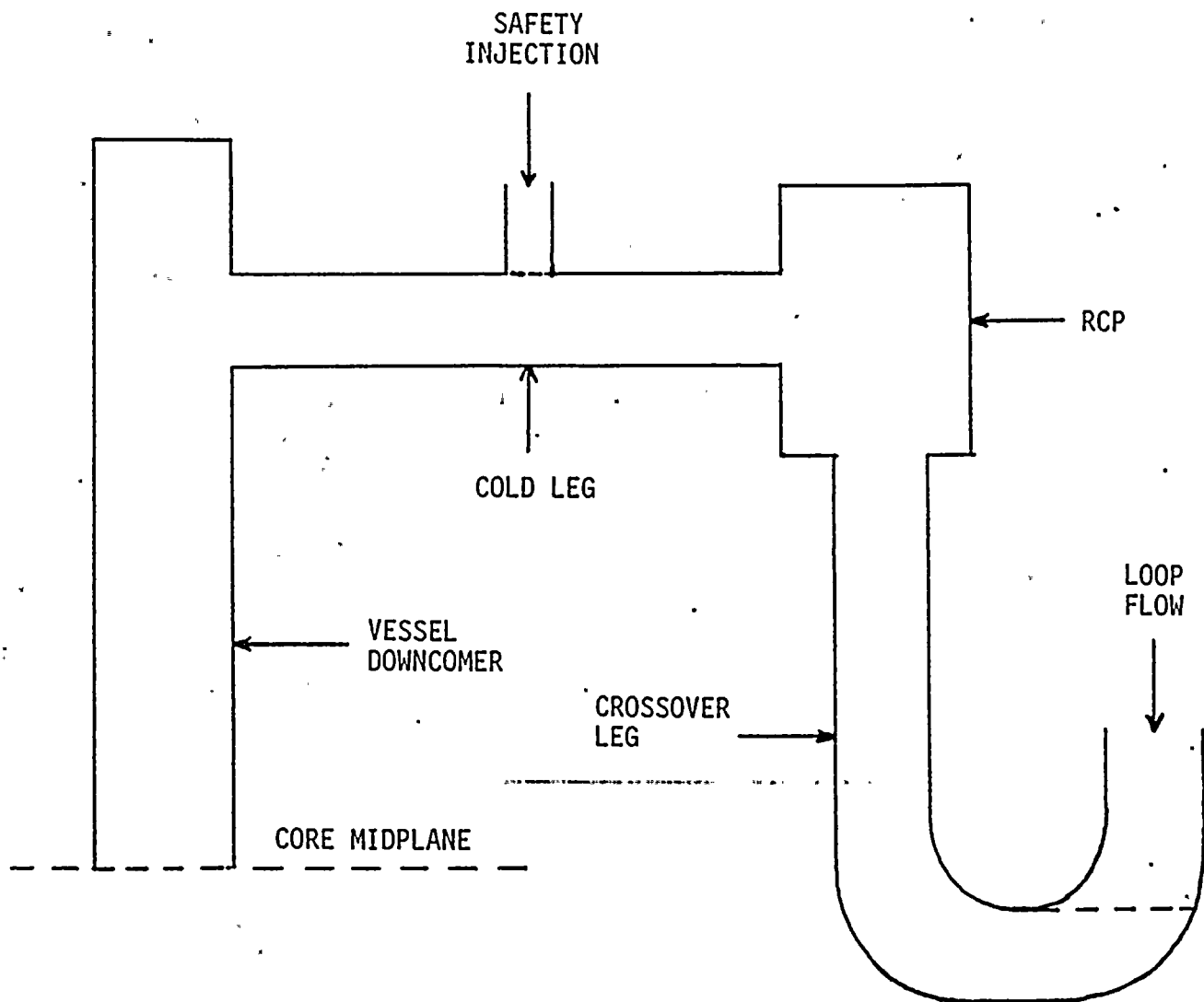


FIGURE II.5.3.2-3 MIXING VOLUME FOR VESSEL DOWNCOMER TEMPERATURE CALCULATION

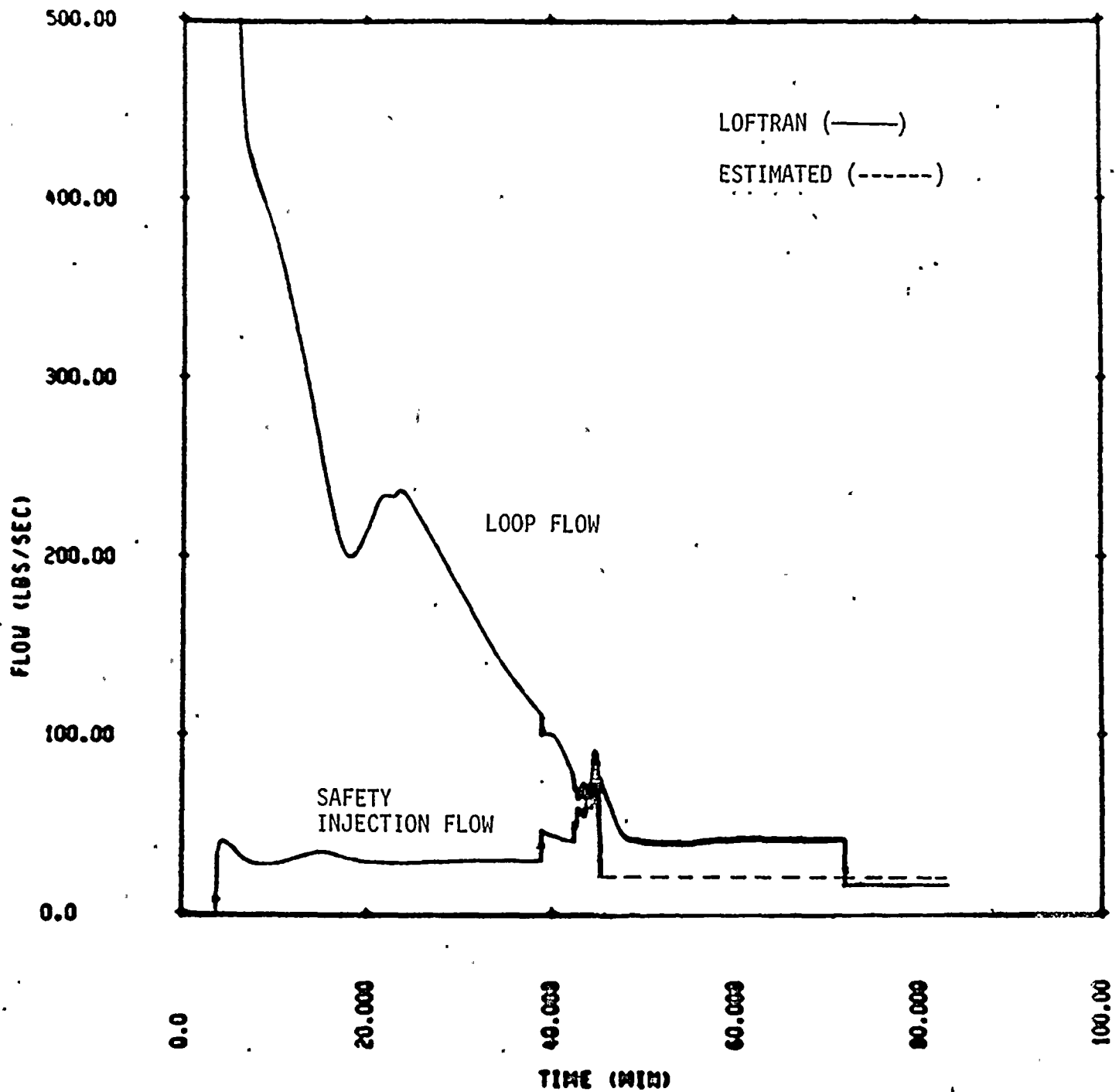


FIGURE II.5.3.2-4 MIXING VOLUME LOOP FLOW AND SAFETY INJECTION FLOW

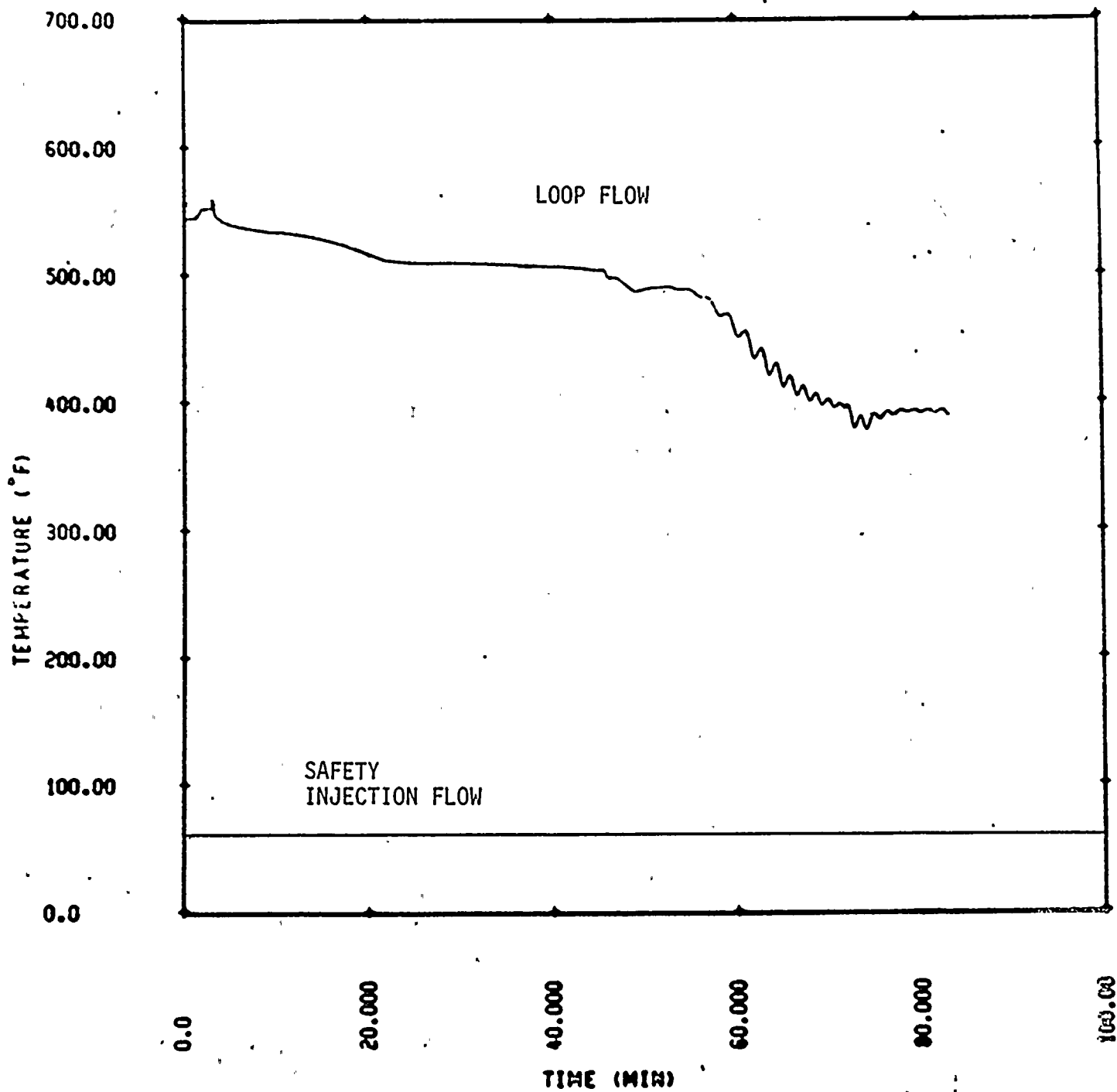


FIGURE II.5.3.2-5 MIXING VOLUME FLOW TEMPERATURES

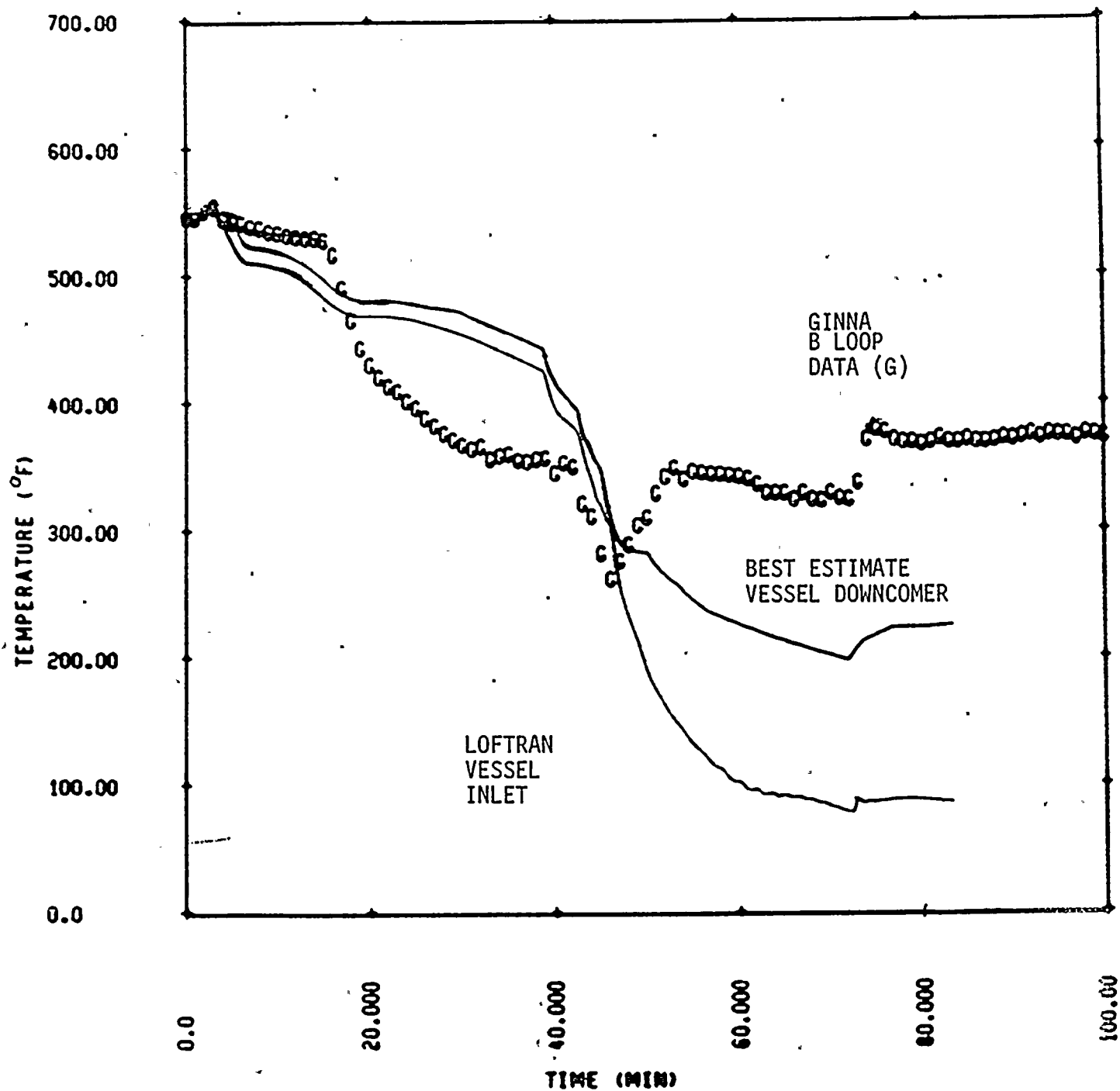


FIGURE II.5.3.2-6 BEST ESTIMATE REACTOR VESSEL DOWNCOMER TEMPERATURE



minimum calculated downcomer fluid temperature at the core midplane elevation to approximately 200°F. In addition, an increase in fluid temperature occurred after safety injection was terminated at 1037 (42 min) as observed during the actual event. These results represent a more realistic estimate of the minimum fluid temperature in the vessel downcomer.

II.5.3.3 Core Exit Fluid Temperature

The calculated core exit fluid temperature is compared to the available data in Figure II.5.3.3-1. Imperfect mixing at the core inlet was simulated in the results presented; consequently, the core exit temperature is slightly different for the core regions adjacent to the faulted and intact loops. The core exit fluid temperature trended the intact loop cold leg and remained subcooled throughout the transient.

Increased reactor coolant makeup following startup of the charging pumps and cycling of the pressurizer PORV decreased the core exit fluid temperature beginning at 10:04 (39 min). This temporarily decreased the core exit temperature below the A loop cold leg temperature as discussed in section II.5.3.1.

II.5.3.4 B Loop Hot Leg Temperature

Primary-to-secondary leakage from the steam generator inlet plenum provided a mechanism for flow through the faulted loop hot leg even for stagnant loop flow conditions. Based on estimates of this break flow, Figure II.5.3.4-1, and the hot leg volume, the faulted loop hot leg temperature was estimated to lag the core exit temperature by less than 10 minutes. The LOFTRAN analysis demonstrated this trend, as shown in Figure II.5.3.4-2. These results indicate that the faulted loop hot leg fluid remained subcooled throughout the event.

II.5.3.5 B Steam Generator Temperature

The tube bundle region fluid temperature of the faulted steam generator was calculated by modelling a single, subcooled control volume in communication with the primary system via primary-to-secondary leakage and specified loop flow. Perfect energy transfer was assumed so that break flow and loop flow



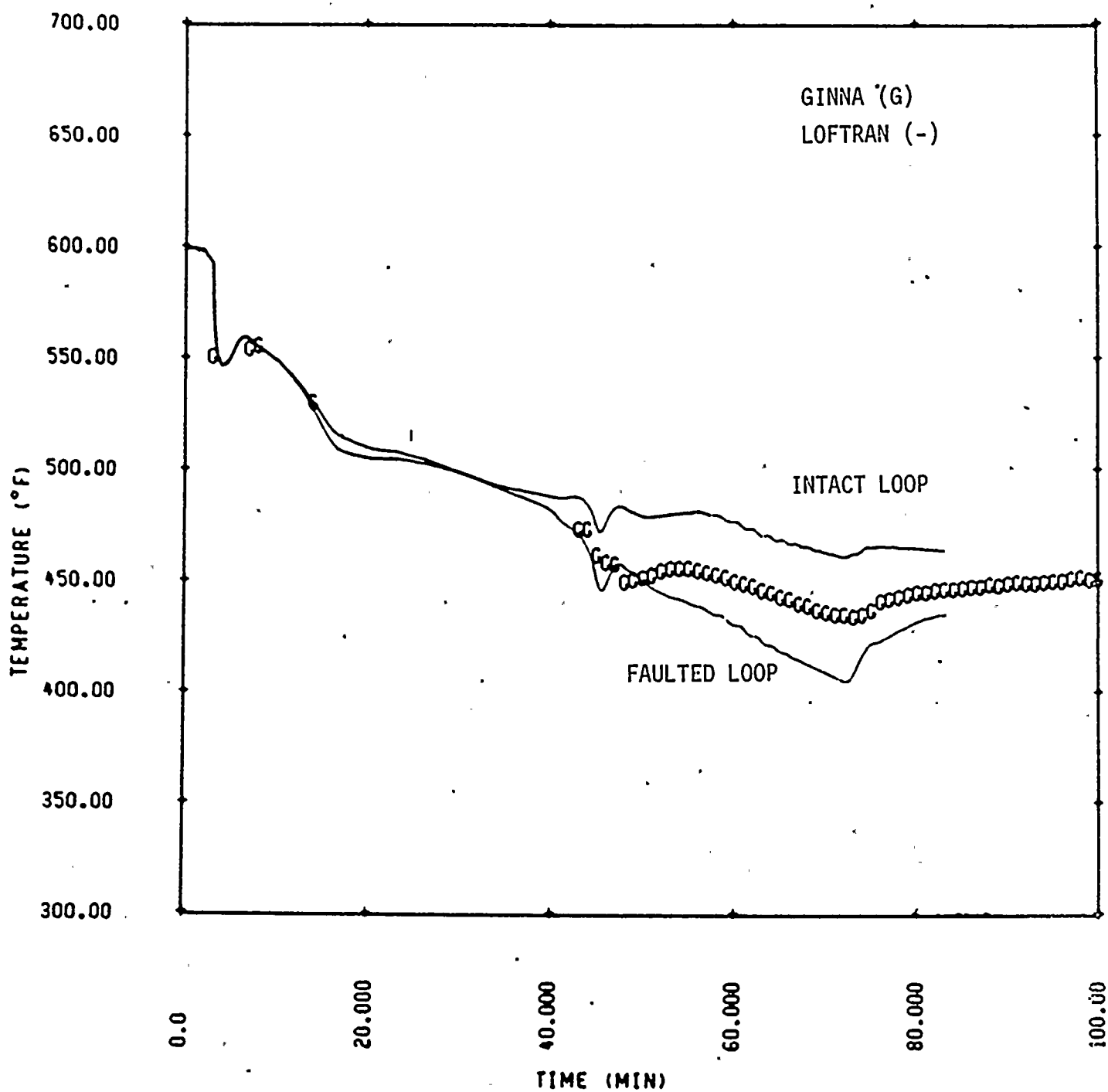


FIGURE II.5.3.3-1. CORE EXIT FLUID TEMPERATURE.



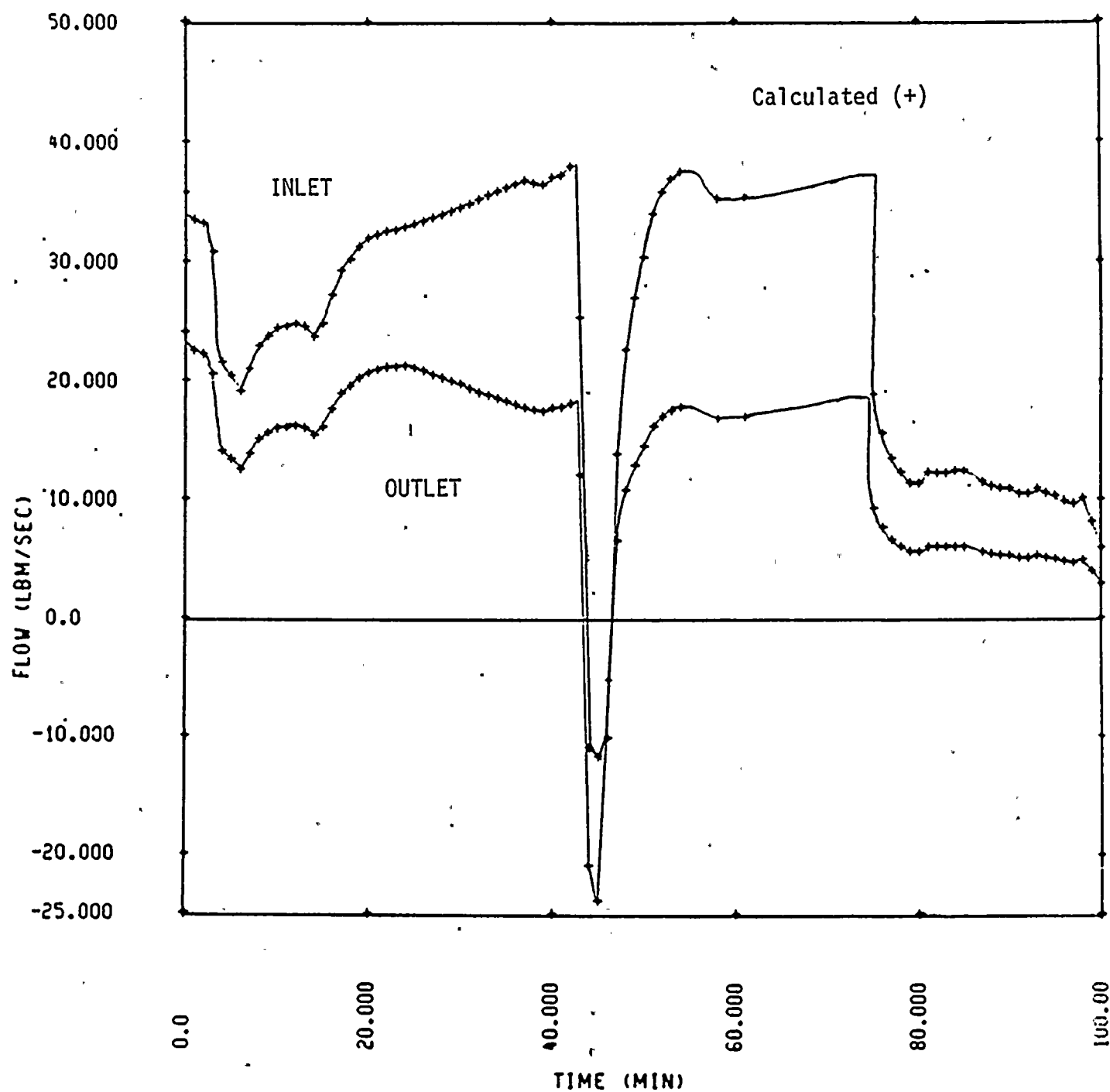


FIGURE II.5.3.4-1. BREAK FLOW FROM S.G. INLET AND OUTLET PLENUMS.



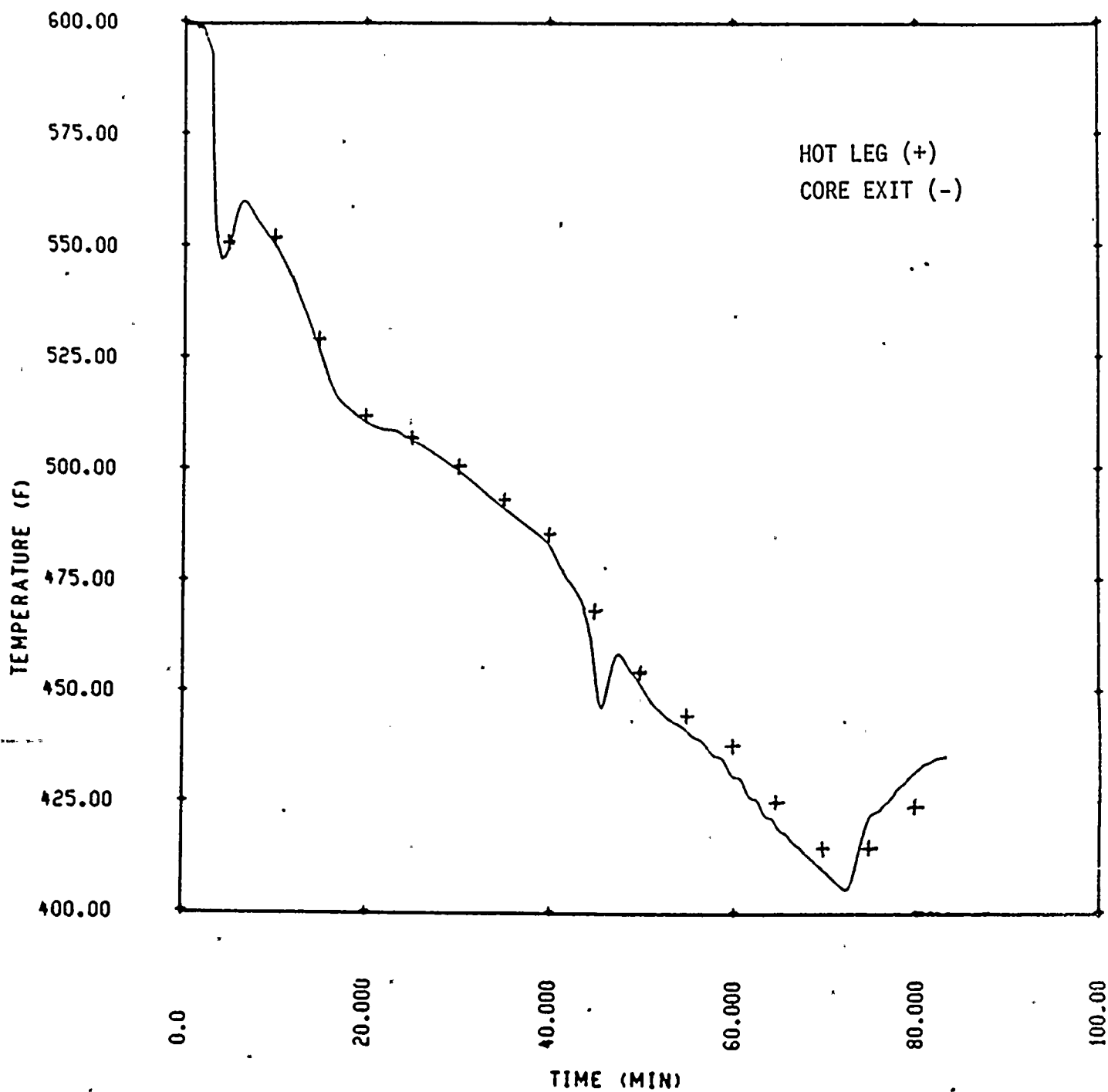


FIGURE II.5.3.4-2. LOFTRAN FAULTED LOOP HOT LEG TEMPERATURE.

achieved thermal equilibrium with the control volume inventory. Two cases of flow from the faulted steam generator outlet plenum were considered: 1) reverse loop flow through the steam generator equal to that presented in Figure II.5.2.1-1, and 2) only primary-to-secondary leakage from the outlet plenum into the faulted steam generator. The temperature of these flows was assumed equal to the indicated B loop cold leg temperature. For both cases, primary-to-secondary leakage from the steam generator inlet plenum was also considered. Figure II.5.3.5-1 compares the results of these calculations with the intact steam generator temperature calculated with LOFTRAN. Case (1) suggests that if sufficient reverse loop flow did occur and produced a mixed temperature response similar to temperatures actually observed, the faulted steam generator would have been colder than the intact steam generator. Since this would promote forward flow in the faulted loop, it is unlikely that such sustained reverse flow occurred. Case (2) indicates that primary-to-secondary leakage effectively cooled the tube bundle region of the faulted steam generator.

II.5.3.6 Upper Head Temperature

During normal operation, a small fraction of the cold leg flow is diverted into the upper head region of the reactor vessel and mixes with flow from the upper plenum to maintain the upper head fluid temperature at Ginna near 595 F. These flows remain nearly constant as long as reactor coolant pumps continue to run. After reactor trip, the core exit temperature decreases rapidly. With reactor coolant pumps running, the upper head fluid temperature will also decrease rapidly but will lag the upper plenum and cold leg temperatures.

The upper head region temperature transient was evaluated assuming constant volumetric upper head flows until reactor coolant pumps were tripped at 9:29:09 (4 min). The average cold leg and hot leg temperatures as indicated by pre-trip data were assumed for the flows from the cold leg and upper plenum, respectively. Figure II.5.3.6-1 presents the calculated upper head region fluid temperature with and without metal heat. For the case with metal heat, the metal temperature was assumed to be equal to the fluid temperature. The fluid temperature was calculated to be approximately 553 F when reactor

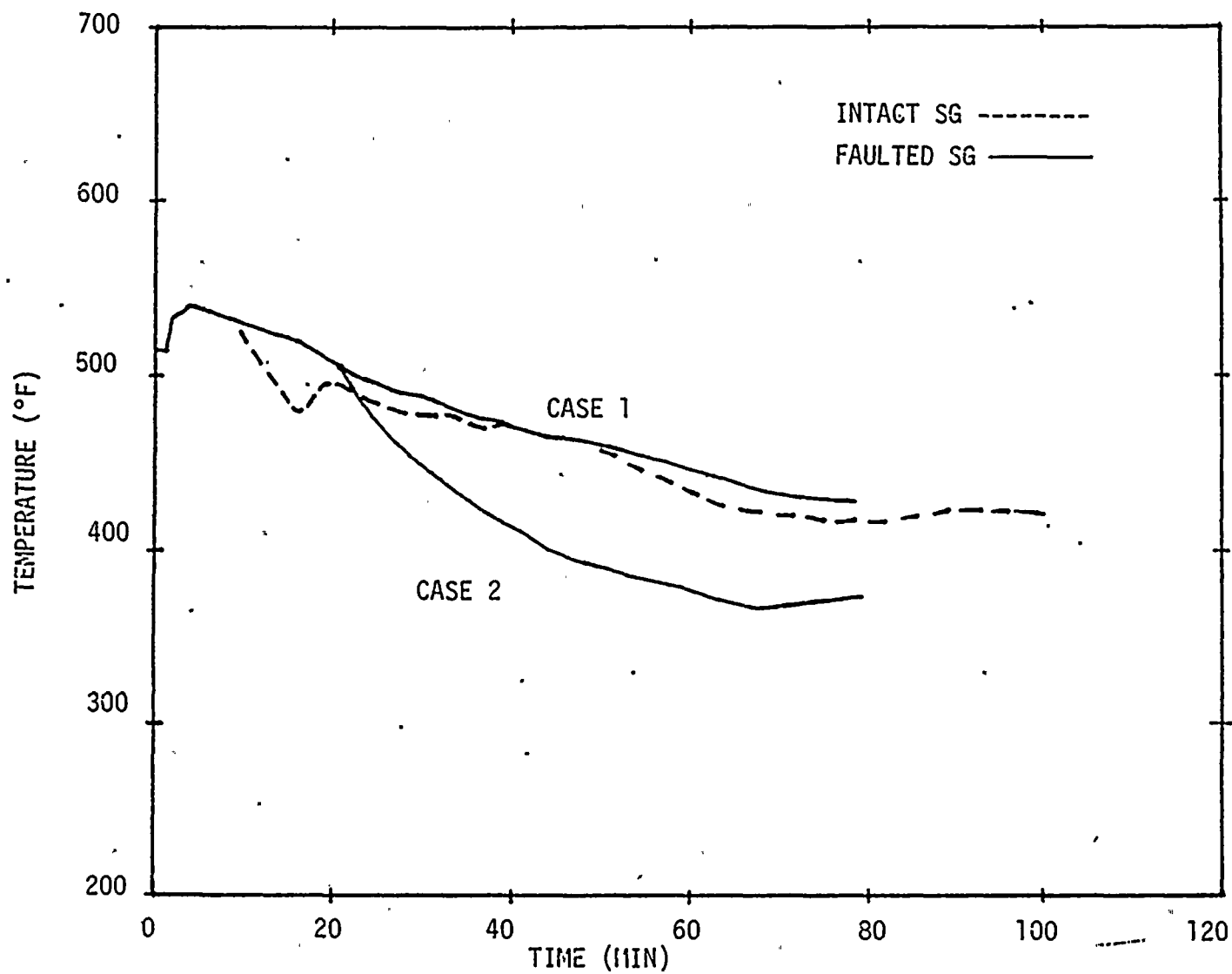


FIGURE II.5.3.5-1. FAULTED SG TUBE BUNDLE FLUID TEMPERATURE.

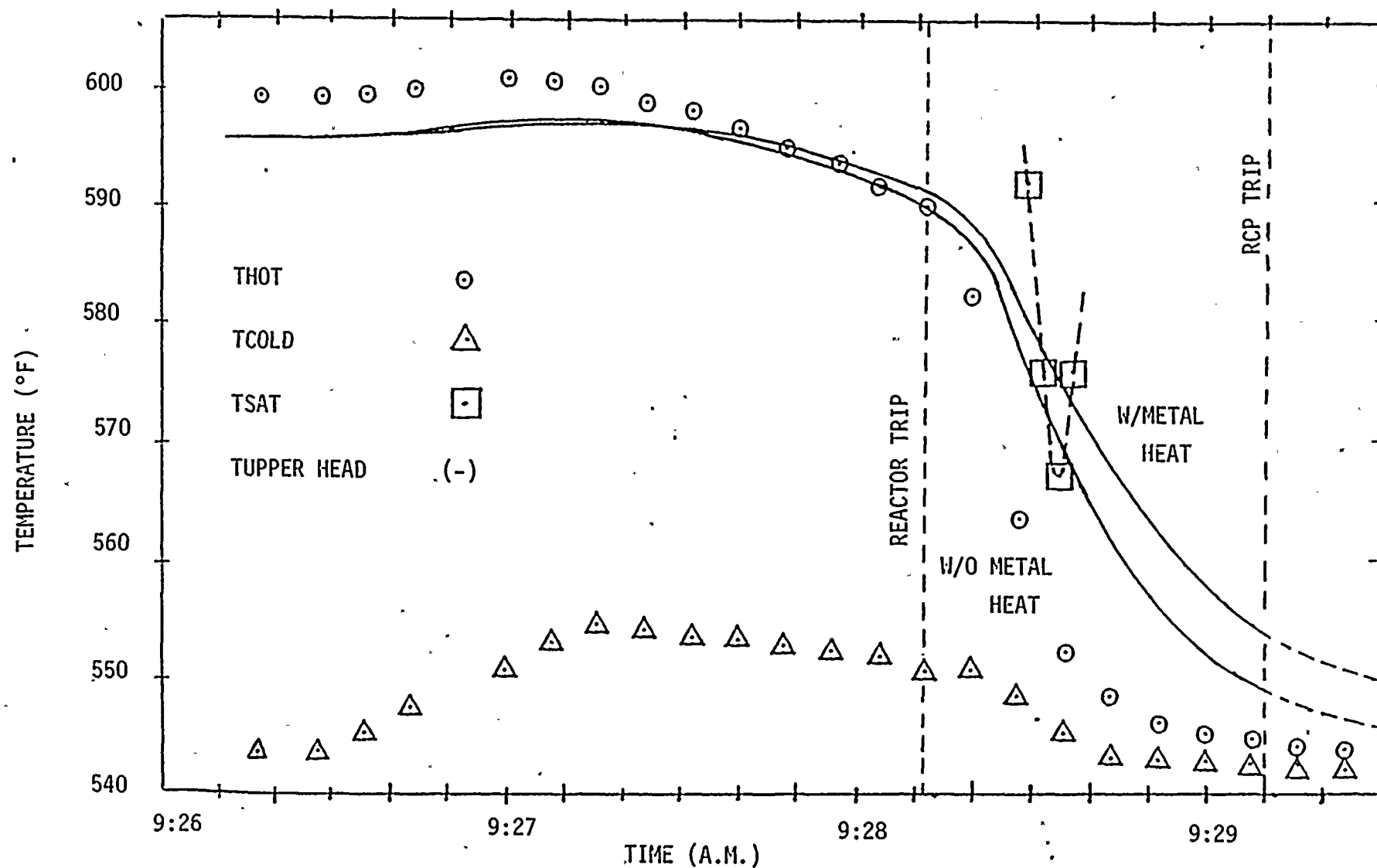


FIGURE II.5.3.6-1. POST-TRIP UPPER HEAD FLUID TEMPERATURE.



coolant pumps were tripped. This is consistent with the upper head thermocouple indication of 556°F at 9:54 (31 min). Note that voiding may have occurred in the upper heat region while reactor coolant pumps were still operating (see section II.5.6.2).

The upper head region temperature calculated by LOFTRAN is shown in Figure II.5.3.6-2. Since flow from the upper plenum through the guide tubes was not modelled, the fluid temperature at reactor trip was less than would be expected. Hence, no upper head voiding occurred immediately following reactor trip in the LOFTRAN results. However, the fluid temperature at 10:07 (42 min), when the pressurizer PORV was cycled, was equal to the measured upper head thermocouple. Hence, the upper head voiding calculated during this period is expected to be representative of the Ginna event.

II.5.4 Pressurizer Level Response

The calculated pressurizer water level indication is compared with plant data in Figure II.5.4-1. The initial decrease in level was predicted by LOFTRAN very well. The pressurizer was calculated to drain by 9:29 (4 min) and begin to refill soon after as safety injection flow repressurized the primary system, as illustrated in Figure II.5.1-3. The pressurizer may have drained a second time between 9:32 (7 min) and 9:38 (13 min) during cooldown via AFW flow. Ginna data indicates that pressurizer level returned on span approximately when the charging pumps were started. An indicated level did not return in the LOFTRAN analysis results until the pressurizer PORV was cycled beginning at 10:07 (42 min).

As primary pressure decreased when the PORV was opened, pressurizer level increased as safety injection flow in excess of break flow, Figure II.5.1-2, replaced vented steam in the pressurizer. Soon afterwards, at approximately 10:09:20 (44 min), the upper head water began to flash. Water displaced from the upper head region rapidly increased pressurizer inventory and the indicated level increased offscale. The LOFTRAN analysis demonstrated similar level response; however, the indicated level remained on span. This appears to be due primarily to the lower initial level prior to depressurization of the primary system. In addition, no reverse flow from the faulted steam



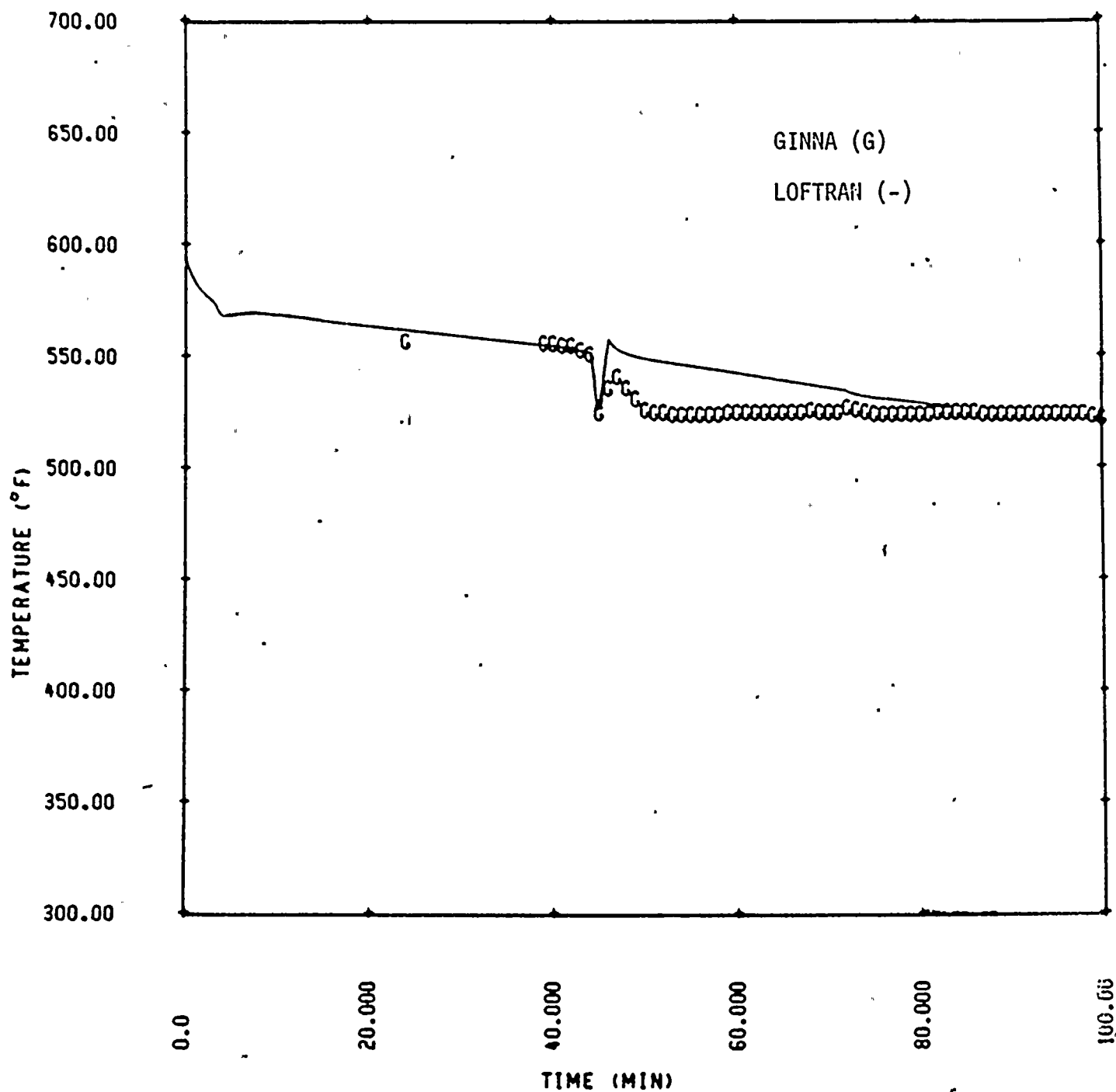


FIGURE II.5.3.6-2. LOFTRAN UPPER HEAD FLUID TEMPERATURE.



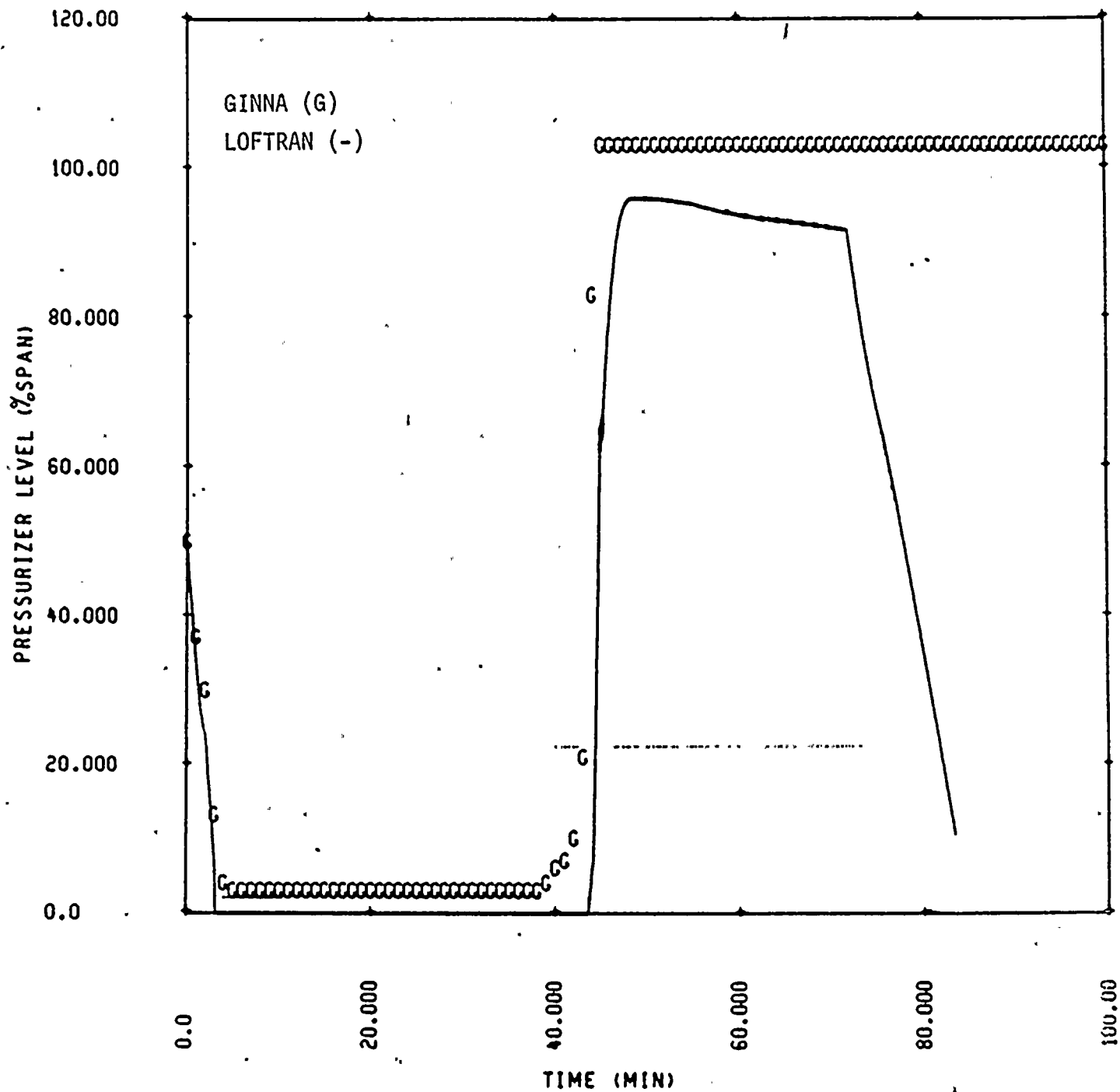


FIGURE II.5.4-1. PRESSURIZER LEVEL INDICATION.



generator occurred in the LOFTRAN results (see section II.5.5). Upper head voiding may have also been slightly underestimated because of the homogeneous modelling, as suggested by Appendix C calculations.

The calculated pressurizer level decreased rapidly after safety injection was terminated at 10:37 (72 min) as break flow decreased coolant inventory. These results indicate that 95 ft³ of water was displaced from the pressurizer as primary pressure decreased to 945 psia. Such a decrease would not have been detected by the level instrumentation if the pressurizer had been nearly water solid. Beyond approximately 10:40 (75 min), the calculated decrease in pressurizer level was unrealistic. Primary-to-secondary leakage was exaggerated after this time because of the unrealistic faulted steam generator pressure calculated by LOFTRAN.

II.5.5 Break Flow

Primary-to-secondary leakage was calculated in LOFTRAN assuming an effective break flow area and a modified Zaloudek critical flow correlation. For unchoked flow, the orifice equation was used. Figure II.5.5-1 shows the primary-to-secondary leakage calculated by LOFTRAN during the Ginna event. Prior to reactor trip, break flow decreased as primary pressure also decreased. Immediately after trip, the rapidly decreasing primary pressure decreased break flow until safety injection flow began to repressurize the reactor coolant system.

Soon after the faulted loop hot leg had cooled below the temperature of the faulted steam generator, 9:37 (12 min), flow through the failed tube was calculated to become unchoked. Beyond this time, the calculated break flow was sensitive to the faulted steam generator pressure. As illustrated in Figure II.5.5-2, the secondary side modelling within LOFTRAN underpredicted the faulted steam generator pressure after 9:46 (21 min). Consequently, secondary-to-primary flow did not occur in the LOFTRAN analysis when the pressurizer PORV was opened.

In order to evaluate the limitations of LOFTRAN break flow modelling and assess the effects on the analysis results, a more detailed model (Appendix B) was developed to calculate the flow from each steam generator plenum. The

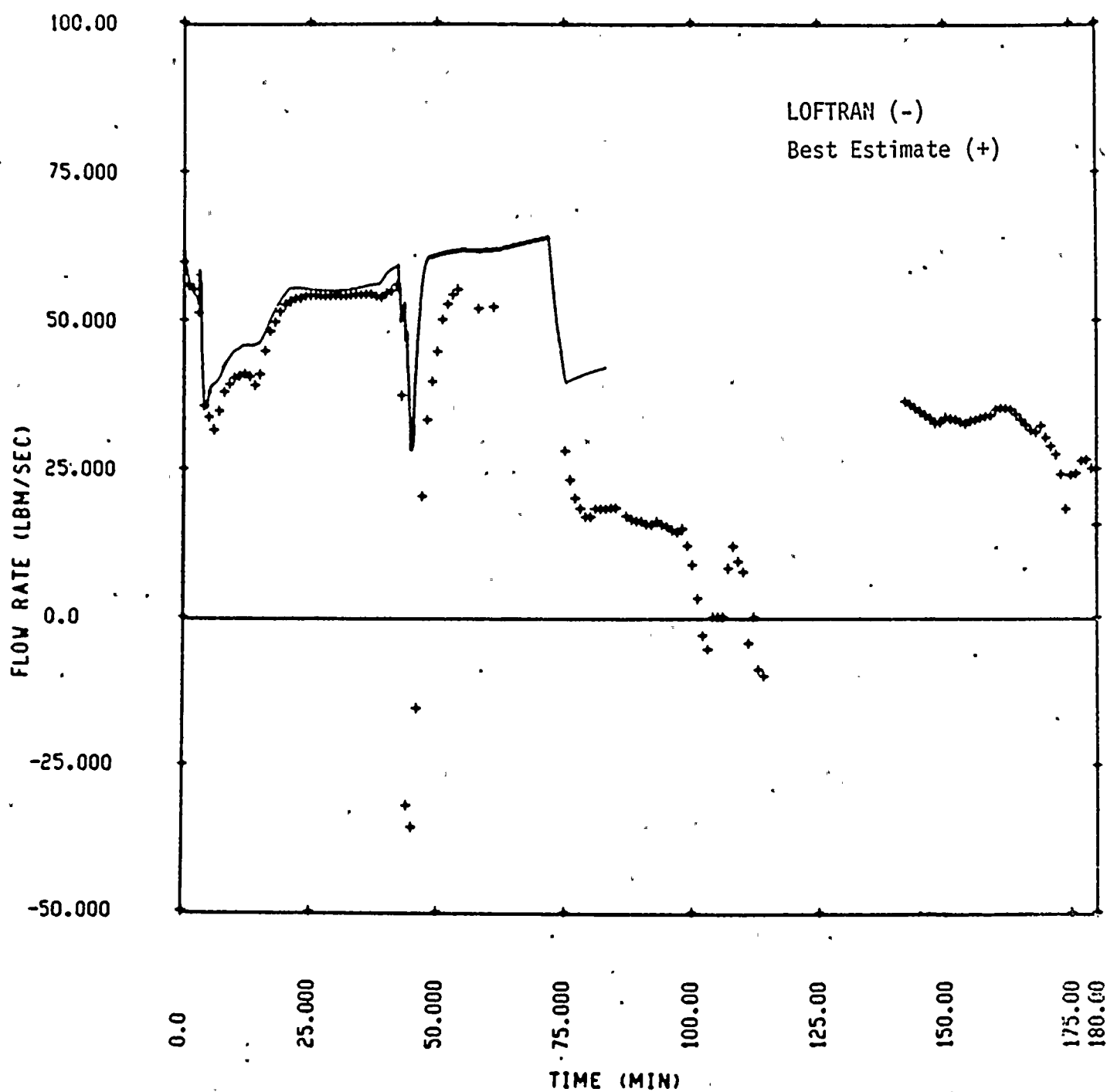


FIGURE II.5.5.-1. LOFTRAN AND BEST ESTIMATE BREAK FLOWS.

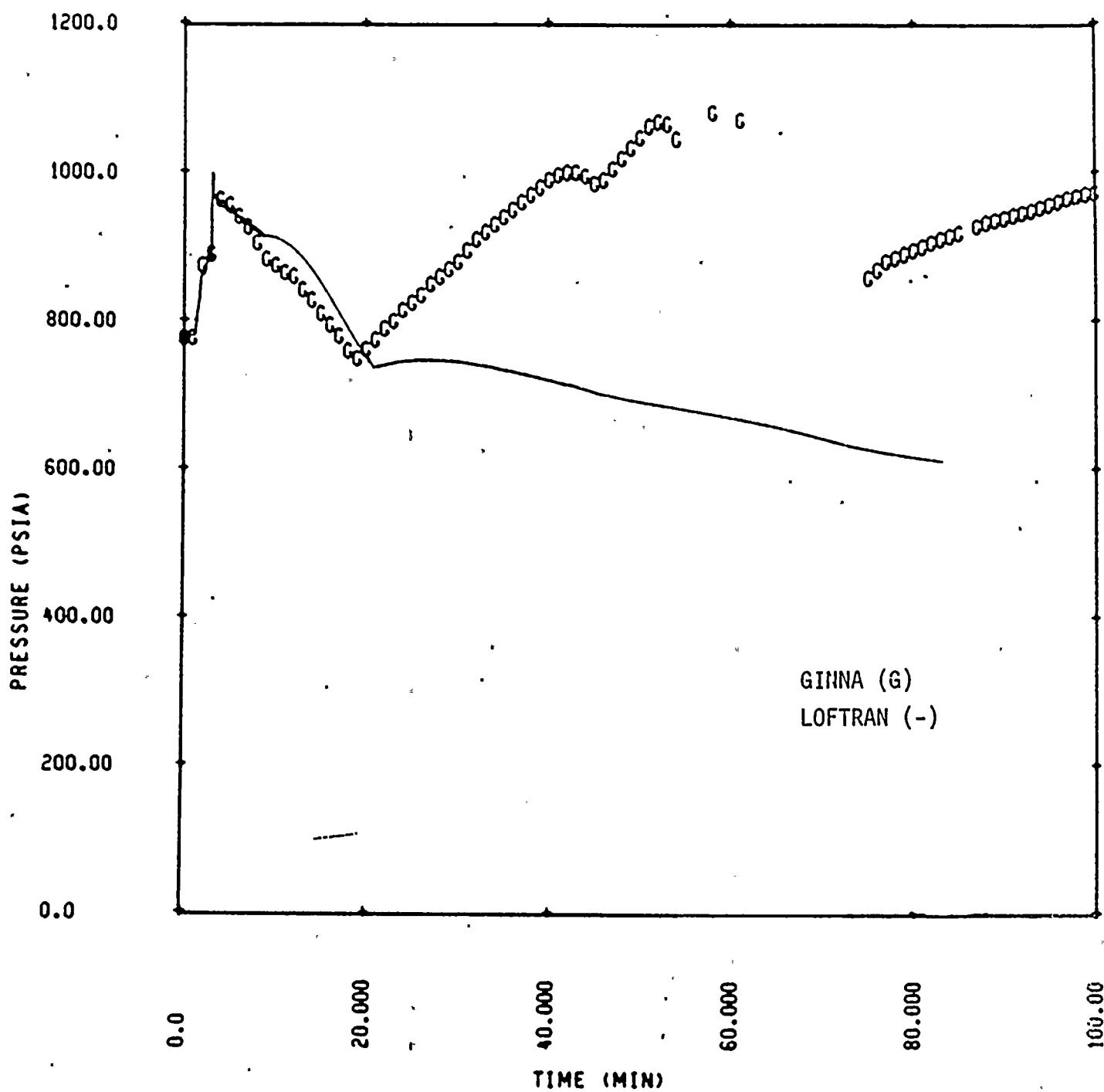


FIGURE II.5.5-2. FAULTED STEAM GENERATOR PRESSURE.



fluid temperature in the steam generator inlet and outlet plenums were taken from the LOFTRAN results. Actual Ginna data was used for the primary and faulted steam generator pressures. Results of these calculations are also shown in Figure II.5.5-1. As demonstrated, LOFTRAN provided a reasonable estimate of the break flow, with the exception of reverse flow through the failed tube, until shortly after safety injection was terminated. After that time, the lower faulted steam generator pressure evident in the LOFTRAN analysis resulted in overestimated primary-to-secondary leakage.

II.5.6 Reactor Coolant Voiding

During natural circulation, portions of the reactor coolant system may stagnate and become effectively isolated from the active coolant regions. Three such regions may exist on the primary side during recovery from a steam generator tube rupture event; the pressurizer, reactor vessel upper head, and the faulted steam generator tubes. As system pressure is reduced, hot fluid in these stagnant regions may flash to steam. The extent of voiding in these regions during the Ginna event was evaluated.

II.5.6.1 Pressurizer Steam Bubble

It is clear from pressurizer level data, Figure II.5.4-1, that a steam bubble existed in the pressurizer until the primary system was manually depressurized beginning at 10:07 (42 min). At that time, the indicated pressurizer level increased rapidly off-scale. LOFTRAN results suggest that the pressurizer did not completely fill, Figure II.5.1-3; however, as previously noted, the increase in pressurizer level may have been slightly underestimated. The pressurizer level response following termination of safety injection suggests that the pressurizer was nearly full at that time. Specifically, pressurizer level did not return on span during the Ginna event when primary pressure decreased by 440 psi.

II.5.6.2 Upper Head Voiding

The calculated upper head temperature history, Figure II.5.3.6-1, indicates that voiding may have occurred in the upper head region prior to reactor coolant pump trip. The maximum volume of this void was estimated to be less than



132 ft³ (Appendix C). Any steam bubble in the upper head at this time would have been quickly condensed since reactor coolant pumps continued to operate. It is unlikely that significant additional voiding occurred prior to manual depressurization of the primary system at 10:07 (42 min) since the calculated upper head fluid temperature remained subcooled.

From 10:07 (42 min) to 10:10 (45 min), upper head thermocouple and pressurizer level responses indicate that voiding also occurred when the pressurizer PORV was opened. The upper head temperature decreased from approximately 556°F when the PORV was initially opened to a minimum of approximately 525°F, as shown in Figure II.5.3.6-2. The upper head region was calculated to completely void during this depressurization (Appendix C). Flashing in the non-active region of the upper plenum, i.e. above the top of the hot leg nozzles, would not be expected because of relatively good mixing characteristics. Consequently, approximately 305 ft³ of steam volume existed in the upper head when the pressurizer PORV was isolated at 10:10 (45 min).

No instrumentation was available above the upper head flange level to track the steam bubble collapse. However, as safety injection repressurized the reactor coolant system, the upper head thermocouples increased approximately along the saturation line from 525°F to 540°F. As pressure continued to increase, temperature then decreased to a stable temperature of 525°F. This suggests flow of colder fluid from the upper plenum past the flange level thermocouples and is indicative of partial steam bubble collapse. This is supported by the slower repressurization of the primary system following isolation of the failed PORV as compared with LOFTRAN analysis results (see section II.5.1).

The size of any steam bubble which existed in the upper head region when safety injection was terminated at 10:37 (72 min) is uncertain. The measured temperature and pressure responses suggest that the upper head was not completely voided and contained significantly subcooled water. The upper head probably voided a third time as primary system pressure decreased to 945 psia following termination of safety injection. Analysis of the primary-to-secondary leakage, charging flow, and reactor coolant expansion suggests a maximum of 125 ft³ of additional voiding may have occurred during this period. This void may have existed until reactor coolant pumps were restarted.



II.5.6.3 B Steam Generator Tube Voiding

The fluid temperature in the faulted steam generator tubes was calculated with LOFTRAN to be 507°F at 10:07 (42 min) when the pressurizer PORV was first opened. This is consistent with plant data which shows that pressure in the B steam generator had decreased to 750 psia by 9:46 (21 min) and is conservative with respect to the calculations presented in section II.5.3.5. Since the calculated tube bundle fluid temperature remained subcooled during depressurization of the reactor coolant system, no steam void would have developed in this region.

II.5.7 Steam Generator Overfill

Primary-to-secondary leakage in excess of steam flow eventually filled the B steam generator with water and lifted the secondary safety valve. The LOFTRAN analysis indicates that the faulted steam generator and main steamline would have filled at 10:18 (53 min), as shown in Figure II.5.7-1. However, this is believed to be earlier than during the actual event for several reasons. In order to simulate the cooldown of the primary system from 9:32 (7 min) to 9:41 (16 min) (see section II.5.3.1), steam release from the faulted steam generator to the condenser was terminated 8 minutes prematurely at 9:32 (7 min). This underestimated the steam released from the faulted steam generator to the condenser by a maximum of 11000 lbm. In addition, the constraints on upper head refill may have increased carryover into the faulted steam generator by a maximum of 300 ft³. The total carryover may have also been slightly overestimated by LOFTRAN since reverse flow during depressurization of the primary system was not predicted. The combination of these effects may have delayed overfill by an estimated 7 minutes. The initial safety valve lifts at 10:19 (54 min) and 10:27 (62 min) would have also decreased steam generator inventory and further delayed overfill.

The mass discharged through the faulted steam generator safety valve was estimated from the primary-to-secondary leakage. LOFTRAN results indicate that 268,000 lbm of primary coolant was transferred into the faulted steam generator prior to termination of safety injection. Approximately 104,000 lbm of this leakage occurred after the steam generator was calculated to fill. Evaluation of the break flow from 10:40 (75 min) until 12:30 (185 min) as shown in



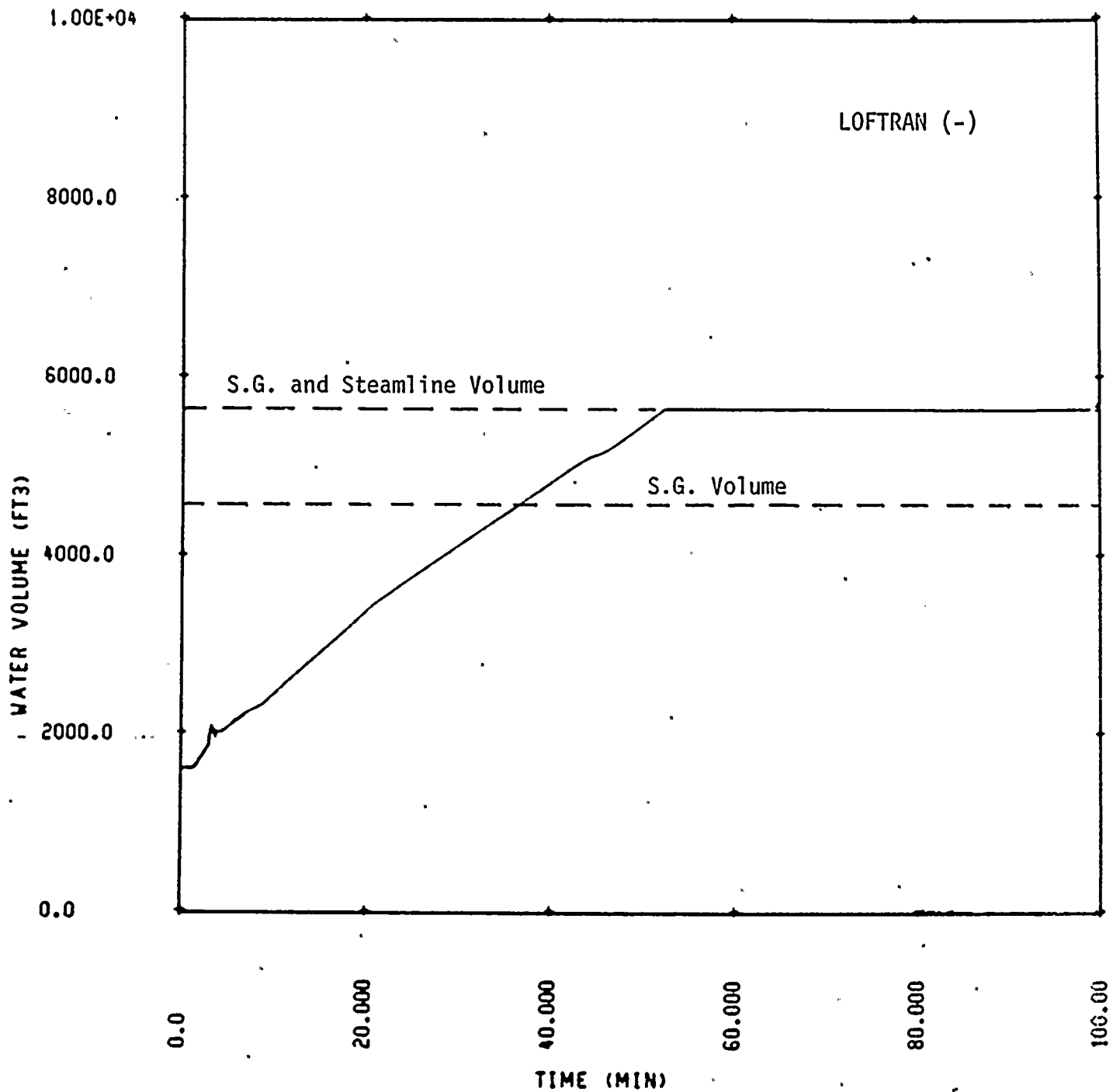


FIGURE II.5.7-1. FAULTED STEAM GENERATOR WATER VOLUME.



Figure II.5.5-1 suggests that an additional 132,000 lbm was transferred from the primary before primary-to-secondary leakage was terminated.

II.6 LONG TERM RECOVERY

When safety injection was terminated at 10:37 (72 min), primary system pressure decreased rapidly from 1370 psia to 945 psia. The LOFTRAN analysis was terminated at this time since the homogeneous equilibrium modelling on the secondary side overestimates the primary-to-secondary pressure differential and, consequently, leakage through the failed tube. Continued charging flow and operation of the pressurizer heaters maintained primary pressure slightly greater than the faulted steam generator pressure, as shown in Figure II.6-1. The B steam generator pressure increased as primary-to-secondary leakage continued. The sequence of events indicates that safety injection was reinitiated at 11:07 (102 min) in preparation for reactor coolant pump restart. However, the effect of the increased coolant makeup on the primary and faulted steam generator pressures is not evident at that time. Although the primary and faulted steam generator pressures increased slowly, the pressure differential decreased. At approximately 11:19 (114 min), a rapid decrease in primary system pressure is evident, probably due to the collapse of an upper head steam bubble (see section II.5.6.2) when a reactor coolant pump was restarted. Although the available data is limited, it appears from the B steam generator pressure response that a safety valve may have lifted at approximately the same time.

Safety injection flow repressurized the reactor coolant system beginning at 11:26 (121 min) until flow was throttled at 11:35 (130 min). The faulted steam generator pressure also increased until the safety valve lifted for the final time at approximately 11:37 (132 min). After this final lift, the faulted steam generator pressure remained approximately 150 psia below the primary suggesting continued leakage into the steam generator. Steam generator blowdown line radiation was also increasing during this same period suggesting flow through this line. Pressurizer level returned on span at approximately 11:53 (148 min), as shown in Figure II.6-2, and continued to decrease indicating a loss of reactor coolant. A safety injection pump was operated intermittently from 12:13 (168 min) until 12:27 (182 min) to control level. By 12:30 (185 min), the faulted steam generator pressure was greater than the reactor coolant system pressure and primary-to-secondary leakage was terminated.

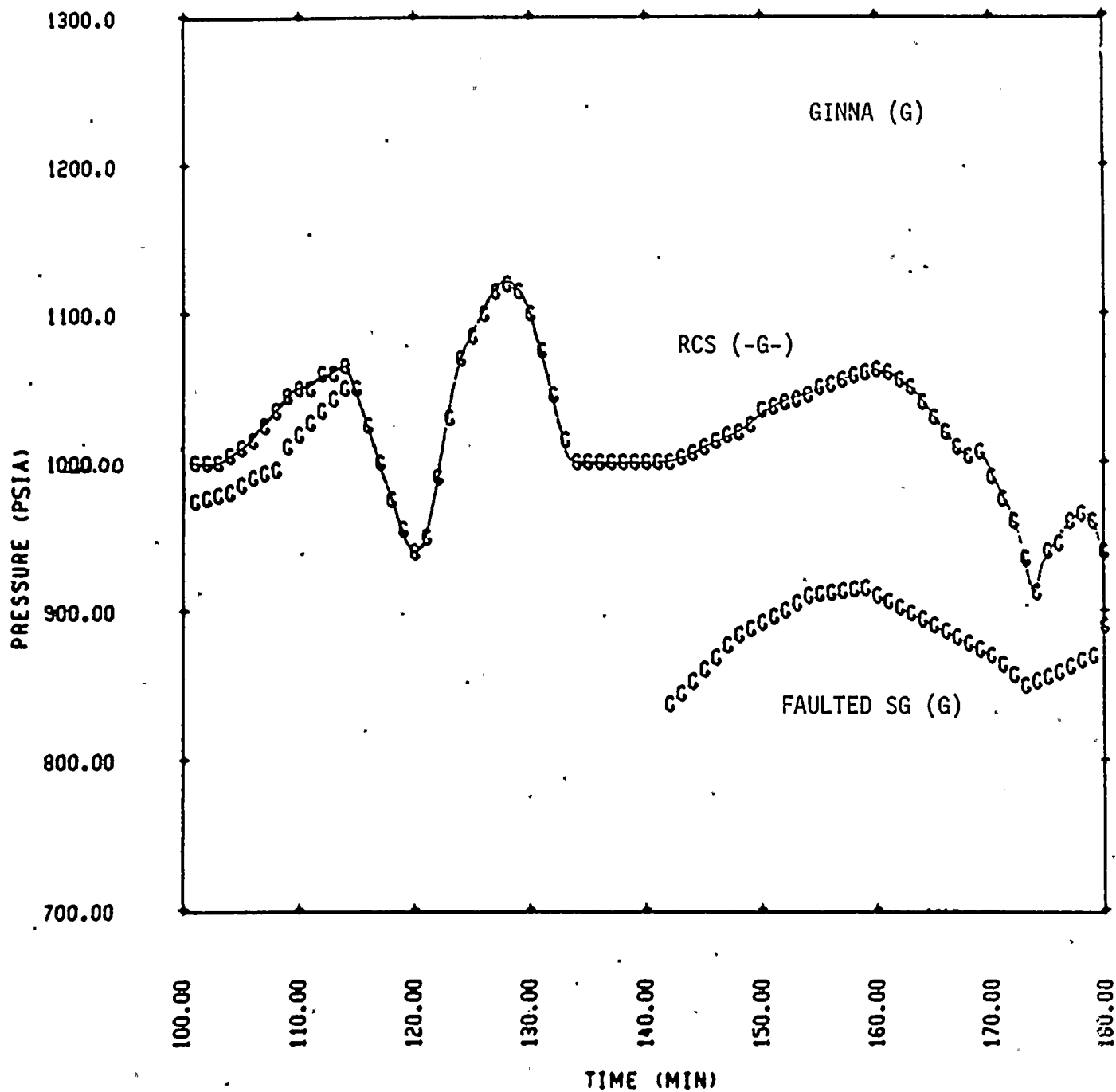


FIGURE II.6-1. RCS AND FAULTED STEAM GENERATOR PRESSURES.



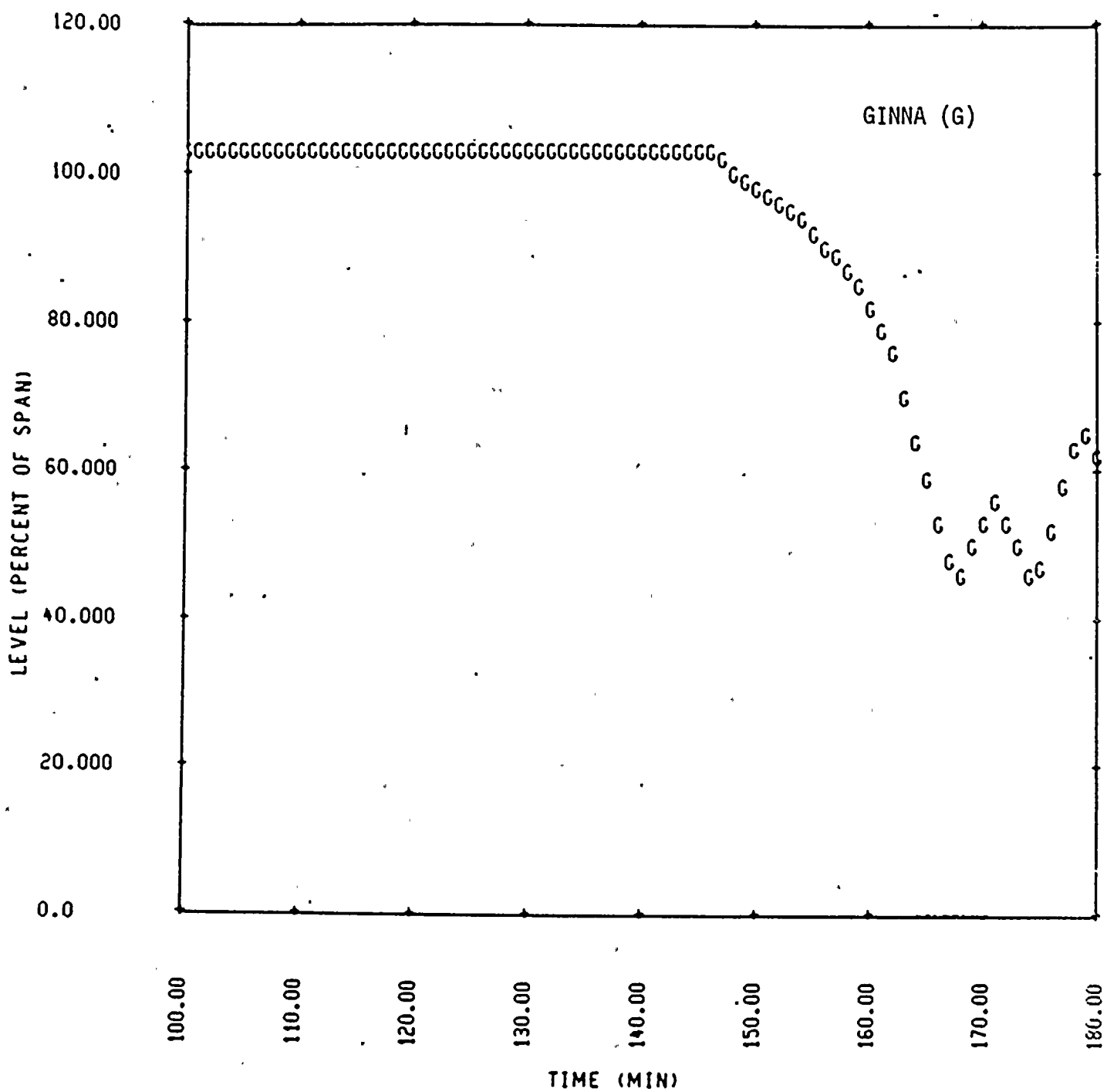


FIGURE II.6-2. LONG-TERM PRESSURIZER LEVEL RESPONSE.



III. SUMMARY AND CONCLUSIONS

The maximum leak rate through the failed tube during the Ginna event was calculated to be 634 gpm. A design basis event with conservative, FSAR assumptions represents an initial primary-to-secondary leak rate of 1147 gpm for the same steam generator. Hence, the initial leak rate was significantly less than design basis.

Break flow depleted primary coolant inventory and resulted in automatic reactor trip and safety injection within approximately 3 minutes of the initiating event. Primary pressure decreased rapidly following reactor trip as coolant temperature decreased and break flow further reduced coolant inventory. Manual reactor coolant pump trip, which occurred within 1 minute of reactor trip, was followed by a smooth transition from forced to natural circulation in both loops. Natural circulation was maintained in the intact loop until a reactor coolant pump was restarted. Isolation of the faulted steam generator in combination with the cooldown of the intact loop eventually stagnated flow in the faulted loop. Analysis results and evaluation of the B loop cold leg temperature suggest that a counter-current flow pattern may have developed in the faulted loop cold leg upstream of the injection nozzle.

With the exception of the upper head region and the pressurizer, the reactor coolant system remained subcooled throughout the event. The upper head may have voided three times. Immediately following reactor trip, a void may have developed before reactor coolant pumps were tripped. No additional voiding occurred until the pressurizer PORV was manually opened to depressurize the primary system. The upper head region completely voided from 10:07 (42 min) to 10:10 (45 min) resulting in a 305 ft³ steam bubble. The relatively slow repressurization of the reactor coolant system from 10:10 (45 min) to 10:17 (52 min) and the upper head thermocouple response suggest that this steam bubble was at least partially collapsed by 10:37 (72 min). However, additional voiding of the upper head probably occurred a third time when safety injection was terminated. This void may have existed when the reactor coolant pump was restarted at 11:19 (114 min). Although LOFTRAN results indicate that the pressurizer did not fill with water, pressurizer level response following termination of safety injection indicate that the pressurizer was nearly full.

The faulted steam generator was estimated to have filled with water by approximately 10:25 (60 min). However, releases during the early safety valve lifts may have reduced steam generator inventory and delayed overfill. An estimated 400,000 lbm of primary coolant were transferred to the faulted steam generator. Approximately 253,000 lbm was calculated to be discharged from the faulted steam generator until primary-to-secondary leakage was terminated at 12:30 (185 min). An estimated 28000 lbm was released as steam to the condenser. The remaining 225000 lbm represents an estimate of the total release from the faulted steam generator safety valve. Consideration of the uncertainty associated with feedwater flow to the faulted steam generator and refilling of the upper head indicates that this estimate may be conservative by up to 48000 lbm. In addition, the calculated leakage into the faulted steam generator from 10:40 (75 min) until 12:30 (185 min) relies on measured system pressures which are subject to instrument uncertainties.



REFERENCES

1. Licensee Incident Evaluation Report on the January 25, 1982 Steam Generator Tube Rupture Incident at the R. E. Ginna Nuclear Power Plant, Docket No. 50-144, April (1982).
2. NRC Evaluation of the January 25, 1982 Steam Generator Tube Rupture Incident at the R. E. Ginna Nuclear Power Plant, NUREG-0909, April (1982).
3. L. A. Campbell, et. al., LOFTRAN CODE DESCRIPTION, WCAP-7878, Rev. 3, January (1977).
4. L. A. Campbell, et. al., WESTINGHOUSE EVALUATION OF LICENSEE EVENT, No. SG 79-11-030, Dec. (1979).
5. F. R. Zaloudek, "Steam-Water Critical Flow From High Pressure Systems Interim Report", Hanford Atomic Products Operation, Richland, Washington, TID-4500, Jan. (1964).
6. J. A. Block, FLUID THERMAL MIXING IN A MODEL COLD LEG AND DOWNCOMER WITH LOOP FLOW, CREARE Inc., Hanover, New Hampshire, EPRI-NP-2312, April (1982).
7. S. Levy and J. M. Lealzer, AN APPROXIMATE PREDICTION OF HEAT TRANSFER DURING PRESSURIZED THERMAL SHOCK WITH NO LOOP FLOW AND WITH METAL HEAT ADDITION, S. Levy Inc., Campbell, California, SLI-8220 August (1982).



APPENDIX A: INITIAL LEAK RATE CALCULATION

The indicated pressurizer level decreased from 32.5% to 11.7% over 104 seconds, as shown in Table II.3-1. This level was adjusted for pressurizer pressure as follows:

$$L_{PRZ} = L_{IND} \times \frac{\left[\frac{1.0}{v_{f_{ref}}} - \frac{1.0}{v_{g_{ref}}} \right] + 100 \times \left[\frac{1.0}{v_{g_{ref}}} - \frac{1.0}{v_g} \right]}{\left[\frac{1.0}{v_f} - \frac{1.0}{v_g} \right]}$$

where,

- L_{PRZ} = actual pressurizer level
- L_{IND} = indicated pressurizer level
- v = fluid specific volume
- Sub f = refers to saturated liquid
- Sub g = refers to saturated vapor
- Sub ref = refers to nominal system conditions

$$\begin{aligned} L_{PRZ}(9:26:18) &= 32.5 \times \frac{\left[\frac{1.0}{0.02698} - \frac{1.0}{0.1569} \right] + 100 \times \left[\frac{1.0}{0.1569} - \frac{1.0}{0.1746} \right]}{\left[\frac{1.0}{0.02617} - \frac{1.0}{0.1746} \right]} \\ &= 32.7 \\ L_{PRZ}(9:28:02) &= 11.7 \times \frac{\left[\frac{1.0}{0.02698} - \frac{1.0}{0.1569} \right] + 100 \times \left[\frac{1.0}{0.1569} - \frac{1.0}{0.1947} \right]}{\left[\frac{1.0}{0.02543} - \frac{1.0}{0.1947} \right]} \\ &= 14.1 \end{aligned}$$

During this time, coolant inventory was depleted at an average rate of

$$\bar{Q}_{BRK} = \frac{(32.7-14.1)\% \text{ span}}{104 \text{ sec}} \times \frac{6.74 \text{ ft}^3}{\% \text{ span}} = 1.202 \frac{\text{ft}^3}{\text{sec}} = 538 \text{ GPM}$$

Considering an excess of 35 gpm from the charging system, the average leak rate was approximately 573 gpm. The initial leak rate was calculated by extrapolating the average rate to the initial system conditions of 2250 psia and 601 F. The average pressure and temperature over the pre-trip period were approximately 2100 psia and 601°F, respectively. Based on subcooled critical flow through the break, the initial flow rate was estimated to be



$$\begin{aligned}\bar{Q}_{BRK} (0) &= 573 \times \left[\frac{(2250 - 0.9 \times 1555) \times 0.02336}{(2100 - 0.9 \times 1555) \times 0.02317} \right]^{0.5} \\ &= 634 \text{ GPM}\end{aligned}$$



APPENDIX B: BEST ESTIMATE BREAK FLOW MODEL

Following a steam generator tube failure, primary coolant flows through the break into the secondary side of the steam generator. The primary-to-secondary pressure differential provides the driving force for this flow. The failure site is connected to two primary fluid reservoirs, i.e. steam generator inlet and outlet plenums, via the segmented tube. Each segment provides a substantial resistance to fluid flow. For larger tube failures, this resistance represents a large fraction of the total resistance between the primary and secondary systems. The break flow model within LOFTRAN does not consider frictional or form pressure losses through each tube segment. For critical flow conditions, this may not be a significant limitation since the pressure drop is essentially localized at the break location or entrance to the failed tube. However, temperature differences between the inlet and outlet plenums will affect critical flow if entrance choking occurs. This temperature effect is also not simulated within LOFTRAN. Furthermore, the primary-to-secondary pressure differential is not accurately predicted. Consequently, a more detailed model was developed which uses primary and secondary pressure data in combination with fluid temperature results from LOFTRAN to calculate break flow.

Flow through the failed tube was simulated as shown in Figure B-1. Frictional pressure losses through each tube segment were represented by an appropriate single phase friction factor, length, and diameter. Entrance and exit losses for each tube segment and at the break location were also included. This system leads to the following set of simultaneous equations which describe flow through the failed tube:

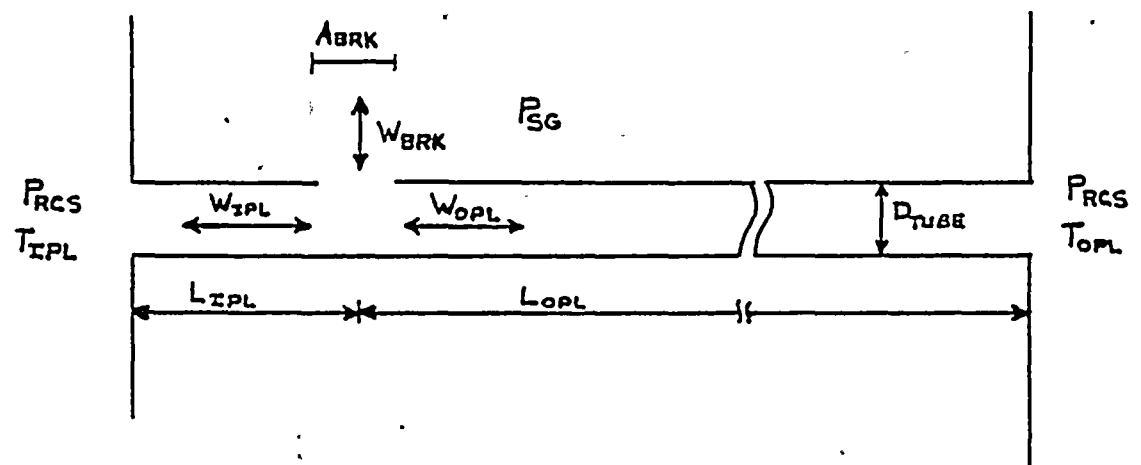
$$\left| P_{BRK} - P_{SG} \right| = \frac{K_{BRK} \times V_{BRK} \times W_{BRK}^2}{2 \times g_c \times A_{BRK}^2} \quad (B-1)$$

$$\left| P_{RCS} - P_{BRK} \right| = \left[K_{ENT} + K_{EXT} + \frac{f L_{IPL}}{D} \right] \times \frac{V_{IPL} \times W_{IPL}^2}{2 \times g_c \times A_{TUBE}^2} \quad (B-2)$$

$$\left| P_{RCS} - P_{BRK} \right| = \left[K_{ENT} + K_{EXT} + \frac{f L_{OPL}}{D} \right] \times \frac{V_{OPL} \times W_{OPL}^2}{2 \times g_c \times A_{TUBE}^2} \quad (B-3)$$



FIGURE B-1. SG TUBE RUPTURE FLOW MODEL DIAGRAM.



$$W_{BRK} = W_{IPL} + W_{OPL}$$

(B-4)

where,

- P = pressure
- W = flow rate
- V = fluid specific volume
- K_{ENT} = Tube entrance loss coefficient
 = 0.4, primary-to-secondary flow
 = 1.0, secondary-to-primary flow
- K_{EXT} = Tube exit loss coefficient
 = $\left[1.0 - \frac{A_{TUBE}}{A_{BRK}} \right]^2$
 = 1.0, secondary-to-primary flow
- f = Moody friction factor
- A = flow area
- D = tube diameter
- g_c = gravitational constant
- Sub BRK = refers to break location
- Sub RCS = refers to primary side
- Sub IPL = refers to steam generator inlet plenum
- Sub OPL = refers to steam generator outlet plenum
- Sub TUBE = refers to steam generator tube

Critical flow through the failed tube was calculated using a modified Zoloudek ⁽⁵⁾ correlation for subcooled critical flow. Choked flow conditions for each tube segment and at the break location were calculated from

$$W_{C_{IPL}} = A_{TUBE} \times C_1 \times \left[\frac{2g_c [P_{RCS} - C_2 \times P_{sat}(T_{IPL})]}{V_{IPL}} \right]^{1/2} \quad (B-5)$$

$$W_{C_{OPL}} = A_{TUBE} \times C_2 \times \left[\frac{2g_c [P_{RCS} - C_2 \times P_{sat}(T_{OPL})]}{V_{OPL}} \right]^{1/2} \quad (B-6)$$

$$W_{C_{BRK}} = A_{BRK} \times C_1 \times \left[\frac{2g_c [P_{BRK} - C_2 \times P_{sat}(T_{BRK})]}{V_{BRK}} \right]^{1/2} \quad (B-7)$$



where,

T = fluid temperature, F

P_{sat} = saturation pressure, psia

WC = critical mass flow rate, lbm/sec

C_1 = entrance effect coefficient (adjusted to match initial leak rate)

C_2 = 0.9

Equations B-1 through B-7 were solved simultaneously for break flow through the failed tube.



APPENDIX C: CALCULATION OF UPPER HEAD VOID SIZE

The upper head region of the reactor vessel was modelled as a single, stratified node with only outward flow as shown in Figure C-1. As system pressure decreased below saturation of the upper head fluid, voiding within the upper head region displaced liquid into the upper plenum. The extent of voiding was estimated assuming thermodynamic equilibrium between phases. Metal in the upper head region was conservatively assumed to be at the fluid temperature.

A mass and energy balance between initial and final states within the upper head volume leads to the following expression for the fraction of final steam volume

$$\frac{V_g}{V_{UH}} = \frac{\left[(h_o - \bar{h})/v_o + (\bar{h} - h_f)/v_f \right] + \frac{MC_p}{V_{UH}} (T_o - T_{sat})}{\left[(h_g - \bar{h})v_g + \frac{(\bar{h} - h_f)}{v_f} \right]}$$

where,

v = fluid specific volume

h = fluid enthalpy

V = Volume

\bar{h} = average enthalpy of displaced fluid

T = fluid temperature

(MC_p) = metal heat capacity

Sub o = refers to initial conditions

Sub f = refers to saturated liquid

Sub g = refers to saturated vapor

Sub UH = refers to upper head region

Table C-1 lists the upper head conditions for the first two incidents of potential upper head voiding during the Ginna event (see section II.5.6.2). The calculated upper head region void fractions from equation C-1 are also presented. For these results, the enthalpy of displaced liquid was assumed to be the linear average of the initial and final states.

FIGURE C-1. UPPER HEAD VOIDING ILLUSTRATION.

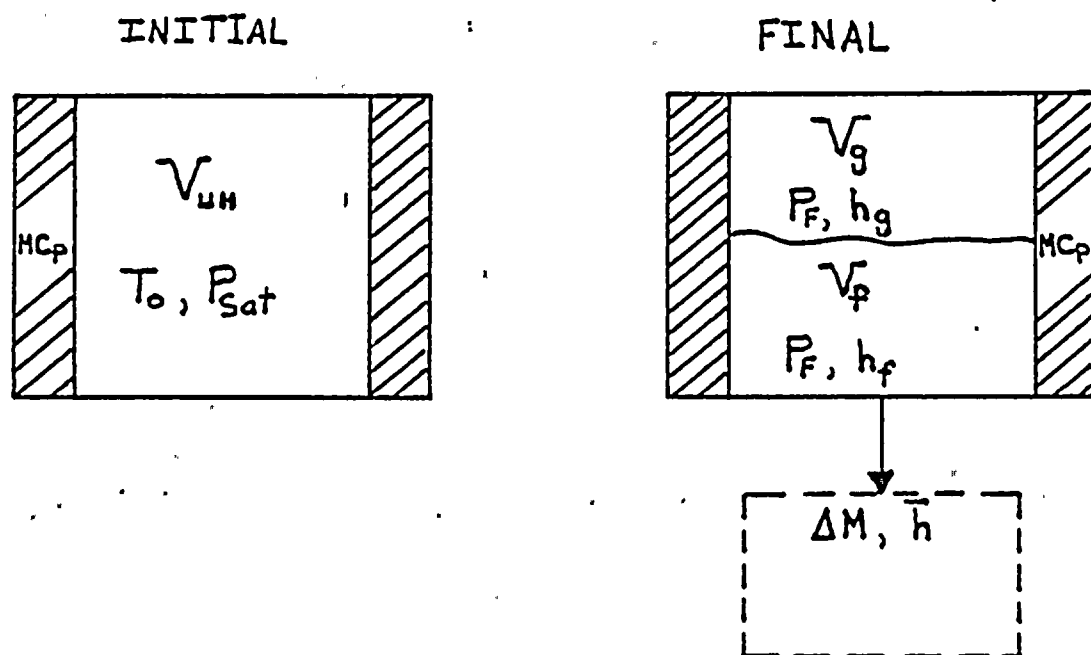


TABLE C-1 UPPER HEAD VOID SIZE

Time	P _o (Psia)	T _o (Psia)	P _F (Psia)	V _g / V _{UH}	V _g (Ft ³)
9:28:30	1300	577.5	1200	0.431	132
10:07	1098	556	845	1.0	305

